SELECTIVE RECOVERY OF SALTS FROM A TERNARY EUTECTIC SYSTEM IN EFC USING SEEDING

Benita Jean Aspeling

Supervisor: Jemitias Chivavava

Co-supervisor: Professor Alison Emslie Lewis

Dissertation submitted in partial fulfilment of the requirements for the degree of Master of Science in Engineering

---

Department of Chemical Engineering

Faculty of Engineering and the Built Environment

University of Cape Town

February 2019

Declaration: *I know the meaning of plagiarism and declare that all the work in the document, save for that which is properly referenced, is mine*

Signed by candidate

.....

Executive summary

Industrial and mining saline streams are often multi-component in nature. Much research within Eutectic Freeze Crystallization (EFC) has focused on the crystallization of ice and single salts from aqueous solutions. However, as a single salt and ice are crystallized, the concentration of the non-crystallizing salt species increase until the system is saturated with more than two species. In such a situation, the sequence and rate of crystallization of each species depends on both the kinetics of crystallization of each salt and the interaction between the different species. Seeding could be employed to control kinetics and thereby achieve selective recovery from multi-supersaturated systems. The aim of this study was therefore to determine the effect of seeding on the yield and purity of the salt product in a system supersaturated with two salts and ice.

A eutectic $MgSO_4$-Na_2SO_4-H_2O system was chosen for this study as these salts are prevalent in saline waste streams in South Africa. A continuous 2 ℓ jacketed, scraped and stirred glass crystallizer was seeded with $Na_2SO_4 \cdot 10H_2O$, $MgSO_4 \cdot 11H_2O$ and ice. The initial salt seed loading and initial supersaturation were varied. The operating conditions used were 30 minutes residence time, a coolant temperature of -11°C, and operating temperature of approximately -5.0 to -5.1°C. An increase in seeding mass was found to increase the yield and proportion of the seeded salt in the salt product due to an increase in salt growth rate. However, in all experiments it was found that $MgSO_4 \cdot 11H_2O$ crystallized out at fractions higher than the eutectic thermodynamic ratio, indicating a higher selectivity towards this salt. Furthermore, the introduction of 30 g of $MgSO_4 \cdot 11H_2O$ seeds produced a pure salt product (above 99.4 wt.% purity) and the highest salt yield. A similar mass of either seeding material resulted in a similar total mass of salt product. This was attributed to $MgSO_4 \cdot 11H_2O$ crystallizing as the majority salt, and therefore its kinetics played a major role in the total salt yield. Initial supersaturation was found to have no significant effect on steady state salt purity and yield. This study showed that multiple steady states exist within this system at the same operating conditions but different initial seeding conditions. Seeding was found to have the potential to engineer the salt purity of the overflow and underflow split fractions by changing the individual salt average particle sizes. Therefore, this study showed that selectivity recovery of one salt is possible in a multi-supersaturated system through seed engineering.

Acknowledgements

The author would like to thank the following people:

- My supervisors, Jemitias Chivavava and Professor Lewis, for their guidance and valuable input regarding the research project. This project would not have been successful without it. An especially large thank you to Jemitias Chivavava for all of his many hours spent guiding me and arguing with me regarding all the finer details of crystallization.
- The Crystallization and Precipitation Research Unit, for funding towards the project. I would also like to thank all the members in this group for all their support and cheer when times were good and when times were tough. I would especially like to thank Dr Qinghai Li who assisted in experimental work, including setting up and taking down the crystallizer multiple times, conducting experiments alongside with me, and assisting with the measurement of magnesium and sodium ion concentrations.
- My husband, who kept on supporting me, financially and emotionally, through all the ups and downs of my experimental journey.
- Most of all, to God who opened all the doors, and made this experience possible. I would also like to thank Him for pulling me through.

  Thank you!

Table of Contents

Table of Figures

List of Tables

Nomenclature

a	Activity [kg/kg solvent]
a_w	Activity of water [kg/ kg total]
A	Pre-exponential factor for primary nucleation
A_s	Total crystal surface area [m^2]
b	Nucleation order
B	Secondary nucleation rate [#/m^3.s]
C	Concentration [kg/kg solvent]
C*	Equilibrium concentration [kg/kg solvent]
C_s*	Critical seed loading ratio
g	Supersaturation exponential factor in growth rate equation
G	Growth rate [m/s]
j	Magma density exponential factor in nucleation rate equation
J	Primary nucleation rate [#/m^3.s]
k	Boltzmann's constant [J/K]
k_b	Secondary nucleation rate constant
k_g	Growth rate constant [$m^{-1}s^{-1}$]
m^*_{seed}	Critical seed mass [g]
M_T	Magma density [kg/m^3 of slurry]
MSZW	Metastable zone width [K] or [kmol/m^3]
R	Universal gas constant [J/mol.K]
r	Ionic radius [°A]
r*	Critical cluster size [m]
S	Supersaturation ratio
T	Temperature [°C]
T_{eq}	Equilibrium temperature [°C]
V_m	Molecular volume [m^3 $molecule^{-1}$]

Greek symbols

ΔC_{met}	Metastable zone concentration [kmol/m^3]
Δm	Mass of solids formed in batch crystallizer [g]
ΔT_{met}	Metastable zone temperature [K]
γ	Interfacial free energy [J/m^2]
γ_{eff}	Effective interfacial free energy [J/m^2]
μ	Chemical potential [J/mol]
$\mu°$	Chemical potential of pure solvent [J/mol]
φ	Wetting factor
τ	Residence time [min]
v	Number of ions per mol solute
x	Mass fraction
x_w	Mol fraction of water [mol/mol total]

1 Introduction

1.1 Background

With an increase in industrialisation and mining, which is associated with an increasing population, our reliance on our water resource is constantly increasing. Although mining and industries make up a relatively small portion of total water use in South Africa, their impact on water sources can be severe (Haggard, Sheridan and Harding, 2015). Some technologies exist to neutralise impacted water if it is acidic, or to remove selected contaminants, but reverse osmosis (RO) is often used as the last step to produce potable or process water from the waste water. Reverse osmosis plants produce a brine stream which is a concentrated volume of water containing all the contaminants previously found in the reverse osmosis feed.

Current normal practice sends brines to evaporation ponds, where solar evaporation takes place, or to evaporative crystallization plants, where the brine is boiled off to produce a mixed dry salt. In either of these cases, the mixed salt still requires disposal to landfill as there are no uses for it. In addition to this, brine ponds may result in seepages to groundwater and are currently being phased out, while evaporative crystallization has high energy requirements.

Eutectic Freeze Crystallization (EFC) is an emerging technology which makes use of cooling as a method for separating salt and water as ice from the mother liquor, by making use of a reduction in salt solubility at low temperatures. Advantages of this technology include a 60-85% reduction in energy requirement (Van der Ham, 1999; Vaessen, 2003; Himawan, 2005; Nathoo, et al., 2009) compared to evaporative crystallization, while producing clean water and potentially pure salts which can be re-used or sold to offset the crystallization costs. The remaining concentrated brine is of a greatly reduced volume, with associated reduced environmental hazard and disposal costs.

Efficient separation of salt product(s) and ice in an EFC process relies on the operating conditions and nature of the system used. In a binary process, a larger crystal size is aimed for, which allows easier separation by gravity from the less dense mother liquor and ice crystals. In a multi-component system, it is aimed to obtain crystals which either crystallize out at separate times and temperatures, or, if the crystals form at the same time, that they should form separate crystals with distinctively different crystal sizes and densities where physical separation can be effected as a post processing step.

Current research and knowledge base largely consist of separation of a single salt and ice from the solution. Therefore, not much research has been conducted on utilising aqueous and solid phase salt properties and interactions between salts to selectively recover a salt from a system saturated with more than one salt, especially within a continuous EFC process. As most waste streams contain multiple contaminants, utilizing EFC for separation of more than one salt as pure products would allow EFC to have far wider applicability throughout South Africa and the world.

In this study, the $MgSO_4$-Na_2SO_4-H_2O ternary system was chosen due to the prevalence of these salts in mining-impacted saline waste streams in South Africa.

1.2 Problem statement

Industrial and mining saline streams are often multi-component in nature. Much research has focused on the crystallization of ice and single salts from aqueous solutions. However, as a single salt and ice are crystallized from such solutions, the concentration of the non-crystallizing salt species increases. Eventually, the system becomes saturated in terms of more than two species. In such a situation, the sequence and rate of crystallization of each species depends on the interaction between ions, the kinetics of crystallization of each species as well interactions between solid surfaces of crystallized species and species still dissolved in solution.

In order to selectively recover one salt in a multi-supersaturated system, nucleation and growth of individual species need to be controlled for a pure salt product to form. Seeding is used as a mechanism of nucleation and growth control, especially within a system which is metastable for one or more species. However, seeding also provides a solid surface which reduces the required energy for crystallization of the non-seeded species. It is therefore necessary to understand the combined effect of seeding on yield and purity of the salt product in a multi-supersaturated continuous process.

1.3 Aim and objectives

The aim of this study was to determine the effect of seeding on the yield and purity of the salt product.

The objectives to address this aim are:

- Conduct thermodynamic modelling to determine the nature of the species in the system;

- Determine the effect of the salt seeding material on the purity and yield of the recovered salt product;
- Determine the effect of seeding temperature on the response of the system to the seeded material; and
- Determine the effect of available seed surface area on the purity and yield of the products.

1.4 Scope of research

This project includes thermodynamic modelling and practical experimentation. OLI Stream Analyser thermodynamic modelling was carried out to determine the theoretical eutectic temperature of the system. This modelling work also provided further understanding on the thermodynamic behaviour of the species. Experiments were conducted on a continuous 2L laboratory scale EFC plant, using a eutectic $MgSO_4$-Na_2SO_4-H_2O ternary system. The effect of seeding material, seeding temperature and seed surface area on salt product yield and purity were investigated and the results are presented in this report.

2 Theory

Crystallization is a separation method in which a solid crystalline material is produced from a melt, solution or vapour (Ulrich and Jones, 2006). Crystallization can only be achieved when the chemical potential of the salt or ice is lower in the solid phase than the liquid phase. This difference in chemical potential is termed supersaturation.

2.1 Supersaturation

The difference in Gibbs free energy of the transferring and transferred state, e.g. solution and crystal states is the driving force for crystallization (Mullin, 2001). When temperature and pressure are constant, Gibbs free energy is the same as chemical potential (μ), and the driving force can then be shown as follows:

$$\Delta\mu = \mu_{i,\mathrm{aq}} - \mu_{i,s} \qquad 2.1$$

The chemical potential [J/mol] is defined in terms of its standard potential μ_0 as follows:

$$\mu = \mu_0 - \nu \mathrm{RT}\, ln\, \mathrm{a} \qquad 2.2$$

In this equation, ν is the number of ions per mole of solute, R is the universal gas constant [J/mol.K], T is absolute temperature [K], and a is the activity of the solute [mol/mol solvent]. As the chemical potential of a solid cannot be calculated in terms of activities, the chemical potential of the dissolved species which would be in equilibrium with the solid is used instead. Substituting the above equation into 2.1 gives the following:

$$\frac{\Delta\mu}{\mathrm{RT}} = -ln\frac{\mathrm{a}_i}{\mathrm{a}_{i,\mathrm{eq}}} = -ln\,\mathrm{S} \qquad 2.3$$

In the above equation, S is the activity supersaturation ratio. Where activity coefficients are not known, a concentration-based supersaturation is usually applied for simplification.

In terms of solvent crystallization, activity is not normally used to determine the supersaturation as it is the major species and therefore its initial and equilibrium activities are very similar, and $\nu \approx 1$. Temperature is therefore used as a measure of supersaturation for solvents such as water.

Taking the activity to remain constant, equations 2.1 and 2.2 can be combined and reduced to the following:

$$\Delta\mu = \mu_{i,\mathrm{aq}} - \mu_{i,s}$$

$$\Delta\mu = \mu_0 - v\mathrm{RT}\, ln\, \mathrm{a} - \mu_0 + v\mathrm{RT}_{eq}\, ln\, \mathrm{a}$$

$$\frac{\Delta\mu}{\mathrm{RT}\, ln\, \mathrm{a}} = \frac{(\mathrm{T} - \mathrm{T_{eq}})}{\mathrm{T}} \qquad 2.4$$

The measure of supersaturation for ice can therefore be calculated as the relative difference in the absolute temperature of the actual solution and equilibrium.

The supersaturation can also be derived using the relationship between the Gibbs free energy and temperature, and solved to obtain the following supersaturation equation:

$$\Delta\mu = (\Delta\mathrm{H}/\mathrm{T_{eq}})(\mathrm{T} - \mathrm{T_{eq}})$$

$$\Delta\mathrm{T} = \mathrm{T} - \mathrm{T_{eq}} \qquad 2.5$$

In these equations, ΔH is enthalpy [J/mol].

The form of supersaturation in equations 2.4 and 2.5 is often called “undercooling” in melt crystallization.

It is important to understand the kinetics of crystallization in order to selectively recover one species over another. Kinetics of crystallization can be divided into nucleation and crystal growth. Nucleation involves the birth of crystals, while crystal growth involves the evolution of the crystal over time.

2.2 Metastability

At low enough supersaturations and in the absence of seeds, no nucleation may take place even given infinite time. The ability of a species to remain in solution without forming a solid phase in the presence of supersaturation is termed its metastability (Myerson, 2002). Conversely, a system is said to be labile if solids are expected to form within a given length of time. Metastability allows a system to be operated below the liquidus or freezing line in a thermodynamic diagram without this species crystallizing out, and therefore potentially allows the selective crystallization of a product in a system supersaturated with multiple species.

As the supersaturation of the system is increased, spontaneous nucleation eventually occurs at a point termed the metastable limit (Mersmann, 2001), which can be described as a concentration or temperature. A system may have metastability below the liquidus/freezing line as a liquid, or above the liquidus/freezing line as a solid without changing phase. This area on the phase diagram is termed the metastable zone.

The metastable zone width is dependent on a number of parameters, such as cooling rate, impurity concentration, agitation rate, solution temperature, size and material of seed crystals (Himawan, 2005, Mullin, 2001). Even given constant conditions as indicated above, the induction time may not be the same for different experiments. This is because nucleation and metastability are stochastic in nature, and therefore follow a probabilistic function, rather than a definite time frame, especially for smaller volumes (Mullin, 2001; Myerson, 2002; Mitchell and Frawley, 2010; Kadam et al., 2012; Randal et al., 2012; Jin et al., 2015). Within the metastable zone, only secondary nucleation and growth occur, and parent crystal seeds are required for this crystallization. This allows the process to be controlled, with crystal formation rate determined by the level of supersaturation of the system. Past the metastable limit, numerous tiny crystals are formed, as is typical for spontaneous nucleation. This negatively impacts crystal size and may cause agglomeration and entrainment in the reactor due to high solids density and small mean particle size.

2.3 Nucleation

In any given solution, ions are continuously coming together and moving apart in an equilibrium. Clusters can form if there is enough driving force in the form of supersaturation or supercooling. These clusters either decay or continue to grow to a threshold size above which the energy required for cluster decay becomes greater than the energy required for cluster growth. From this point, the cluster is termed a nucleus, and represents the birth of a crystal. However, if large enough clusters do not form, the system may be supersaturated but metastable and potentially remain in this state for long periods of time.

2.3.1 Primary nucleation

Nucleation can occur in the form of primary or secondary nucleation. Primary nucleation describes nucleation in the absence of parent crystals of the species in question. Secondary nucleation describes nucleation of crystals due to the presence of parent crystals.

Primary nucleation can be subdivided into homogeneous nucleation and heterogeneous nucleation. Homogeneous nucleation occurs within a system devoid of dust particles, movement and surfaces. This type of system does not encourage cluster growth, and therefore requires the highest level of supersaturation in order to break the energy threshold for crystallization (Myerson, 2002).

Heterogenous nucleation is primary nucleation that occurs in the presence of dust particles, agitation, solid surfaces, etc. This type of nucleation occurs most often in nature, and requires less energy for nucleation than homogeneous nucleation.

Primary nucleation is dependent on many factors, such as vibrations, presence of particles or surfaces, and even the presence of dissolved ions which are in a constant state of motion. By its very nature, spontaneous nucleation is a probabilistic function dependent on the supersaturation of the system and the rate of clustering together of particles. However, in addition to this probabilistic nature, differences in agitation and non-homogeneity in the solution results in local areas of higher supersaturations and higher "probabilities" of nucleation than other areas, also making this a stochastic process (Kadam et al., 2012).

In a multi-component system, the induction time of the unseeded salt is a function of supersaturation and the presence and nature of surfaces, including crystals of the seeded species (Mullin, 2001). The supersaturation of the unseeded salt is also affected by the rate of crystallization of other species. These crystallization rates are further dependent on the level and spread of supercooling and interactive supersaturation generation, where two or more species are crystallizing. Therefore, it is expected that the induction time for nucleation of the unseeded salt will vary with each experiment even with seeding of other species, providing a varying length of time for growth, and therefore a variation in both yield and purity of the product.

The particle size to which clusters need to grow in order to reach the energy threshold for nucleation is termed the critical size. This size is determined by the Gibbs free energy (ΔG) of the nucleus.

The Gibbs free energy of the nucleus is calculated from the Gibbs free energy of the surface cluster's surface and volume (Myerson, 2002; Ulrich and Jones, 2006). This relationship is shown in Figure 2.1 below.

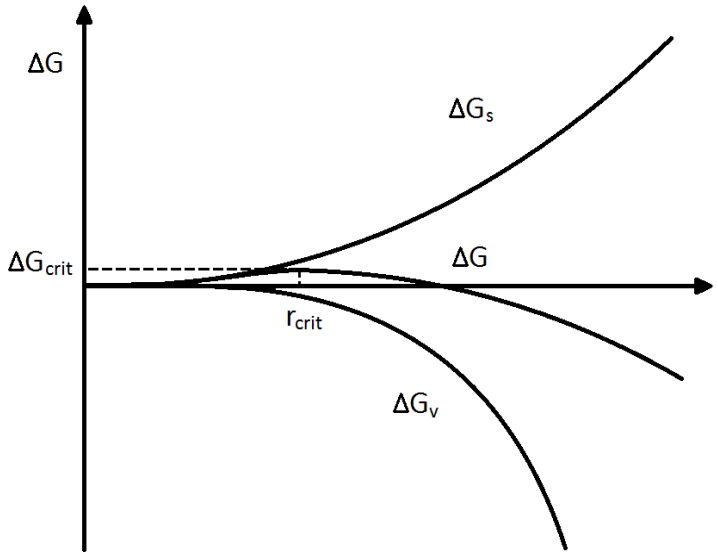

Figure 2.1: Gibbs free energy with radius of nucleus [redrawn from Ulrich and Jones, 2006]

For a spherical particle, the volume and surface of the cluster can be calculated based on a particle radius of r and given number of particles n. The critical radius of the particle can be determined to be as follows:

$$r^* = \frac{2\gamma V_m}{\Delta\mu} \qquad 2.6$$

In this equation, γ is the interfacial free energy [J m^{-2}] and V_m is the molecular volume [m^3.$molecule^{-1}$]. The corresponding critical Gibbs free energy is then:

$$\Delta G^* = \frac{16\pi\gamma^3 {V_m}^2}{3\Delta\mu^2} \qquad 2.7$$

The interfacial free energy is dependent on the surface where nucleation takes place. If no surface is used (homogeneous nucleation), the interfacial free energy is at a maximum. The more similar the nucleation surface is to the crystal which is to be formed, the smaller the wetting factor (φ) becomes, thus the lower the free energy required for nucleation will be and the greater the probability for clustering and eventual nucleation of crystals.

$$\gamma_{eff} = \varphi\gamma \qquad 2.8$$

The heterogeneous nucleation rate can be written in terms of the critical Gibbs free energy and supersaturation (Lewis et al., 2015):

$$J = AS \exp\left[-\frac{16\pi{\gamma_{eff}}^3 {V_m}^2}{3kT\Delta\mu^2}\right] \qquad 2.9$$

In the above equation kT is used instead of RT since it is related to one solute entity or molecule rather than a mol, where k is Boltzmann's constant [J/K]. A is a kinetic factor that depends on whether nucleation is surface integration controlled or volume diffusion controlled, which will not be discussed here. These equations show that nucleation is directly dependent on supersaturation and are also largely affected by the nature of other surfaces present.

2.3.2 Secondary Nucleation

Secondary nucleation is the most common form of nucleation in industry, and requires the active participation of crystal surfaces (Myerson, 2002). It occurs by parts of crystals separating and thereby providing additional surface for nucleation. The various mechanisms of secondary nucleation include initial breeding, where nuclei form due to particles washing off crystals that have been placed into the supersaturated solution, collision breeding and fluid shear, where fragments of existing crystals are broken off by mechanical impact and the shear of the moving liquid, respectively, to provide new crystals for nucleation (Ulrich and Jones, 2006). Collision breeding is the most common form of nucleation, once initial crystals have started forming. This allows continued crystal formation until steady state in continuous crystallization.

Secondary nucleation is related to magma density in the following equation, taken from Tavare (1995):

$$\mathrm{B} = k_b M_T^j \Delta C^b \qquad 2.10$$

In this equation, k_b is the nucleation rate constant, which is a function of many variables such as temperature, hydrodynamics, presence of impurities, among others. M_T is magma density [kg/m^3 of slurry], j is a factor usually between 0 and 1, and the nucleation order, b, is typically between 0.5 and 2.5.

2.3.3 Seeding

Seeding is the addition of crystals to a crystallizer to initiate crystallization of metastable species. This ensures that crystallization can occur well within the metastable zone, such that nucleation is suppressed and growth is optimised (Mersmann, 2001; Bergfors, 2003).

There are a number of important factors to consider regarding seeding, in order to produce an optimal crystalline product (Ulrich and Jones, 2006). The surface area of the seeds must be large enough to avoid additional spontaneous nucleation in the early stages of the process, ensuring that a bimodal crystal size distribution does not form. However, the surface area needs to be small enough to produce the desired mass of product in the process. Seeds that are too

large in size produce a low yield while seeds that are too small yield a product with a small crystal size, which could result in entrainment and difficulties in product handling processes. Additionally, the supersaturation of the process needs to be controlled within the optimal region for crystal growth throughout, as the crystal surface increases and the solution concentration changes. In terms of seeding temperature, it has been determined that seeding has no effect on the average size of the product within 40% of the metastable zone width temperature (ΔT_{met}) (Myerson, 2002). However, as the supercooling increased above this point, progressively more fines were observed.

The optimal mass of seeds to be used is usually determined experimentally per system rather than using science (Ulrich and Jones, 2006; Aamir et al., 2010, Myerson, 2002). According to Lewis et al. (2015), a critical seed loading ratio for a batch system is determined as the ratio of seed to expected product mass required to ensure that no spontaneous nucleation occurs upon seeding. From various systems, it has been determined that the critical seed loading ratio is directly dependent on seed size, and therefore the critical seed mass can be calculated simply from a knowledge of the seed size and mass of product that is to be produced.

$$C_s^* = 2.17 \times 10^{-6} L_{seed}^2 \qquad 2.11$$

In the above equation, C_S^* is the critical seed loading ratio.

2.4 Crystal growth

Crystal growth is the increase in size and mass of existing crystals past the critical nuclei size. Crystal growth from solutions happens by means of bulk diffusion and surface integration (Markov, 1995). Solutions are usually agitated, however if they are not, the molecules will move through convection in order to allow crystal growth. The fluid closest to the crystal particle is stationary. This is referred to as the boundary layer of the crystal.

Within the boundary layer of the crystal, growth of the crystal occurs by diffusion, where the growth material diffuses from the outer edge of the boundary layer to the crystal surface. The concentration of the growth units at the outer edge of the boundary layer is the same as that in the bulk solution, while the concentration at the crystal surface is at its lowest (Markov, 1995). The boundary layer can be reduced by agitation, speeding up the rate of mass transfer to the growing surfaces of the crystals.

Surface integration is the step whereby growth units are incorporated into the crystal structure. This is thought to be a layer by layer process (Myerson, 2002). The method of incorporation

of growth units is dependent on the level of supersaturation, with the largest and most perfect crystals formed at the lowest supersaturation.

A crystal releases heat when it grows. Similar to mass transfer, heat is also transferred through the boundary layer, from the crystal into the bulk liquid (Markov, 1995). In cooling crystallization, which is a system where solute species are crystallized from the solution, if this heat is not removed from the system, the solution will heat up until the bulk solution temperature reaches the equilibrium temperature, and crystal growth will cease. Agitation also reduces the thickness of the thermal boundary layer so that the temperature at the surface of the crystal is similar to the bulk temperature of the crystallizer. It is important to ensure a sufficient rate of heat removal from the crystallizer as well as a reduction of the thermal boundary layer, especially in an EFC, as the heat of crystallization may undermine the effects of supercooling applied on the system.

Growth rate is a function of supersaturation at the growing surface of the crystal. The linear growth rate can be related to the supersaturation through equation 2.13 (Jones, 2002):

$$G = k_g A_S S^g \qquad 2.12$$

In this equation, k_g is a growth rate constant [$m^{-1}s^{-1}$], A_s is surface area [m^2], S is the supersaturation ratio and g is an exponential factor. It is seen that both nucleation and growth rate increase with an increasing supersaturation. As a species in multiply-supersaturated system crystallizes, the supersaturation of the species decreases (therefore growth rate decreases) while the supersaturation of the non-crystallizing species increases.

2.5 Multi-component solutions

Ions in solution can have a number of interactions with each other, as well as the solvent that they are dissolved in.

2.5.1 Colligative properties

Colligative properties of a solution include vapour pressure lowering, boiling point elevation, freezing point depression and osmotic pressure. These properties depend on the entropy of the solution that contains solute particles. Mixing a solute into a solution raises the entropy of the solution. If the solid or vapour phase of the solvent do not contain elements of the solute, these phases will not have the same increased entropy. As a system prefers to remain in a state with the highest entropy, the system's preference for the liquid phase rather than the solid or vapour

phase increases as a solute is added to the solution. This explains the boiling point elevation and freezing point depression of the solution.

The change in entropy causes the chemical potential of the solvent to change as follows:

$$\mu_{\text{solvent}} = \mu^{0}_{\text{liquid}} + \text{RT}ln\text{a}_{\text{w}} \qquad 2.13$$

In the above equation, μ^0 refers to the chemical potential of the pure solvent [J/mol] and a_w is the activity of water [mol/mol total].

In a binary system with a low solids concentration, the activity of water can be approximated by using x_w which is the mole fraction of the solvent (water) [mol/mol total]. However, when impurities are added, they have a greater effect on the activity of water than they would have on the mole fraction. Therefore, the addition of more solute(s) into the solution causes a further depression in the freezing point.

In addition to the effect of the impurities on the activity of water, these impurities surround themselves with water molecules. This is called hydration. Hydration causes water molecules to be unavailable to the solution in general, and thus reducing the effective activity of water. At higher concentrations, ions in solution may start to share the bonded water molecules thus reducing their effect on the solution (Balomenos et al., 2006).

Different ions have varying hydration shells around them, with varying numbers of water molecules within these shells. Therefore, the shielding effect of these water molecules is different for different ions. For example, sodium and magnesium ions each bond to a total of 18 water molecules (Bock, 2006). However, the water molecules are arranged in three shells around the sodium ion, whereas they are arranged in two shells around magnesium. This indicates that the molecules result in a much stronger shielding effect around magnesium as they are arranged more closely together, while sodium ions reduce the strength of hydrogen bonds further away from it.

As sodium and magnesium have an equal hydration number, they are expected to have an equal effect on the freezing point depression of water for the same concentration. However, at higher concentrations, it is expected that sodium ions are more likely to share the water molecules between hydration shells as they are not so closely bonded. This increases the effective mole fraction of water. This means that magnesium would cause a higher freezing point depression than sodium at high molality concentrations.

2.5.2 Ionic interactions

There are a number of interactions that occur between dissolved ions. Ions can also interact with polar molecules or induce dipolar characteristics in non-polar molecules. When a salt is dissolved in water, the ions interact with the positive and negative heads of polar water molecules. Due to this interaction, salts generally have a higher solubility than in their free form (Mantri et al., 2017). The strength of ionic interactions depends on the charge density of the ions, as well as the properties of the solvent, including dielectric constant and temperature. Other than the intermolecular forces caused by the positive and negative charges of the ions, solubility of a species is also affected by other factors. A factor of interest in this project is the common ion effect.

According to Le Chatelier's principle, when a common ion is added to a solution, it causes the equilibrium to move away from that ion. For example, if the system started off with sodium and sulphate as shown in Equation 2.15, and magnesium sulphate were dissolved into the solution, more sodium sulphate salt would precipitate from solution.

$$2Na^+ + SO_4^{2-} \leftrightarrow Na_2SO_4 \qquad 2.14$$

2.6 Phase Diagrams

Phase diagrams are graphical representations of the equilibrium relationships between phases of various species within a system. Phases are dependent on temperature, pressure and concentration, are drawn using two of these three variables in two dimensional plots.

Because phase diagrams show equilibrium behaviour, they give an indication of how a system would behave given infinite time and infinitely fast reaction/crystallization rates.

2.6.1 Binary systems and EFC

In Eutectic Freeze Crystallization, the main interest is in the liquid and solid phases of a system, and since pressure has little effect on solid and liquid systems, the pressure is normally ignored (kept at atmospheric), while the temperature and concentration are used as the axes of the diagrams.

There are various kinds of binary systems, which include simple eutectic, compound formation, where solute and solvent combine to form one or more compounds, and solid solutions, where a phase state does not form pure components (Mullin, 2001). A simple eutectic phase diagram depicts a system of components that do not combine to form a chemical compound. This is a

typical example of the kind of system would be found in a binary EFC system, if any hydrate form of the solute is ignored. An example of a simple eutectic system is shown in Figure 2.2.

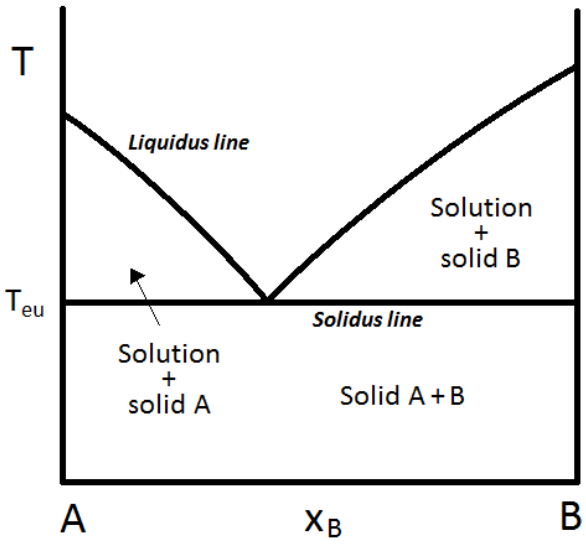

Figure 2.2: Binary phase diagram for simple eutectic system

Figure 2.2 shows that the freezing temperature of water decreases with increasing concentration of solute. In this phase diagram, if it is assumed that the solution is at a temperature above which any crystals may form, the starting point will be above the liquidus lines. The solution is said to be undersaturated. As it is cooled, it will eventually approach one of the liquidus lines if the composition is not at the eutectic point composition. Once it has reached the liquidus line, it becomes saturated. With further cooling it becomes supersaturated, resulting in the crystallization of the solute or solvent. As crystals form, the mixture will move along the liquidus line until it reaches the eutectic point, where both the solute and solvent will form crystals if cooling continues. The system remains at the eutectic point with further heat extraction until all of the liquid has crystallized, before the temperature continues to drop. If the starting composition is the eutectic composition, the mixture will form both solute and solvent crystals once the system has been cooled to below the eutectic temperature.

In industry the conventional terms of melt/freeze crystallization, solution crystallization and Eutectic Freeze Crystallization are all applicable to the diagram given above. Solution crystallization considers the case where the solute is removed from solution. In melt crystallization, ice is crystallized from the liquid. Eutectic Freeze Crystallization is a unique case where crystallization is undertaken at the eutectic point, such that both solute and solvent are crystallized at the same time, thereby combining both melt and solution crystallization.

2.6.2 Multi-component systems

In ternary systems, there are four degrees of freedom with the addition of a second solute species. It is impossible to show all of these variables on a two-dimensional graph, even if pressure is excluded for a liquid-solid system.

Ternary systems can be drawn on an equilateral triangle from where tie lines can be used to determine relative compositions. However, these diagrams show compositions of solids at a specific temperature, where equilibrium liquidus lines can be drawn, and are not useful in determining compositions at varying temperatures. Alternatively, as shown in Figure 2.3, temperature lines are shown indicating the third dimension of the liquidus surface, at which the liquid and solid interface occurs.

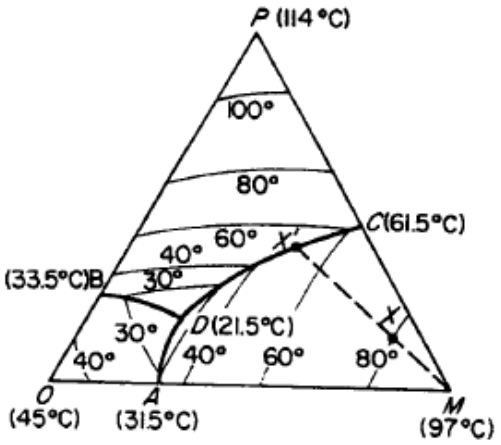

Figure 2.3: Ternary system of o-, m- and p-nitrophenol, taken from Mullin (2001)

In this figure, viewing the diagram from any of the sides (eg, the OM face) would show a typical binary phase diagram without the third species (in this case, P). As the concentration of P increases, the binary eutectic composition changes along the AD line. This is usually associated with a decrease in temperature. Point D denotes the ternary eutectic point. This diagram can also be used to determine the composition of solid and liquid phase produced upon cooling. For instance, a starting composition of X would, upon cooling, produce a solid of composition M and result in a change in liquid concentration along the MX' line. Eventually, once the liquid composition has changed to X', a solid of composition X' would be formed.

In order to show all of the parameters (all three of the component concentrations and temperature), a three-dimensional graph must be used. Such a graph helps to visualise the situation, but is not easy to work with when determining specific concentrations and temperatures. A three-dimensional graph is shown in Figure 2.4.

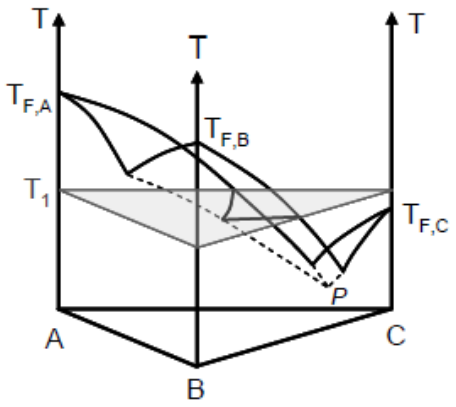

Figure 2.4: Three-dimensional image of a ternary system (Beckmann, 2013)

The above figure shows the equilateral triangle at constant temperature overlaid on the three-dimensional ternary system.

Another method of depicting the system is by showing the mole fraction of two of the components and ignoring the third. This may be useful in a mixture which includes water as the solvent. Such an example is shown in Figure 2.5. The level of dilution of the salts in the solvent is not shown, but it does affect the temperature of crystallization.

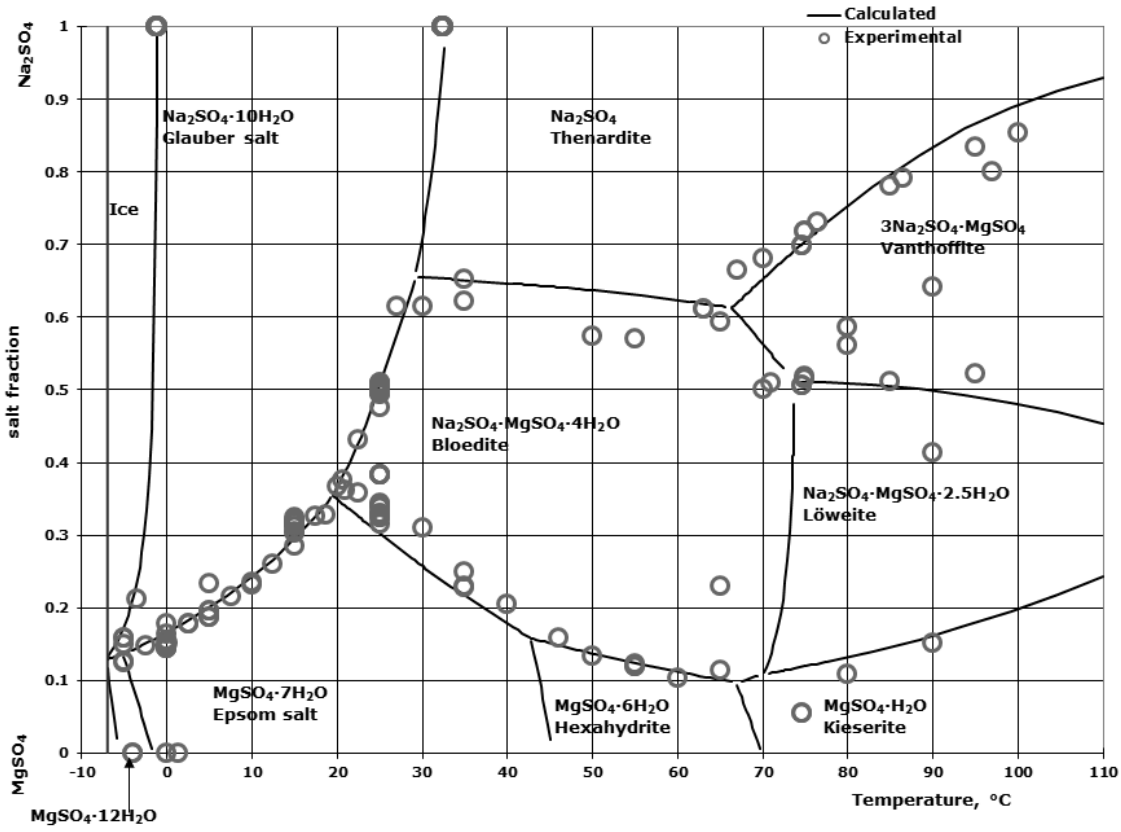

Figure 2.5: Ternary phase diagram of Na_2SO_4 - $MgSO_4$ - H_2O where mole fraction of H_2O is not shown (Thomsen, 1997)

This sub-section has only described ternary systems. However, more complicated systems do exist, and have been described for quaternary and pentenary systems in literature. With each new species, a further degree of freedom is added.

2.7 Crystal impurities

EFC is partly attractive because of its potential to produce pure crystalline products. Ice has been shown to form pure crystals through multiple studies with various impurities (Vaessen, 2003; Gartner et al., 2005; Himawan et al., 2006; Witkamp, 2008; Lewis et al., 2010). This is particularly as ice crystals differ significantly in structure to most salts. Theoretically, two salts with different crystal structures and different crystal unit sizes should also produce pure crystals purely by the nature of rigid crystal structures. However, crystals do not always form perfectly, and in some cases single ions can be substituted for foreign ions as the crystals form. Ways in which impurities can occur include liquid inclusions and isomorphous inclusions (Apsey, 2011).

2.7.1 Liquid inclusions

Liquid inclusions are chambers within crystals which contain mother liquor. There are multiple theories on why liquid inclusions occur, but the mechanism of their formation is still not fully understood. Liquid inclusions are postulated to form because of damaged crystal surfaces, macro-step generation, mechanical impacts or adhesion of fine crystals to larger crystal surfaces (Saito et al., 2001). Liquid inclusions also take place through agglomeration, where crystals join together to form groups of crystals or agglomerates, which causes mother liquor to be trapped within the mass of crystals.

2.7.2 Isomorphous inclusions

Individual impurity ions may form within a crystal by substituting out a similar ion of the crystallizing salt. Findings indicate that most impurities found in crystalline products formed in well-agitated and slow crystallization environments are as a result of isomorphous inclusions in solid solutions, rather than inclusions of mother liquor (Zhang and Grant, 1999). It is generally understood that growing crystals tend to reject foreign particles. This is because of the energy cost of crystal structure disruption (Myerson, 2002). However, because crystal formation is not a perfect process, it is possible for foreign substances to be included in the crystal lattice during crystal growth.

Impurities can be interstitial or substitutional. Interstitial impurities are more common with metals, where elements such as carbon are included in between the metals in the solid structure.

This form of impurity is less common in salt crystals due to the rigidly arranged crystalline structure of the salt, although trace impurities may be found in salts produced by EFC. Substitutional impurities need to be similar to the host ion in order to be included in the crystal lattice. Goldschmidt (1937) proposed that the key variables affecting partitioning of impurities are molecular size and charge. Two ions must have a similar charge. Also, according to the Hume-Rothery rules, the ionic radii must be within 15% of each other in terms of size in order to substitute each other in a crystal lattice, as follows:

$$\%\ \text{difference} = \left(\frac{r_{solute} - r_{solvent}}{r_{solvent}}\right) \times 100\% \leq 15\% \qquad 2.15$$

In the equation, the solvent refers to the host crystal, and r refers to ionic radius in Angstroms [°A].

As an example, the ionic radius of Mg^{2+} is 0.65°A and the ionic radius of Na^{+} is 0.95°A, as taken from Remko (1997). The % difference between them is therefore 32%, which is greater than 15%. This means that the chance of isomorphic substitutions taking place between sodium and magnesium in a crystal lattice is very low, if charge is not considered.

3 Literature Review

This section is a review of literature associated with selective crystallization in the presence of impurities and thereafter in a multi-supersaturated system. Within a multi-supersaturated system, a number of factors affect the possibility of selective crystallization. The nature of the species present is one such factor, and can include aspects such as solubility-temperature dependency, the presence of common ions, and crystallization kinetics. Another factor is seeding, which affects the initial energy barrier for nucleation of a species, thus overriding some aspects of the natural state of the species.

3.1 Crystallization in the presence of impurities

Hypersaline brines often contain multiple dissolved components depending on how the brine was generated. The interaction between these components make up systems which are thermodynamically different to binary salt-water systems. Several studies have been undertaken which found that a high purity ice and salt product can be recovered from these systems in the presence of minor impurities (Vaessen, 2003; Gartner et al., 2005; Himawan et al., 2006; Witkamp, 2008; Lewis et al., 2010). However, although it is known that a high purity product can be produced, it is also possible for impurities to occur in appreciable concentrations (Apsey, 2011). Most of these studies explored minor impurity concentrations and therefore did not consider potential hampering of movement of ions through the bulk to the growing surface, and the possibility of other salts crystallizing out, on the purity and yield of the major crystallizing salt.

Almost all of the studies listed above included washing of ice and salt products, which has been shown to greatly improve the purity of the products. The increase in purity was so sharp, that Vaessen (2003) suggested that this could mean that the impurities were due to mother liquor entrainment, and that the crystals themselves are pure. Lewis et al. (2010) and Reddy et al. (2010) both found that this was indeed the case in a system of $Na_2SO_4 \cdot 10H_2O$ and multiple impurities, with washed salts showing no trace of any of the impurities in the solution.

However, Gartner et al. (2005) used laser ablation to study the purity of $MgSO_4 \cdot 12H_2O$ crystals in the presence of various impurities such as Cl^-, Ca^{2+}, Mn^{2+} and Na^+, among others. This study found that of all the impurities, only molybdenum was detected in the salt crystals, and although the concentration was very low (estimated in the ppb range), it was evenly distributed throughout the crystal, which suggests that impurities were evenly incorporated into the crystal lattice of some crystals, possibly by substitutions of ions. Another study by Himawan and co-

workers (2006) on impurities (K, Na, Cl, Ca and Mn) in $MgSO_4 \cdot 12H_2O$ crystallization showed that impurity incorporation was low for all impurities except Mn, which was attributed to a similarity in ionic radius and charge between Mg and Mn.

A study by Apsey (2011) investigated sodium selenate and selenite incorporation into sodium sulphate decahydrate. The salts were not washed, but only filtered, which may have resulted in a higher impurity level than actually present. The selenite impurity was very low and was therefore attributed to mother liquor entrainment and not incorporations into the crystal structure. However, the selenate impurity content increased with increasing concentration of sodium selenate in solution. This also occurred when the presence of other common ion compounds (sodium chloride) was increased which indicated that selenate was incorporated into the crystal structure. The incorporation of selenate into the $Na_2SO_4 \cdot 10H_2O$ crystal structure was attributed to isomorphous substitution due to the similar structure, size and charge of the polyatomic selenate and sulphate ions. Reddy and Lewis (2009) also showed that selenate had the highest concentration level in the sodium sulphate decahydrate product, followed by HCO_3^- and chloride, respectively. This was despite chloride having the highest concentration, and selenate having the lowest concentration of these species in the brine. This study showed that various polyatomic and monoatomic ions had different affinities to forming inclusions within the salt crystallized in the system. Although washing removes mother liquor entrainment from the salt product, it may not remove impurities which are incorporated in the crystal lattice.

In terms of salt and ice nucleation temperatures, Lewis et al. (2010) and Reddy et al. (2010) found that the presence of a common ion in solution increased the nucleation temperature of the $Na_2SO_4 \cdot 10H_2O$ by changing its solubility. However, impurities caused the eutectic point, or the ice nucleation temperature, to decrease due to freezing point depression.

Several studies have been conducted on ternary systems, where the impurity was a major salt, thus with a significant concentration, interacting to a much greater degree. However, these studies included an acid compound, for example, Na_2CO_3-$NaHCO_3$-H_2O and KNO_3-HNO_3-H_2O (Vaessen, 2003; Rodriguez Pascual, 2009; Van Spronsen et al., 2010). These findings showed that it is possible to operate within the metastable zone of the acid, while only producing the desired salt compound. However, as these compounds can morph into each other depending on the pH of the system, this may introduce some effects, including improved operation of the crystallizer by pH adjustment, which may not apply to the current inorganic salt-pair study.

3.2 Crystallization in a multi-supersaturated system

There are a number of factors that affect the way species crystallize out in a system which is supersaturated with multiple species. Some of these factors are explored in this section.

3.2.1 Nature of species

3.2.1.1 Metastability

In a multi-supersaturated system, metastability determines which species will crystallize first upon cooling of the system, if it is near the eutectic point. Metastability is determined based on a change in concentration or temperature. Upon initial cooling, temperature related metastability is the determinant for which species will spontaneously form as concentration does not change. However, crystallization of ice results in the removal of the solvent which increases the concentration of the solution, while increasing its temperature. This results in an increase in the supersaturation of non-crystallizing species in terms of concentration, while reducing the supersaturation in terms of temperature. At this stage, the concentration change becomes the determinant for spontaneous nucleation in a system supersaturated with more than two species. As the solute species usually have a relatively low concentration in comparison to the solvent, a small change in concentration has a larger effect on the supersaturation of the solute than the solvent.

Many studies have been conducted on the metastability of binary systems at room temperature. $Na_2SO_4 \cdot 10H_2O$ has been found to have a Metastable Zone Width (MSZW) of 0.3K or 0.04 kmol/m^3 (defined as ΔT_{met} and ΔC_{met}) while that of $MgSO_4 \cdot 7H_2O$ was 1K or 0.043 kmol/m^3 at the same conditions (Mersmann, 2001). Genceli et al. (2005) conducted studies on accuracy of conductivity and refractive index in measuring the MSZW of a $MgSO_4$-H_2O system between 10 and -5°C, measured at a cooling rate of 4°C/hour. Although these studies did not focus on comparing metastability of the different species in the system, the diagram that was developed in the study showed that the metastability of $MgSO_4 \cdot 11H_2O$ (mistakenly labelled as $MgSO_4 \cdot 12H_2O$) was greater than that of ice in terms of temperature, although the metastability with a change in concentration alone, defined as (C*-C)/C* was very similar. Himawan et al. (2006) found that at concentrations above and below eutectic for a $MgSO_4$-H_2O system in batch, ice always crystallized first within the range of 16.5-19.5 wt.% $MgSO_4$. They also showed that the metastable zone width (ΔT_{met}) for $MgSO_4 \cdot 11H_2O$ was far greater than for ice. The ice MSZW at the eutectic was determined to be approximately 0.85°C (from a straight line calculation based on their diagram). The points for the salt MSZW were relatively spread such that an accurate number could not be estimated for the MSZW, but is likely to be approximately

double that of ice, in terms of temperature. The concentration related MSZW (ΔC_{met}) of $MgSO_4 \cdot 11H_2O$ was determined to be between 0.16 and 0.25.

Randall (2010) conducted a study on the metastability of ice and $Na_2SO_4 \cdot 10H_2O$ in a binary $Na_2SO_4 \cdot 10H_2O$-H_2O system. The MSZW of ice was found to be between 2.2 and 2.6°C, depending on the volume of crystallizer and the concentration of Na_2SO_4 used. He further found that in a hyper-eutectic system, once salt had nucleated, ice only nucleated upon reaching the MSZW. This indicated that the presence of salt crystals did not noticeably lower the energy threshold for heterogeneous nucleation of ice. The concentration-based MSZW of $Na_2SO_4 \cdot 10H_2O$ was not determined. A comparison of these two binary systems shows that the MSZW of ice differs depending on the salt present.

Deng (2012) conducted a study on numerous salt lakes. This study compared stable and pseudo-phase diagrams, developed at a very specific cooling or heating rate. He found that some phases on the pseudo-phase diagram would become smaller or disappear completely in comparison to the thermodynamic phase diagram, while others would become more prominent. This showed a reduction in metastability, or an increase in the tendency to form solid crystals for some salts, and the opposite tendency for other salts. This is because a species which has a high metastability would not easily form given some supersaturation, while other species with a low metastability would form given a very slight supersaturation. A species with low metastability would therefore feature more prominently on the pseudo-phase diagram. These findings thus indicated that kinetics play an important role in the response of the system, in addition to thermodynamics. There was no clear trend in terms of the presence of double salts or number of waters of hydration. The response of the system is therefore largely experimental and dependent on all the major species present, and cannot be predicted based on similarity of salt formulas or types.

Rousseau and O'Dell (1980) conducted selective seeding experiments in batch on a number of two-salt systems. It was observed in one system that rapid primary nucleation of both salts occurred upon reaching a slight supersaturation and therefore providing no time for seeding (KCl-KNO_3-H_2O system). It is assumed that the metastable zone widths of these salts were too low for selective salt recovery.

Rodriguez Pascual (2009) used a continuous crystallizer to conduct experiments on a ternary Na_2CO_3-$NaHCO_3$-H_2O system. In addition to studying the safe operating zone within the bicarbonate metastable zone, he also found that when sodium bicarbonate spontaneously

crystallized out from solution, it would form needle like structures in between the sodium carbonate decahydrate crystals, making it difficult to filter, and impossible to separate these crystals. See Figure 3.1 for a diagram of the mixed salt product.

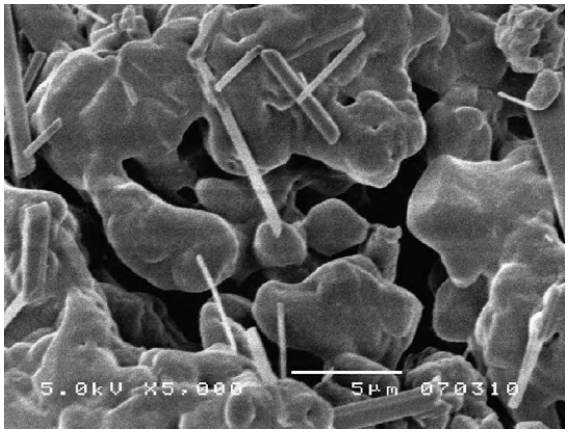

Figure 3.1: Needle-like sodium bicarbonate crystals interspersed within sodium carbonate decahydrate crystals [taken from Rodriguez Pascual, 2009]

Van Spronsen et al. (2010) further found that when trying to wash the salts in an effort to dissolve some of the needle-like sodium bicarbonate, the carbonate was more prone to re-dissolving than the bicarbonate, which means that this was not a means of purification of the salt product, in this case.

In both of these systems, sodium bicarbonate formed spontaneously. It was therefore uncontrolled and unseeded crystallization through primary heterogenous nucleation, induced by sodium carbonate decahydrate. It was furthermore widely dispersed as is the nature of spontaneous nucleation. Therefore, although it was within the expected metastable zone width for both crystals, the findings suggest that the sodium carbonate decahydrate surface reduced the energy threshold required for sodium bicarbonate crystallization, and therefore caused sodium bicarbonate to crystallize out. This system showed that the lower energy threshold for crystallization requires that the system supersaturation be significantly reduced to prevent spontaneous heterogeneous nucleation.

These studies showed that it is possible to selectively crystallize a pure salt product, provided that the system has sufficient metastability and remains at a low supersaturation, and therefore producing a low yield of product.

3.2.1.2 Growth kinetics

Growth rate information is available for binary ice-salt systems. For example, the following growth rate information has been obtained for $MgSO_4$-H_2O and Na_2SO_4-H_2O binary systems:

- Ice growth rate was found to be 9x10-9 to 5x10-8 m/s in a $MgSO_4$-H_2O system at cooling liquid temperatures between -7.6 and -11.7°C and residence time between 1.1 and 3 hours in a scraped cooled disk column crystallizer (Genceli, 2008)
- Ice growth rate was $3.9x10^{-7}$ to $4.9x10^{-7}$ m/s in a Na_2SO_4-H_2O system using a coolant temperature of -2.6°C and residence time of 30 min in a stirred glass crystallizer (Peters, 2015). It is noted that accuracy of these results was affected by agglomeration, resulting in a larger perceived growth rate.
- $MgSO_4 \cdot 11H_2O$ growth rate was $9x10^{-9}$ to $6x10^{-8}$ m/s (Genceli, 2008), and therefore similar to ice in this system
- $Na_2SO_4 \cdot 10H_2O$ growth rate was $1.5x10^{-8}$ to $1.6x10^{-8}$ m/s (Peters, 2015), thus slower than ice for this system.

These findings show that ice growth rate changes according to the system, therefore the growth rate of a species is affected by the presence of other species. The growth rate of $MgSO_4 \cdot 11H_2O$ is similar to that of ice, while $Na_2SO_4 \cdot 10H_2O$ is slower than ice, in the respective binary systems. In a ternary system, a third species may increase or decrease a salt's growth rate, as it has an effect on the supersaturation of the system and may have other interactions with the crystallizing species. See Section 3.2.4 for more detail on the effect of aqueous and solid species interactions on growth rate.

3.2.1.3 Common ion systems

The addition of a common ion into a system results in the increase in the formation of the crystallizing species due to a decreased solubility. In Apsey's work (2011) a thermodynamic study showed that a decrease in solubility was evident for both sodium selenate and sodium sulphate decahydrate for an increase in the common sodium ion, but this decrease was more pronounced for selenium. However, the actual selenium concentration in solution was much lower than its thermodynamic solubility limit. Yet, even with this low concentration, an increase in concentration of the common ion increased the rate of selenate incorporation.

In addition to a decrease in solubility, the system also experienced the presence of a salt with a similar structure to sodium selenate. Therefore, there was a kinetic effect caused by a reduction in the energy threshold of formation of the impurity, allowing it to form as a substitution into the major salt. The decrease in its solubility thus had an impact on its crystallization even though a pure sodium selenate solution would not crystallize at these concentrations. This is an indication that the presence of a similar structured salt in solution has a vast effect on the energy barrier for crystallization, and a common ion can drastically reduce the solubility of a species, assisting in its formation.

3.2.1.4 Solubility temperature dependence

In brine treatment with eutectic freeze crystallization, the removal of a first salt and ice results in the increase in concentration of the remaining salts, to the point where the system is at the ternary eutectic with a second salt. Randall et al. (2011) attempted to show the above treatment protocol through an investigation on a system which had $CaSO_4 \cdot 2H_2O$ as its first salt and $Na_2SO_4 \cdot 10H_2O$ as its second salt. This investigation was done in a batch crystallizer. According to thermodynamic modelling, the $CaSO_4 \cdot 2H_2O$-H_2O eutectic point was at about -0.5°C. However, it was not possible to crystallize $CaSO_4 \cdot 2H_2O$ in practice, with only ice being removed in the first stage. This was attributed to $CaSO_4 \cdot 2H_2O$'s very low solubility-temperature dependence, which resulted in a very low supersaturation for $CaSO_4 \cdot 2H_2O$. Slow kinetics and high metastability may also have played a role in preventing its crystallization. When the solution was left at room temperature for 24 hours, the $CaSO_4 \cdot 2H_2O$ precipitated out due to increased nucleation and growth kinetics at the higher temperature. The $Na_2SO_4 \cdot 10H_2O$ was successfully crystallized out in the last stage of the operation, as it has a significant solubility-temperature dependence. The $CaSO_4 \cdot 2H_2O$ product was obtained at 98% purity. All impurities in this product were due to mother liquor entrainment, as the salt was not washed. The purity of the $Na_2SO_4 \cdot 10H_2O$ product was 96.4%, which included some $CaSO_4 \cdot 2H_2O$ as an impurity due to co-crystallization. This study showed that both solubility-temperature dependence and crystallization kinetics are important for effective crystallization.

Randall et al. (2009) and Randall (2010) conducted several studies on multi-component brines, comparing real systems to thermodynamic models, as well as crystallizing out salts sequentially by changing operating conditions or seeding. One of the systems considered was a ternary system of $Na_2SO_4 \cdot 10H_2O$ and $MgSO_4 \cdot 7H_2O$ and water without ice crystallization, where he seeded with each of these salts and with silica sand, respectively. Experiments were conducted with a solution saturated with both salts at 14.1°C which was cooled to 12°C, causing it to become supersaturated with both salts, as both salts become less soluble when cooled. It was found that $Na_2SO_4 \cdot 10H_2O$ preferentially crystallized out regardless of the seeding material used. This is despite magnesium ions being present at a greater abundance in the solution than sodium ions. Thermodynamic modelling of this system (see Figure A1.2 in Appendix A1) shows that $MgSO_4 \cdot 7H_2O$ has a far lower solubility-temperature dependence, indicating that for a given supercooling, $Na_2SO_4 \cdot 10H_2O$ would be more supersaturated than $MgSO_4 \cdot 7H_2O$. This may explain why $Na_2SO_4 \cdot 10H_2O$ preferentially crystallized out. This study also shows that

$MgSO_4 \cdot 7H_2O$ had a high metastability, which allowed the selective recovery of $Na_2SO_4 \cdot 10H_2O$.

In the K_2CrO_7-K_2SO_4-H_2O system, which was studied by Rousseau and O'Dell (1980), K_2CrO_7 always crystallized out regardless of which salt was seeded. This study suggested that the low solubility-temperature dependence of K_2SO_4 may have resulted in its supersaturation not increasing significantly with a large change in temperature, causing K_2CrO_7 to spontaneously nucleate in each case.

The findings from these sources suggest that, for a system on a binary eutectic line, the species with the highest solubility-temperature dependence is most likely to crystallize out at a given supercooling due to a higher supersaturation. Although other factors may affect crystallization potential, such as crystallization kinetics, it is likely that these factors could be related to this thermodynamic property, and thus play a less significant role. If the difference in solubility-temperature dependence between the species is large enough, it may therefore only be possible to selectively crystallize the species with the highest supersaturation at the given conditions.

3.2.1.5 Simultaneous crystallization of organics

In industrial and pharmaceutical applications, continuous crystallizers have been used to preferentially crystallize one organic species, or enantiomer, over another. Inorganic salts have, for the most part, been formed as a pure single salt, where no second salt is supersaturated. Some studies that considered simultaneous salt formation have been discussed in this section. However, simultaneous crystallization is most common in the preferential crystallization of organics to control chirality. This is used specifically for conglomerate forming enantiomeric species. Chirality can be divided into a few sub-categories, the most common of which are the following:

- Conglomerate forming species, where each species preferentially crystallizes on its own type of crystal, therefore the resulting solid is a physical mixture of pure crystals
- Racemic compound forming species, where the crystals form in a structured 1:1 ratio of each enantiomer
- Solid solution forming species, where there is no preference, and the solid that is formed is a mixture of the two enantiomers in no specific ratio or order.

The conglomerate forming species have similarities to multicomponent inorganic salt crystal species. These include the formation of individual pure species which preferentially crystallize on its own species. Also, they both follow the same responses to supersaturation and seeding

in terms of primary and secondary nucleation and growth (Villamil Ramirez, 2016, Zhang et al., 2017). The solubility of both types of crystals increases with cooling, therefore cooling is used to form crystals in both cases. The major difference is that chiral species do not involve solvent removal in the form of ice. Therefore the supersaturation experienced by these species is far less, which makes the control of the system within the metastable zone for the prevention of primary nucleation of the unseeded species much easier. However, it may be useful to apply the learnings from studies done on organic conglomerate forming species to the crystallization of multicomponent inorganic species.

Batch crystallizers for preferential enantiomer crystallization is a well-known and well-tested method (Zhang et al., 2017). However, research and development is moving into the continuous crystallization arena as continuous crystallizers are easier to control and are preferred for large-scale applications. Continuous crystallizers which use other methods than cooling will not be discussed here. For cooling crystallizers, single stage systems make use of isothermal systems with fine temperature control to prevent the system from exceeding the metastable limit for the unseeded species (Rougeot and Hein, 2015). Enantiomers are known to have a low crystallization rate (Chaaban et al., 2013), which is why many crystallizers make use of solids recycling or continuous seeding to ensure that the crystallization rate is fast enough to produce the desired yield. The slow crystallization rate makes control of these operations simpler than for inorganic salts, which have a higher growth rate.

A relatively new development among continuous crystallizers is the coupled preferential crystallizer (see Figure 3.2), which has been modelled by Hofmann and Raisch (2013) and Qamar et al. (2013) and applied practically by a number of researchers, including Chaaban (Chaaban et al., 2013). This is a system of two crystallizers, each seeded with one of the enantiomers, and which have mother liquor exchange pipes sending the filtered solution supersaturated with the unseeded species to the other crystallizer where this species is then seeded and crystallized. Feed solution is continuously added to each crystallizer, and mother liquor is bled from both crystallizers. In this system, the concentration in each crystallizer remains constant, and the feed solution in the exchange pipe to each crystallizer is concentrated in the crystallizer's seeded species, allowing the formation of both species at a high yield and high purity. An additional advantage is that the process is robust and able to recover if counter-enantiomer crystals appear, as long as melting of fines is employed (Zhang et al., 2017).

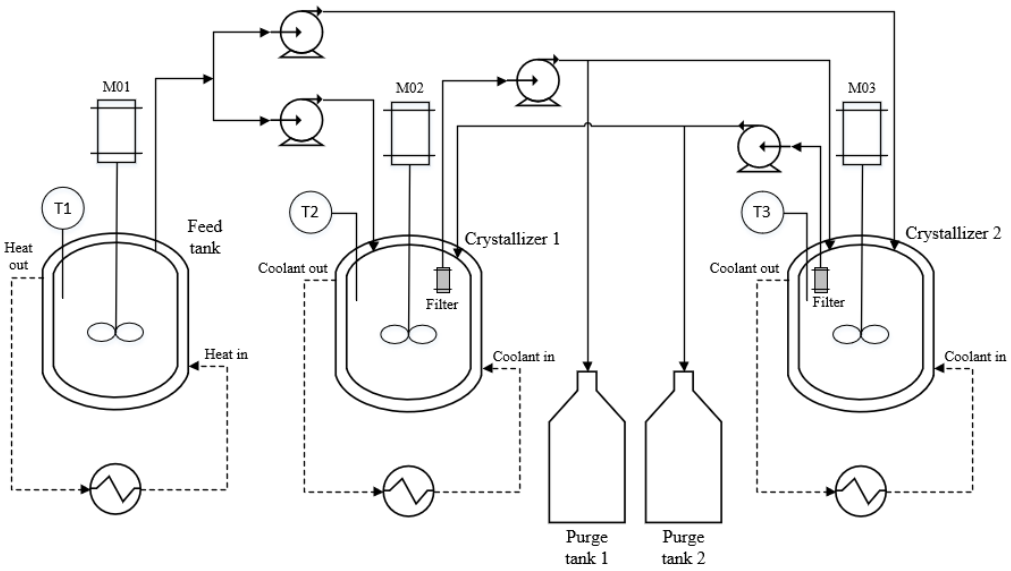

Figure 3.2: Diagram of coupled crystallizer setup (based on Chaaban et al., 2013)

The major disadvantages of this system include the memory of the solution (Mullin, 2001), meaning that even a filtered solution would result in the formation of the species which previously crystallized. This type of behaviour has been observed in crystallization applications and results in a smaller metastable zone for the system (Villamil Ramirez, 2016). Another disadvantage is that if the undesired salt spontaneously nucleates, the system quickly becomes unstable, where it is defined as a system with a mixed product. In such a situation, the process needs to be halted or restarted. A possible solution to this is the melting of fine particles modelled by Qamar et al. (2013) and Vetter et al. (2015). Primary nucleation results in the formation of a multitude of minute crystals, which can be separated from the larger size fraction and melted prior to being added to the feed to the other crystallizer. This means that primary nucleation of the unseeded species can be allowed without leading to unstable operation by allowing these crystals to grow. Vetter and co-workers' model (Vetter et al., 2015), found that even if the system was started with an impure product, or typical unstable operation, it would become stable over time if melting of fines was incorporated, without the requirement of further intervention. This type of operation is a possibility for selective recovery of crystals from a multi-supersaturated inorganic solution, with some design adjustments to allow for ice crystallization.

3.2.2 Effect of supercooling on the crystallization process

In Eutectic Freeze Crystallization, refrigerant is used to cool down the process liquid. However, the difference between the refrigerant and suspension temperatures does not necessarily point to a change in the supercooling of the actual process liquid due to multiple effects occurring

within the crystallizer. For instance, heat is released by the crystallizing species in response to cooling applied by the cooling system, resulting in a small or no change in suspension temperature. Furthermore, the heat of crystallization released is different for different species. This may result in variations in solution temperature within a single system depending on which species crystallize out. Also, a temperature difference between coolant and process liquid for different experimental setups would not cause the same process supercooling due to variations in design and insulation. Therefore, although various studies (Sadek, 1966; Margolis et al., 1971; Denton et al., 1974; Kane et al., 1975) show various outcomes of the effect of a difference between refrigerant temperature and process liquid temperature, these studies might not necessarily be comparable to each other.

Kane et al. (1975) did however find that solution supercooling affected nucleation rate of crystals to a great extent. The response of the system to supercooling was also larger at higher salt concentrations.

Vaessen (2003) measured the supercooling as the difference between the applied temperature of cooling and process liquid within the crystallizer rather than the actual process liquid supercooling. In this study, it was found that the production rate, determined by the amount of ice and salt produced, increased for both species with a decreased refrigerant temperature. Production rate for both ice and salt was observed to be proportional to the heat transfer driving force between the solution and the coolant.

Vaessen (2003) showed that heat transfer driving force has an insignificant effect on purity of crystals, as the purity of both ice and salt remained constant at different coolant temperatures. However, Van der Ham et al. (2004) proposed that at a low super cooling, and therefore slow crystal growth, impurities are incorporated less into crystals. This also causes low nucleation rates, and so ensures a larger crystal size, which makes washing easier.

Apsey similarly undertook a study to test whether a greater cooling rate increased the rate of impurity incorporation (Apsey, 2011). He specifically investigated the effect of cooling rate on purity of crystals and found that the crystal growth rate increased with an increase in the cooling rate. However, there was no clear correlation between impurities and crystal growth rate at the cooling rates tested.

Using the theory of liquid and isomorphous inclusions with the findings of Gartner et al. (2005) and his laser ablation studies, it can be concluded that isomorphous inclusions take place evenly throughout a crystal, and are not vastly affected by the heat transfer rate. However, the

possibility remains that irregularities may occur at a very high crystal growth rate, thus causing an increase in impurities. Such high crystal growth rates could not be achieved for inorganic salt crystallization in these studies.

3.2.3 Effect of nature of seeds on the crystallization process

An unseeded supersaturated system will not produce any crystals as long as it remains within the metastable zone. As seeds are introduced, they reduce the Gibbs free energy for crystal formation of all species in solution, especially those most similar to the seeds added. Species most similar to the seeds have a smaller wetting or contact angle for attachment to the seed surface, which reduces the surface energy for nucleation more than for more dissimilar species. The formation of crystals changes the concentration of the system. This may cause the supersaturation of other species in the system, and hence their Gibbs free energy, to increase above their required Gibbs free energy of crystallization, therefore causing these species to crystallize out spontaneously. The nature of the seeding material determines the crystal species which will nucleate upon seeding, as well as how the system will continue to behave until steady state is reached, as each species is likely to affect all other species present. This section only considers the seed material, rather than the size and mass of seeds.

There are several studies that have been conducted where seeding was used within a multi-supersaturated system. The most common of these studies are seeding with ice and/or salt in a binary ice-salt eutectic system. An example of this is a study on the binary $Na_2SO_4 \cdot 10H_2O$-H_2O system undertaken by Randall (2010) which found that salt seeds did not cause ice to crystallize below its metastable limit. This indicates that the ice and salt crystals were different enough that the salt did not lower the energy threshold for heterogeneous nucleation of ice. The difference in their structure may render this true vice versa, with ice seeding in the presence of a supersaturated salt.

Salts have been shown to have a significant effect on the energy threshold for heterogeneous nucleation of other salts. Rodriguez Pascual's study (2009) on a sodium carbonate, sodium bicarbonate and water system, showed that it was possible to operate the system while only producing sodium carbonate decahydrate crystals. However, the system had to be well within the metastable zone for sodium bicarbonate, as it would otherwise form spontaneously. This study shows that the presence of sodium carbonate decahydrate crystals lowered the energy threshold of formation of sodium bicarbonate.

In Rousseau and O'Dell's (1980) study, one system showed that although single crystals were of high purity, it was possible for heterogeneous nucleation and/or epitaxial "growth" to occur where the crystal of one salt grows on the surface of another salt. This occurred in the KNO_3-$NaNO_3$-H_2O system. It was unclear if the growth was due to epitaxial growth or heterogeneous crystallization of the other salt. The lattice units of the crystals have very different structures, and therefore the growth could not have been due to any form of interstitial or substitutional phenomena.

In Randall and co-workers' (2011) study on the $CaSO_4$-H_2O system, $CaSO_4 \cdot 2H_2O$ had a low solubility-temperature dependence as well as slow kinetics and high metastability, which hindered its crystallization. However, upon further solvent removal to the ternary $CaSO_4$-Na_2SO_4-H_2O eutectic point, the $Na_2SO_4 \cdot 10H_2O$ formed with a purity of 96.4 wt.%. This indicated that there was co-crystallization of both salts. The formation of $CaSO_4 \cdot 2H_2O$ at these low-temperature conditions was likely possible due to a combined concentration increase due to both ice and $Na_2SO_4 \cdot 10H_2O$ crystallization, solution supercooling, and a large presence of salt crystal surface area. Therefore, where crystallization kinetics and solubility-temperature dependence are low, crystallization of a salt cannot be discounted. Contamination of the desired salt product is still possible as the change in solution concentration and presence of salt surfaces encourage the formation of the unseeded salt.

3.2.4 Effect of seed surface area on the crystallization process

Seeding is important to ensure control of the species to be crystallized in the process. In order to produce large crystals with an even size distribution in a typical system with the formation of a single species, it is required to operate at a low supersaturation that does not allow spontaneous or primary nucleation, and therefore well within the metastable zone. At this level of supersaturation, seeding is required to initiate crystallization. In a multi-supersaturated system, it is more crucial to operate well within the metastable zone of the unseeded species to ensure the formation of a pure product of the seeded species by preventing nucleation of any unseeded species (Rodriquez Pascual, 2009).

In a seed-free environment, primary nucleation may occur, which forms numerous tiny crystals. Based on Equation 2.10, this type of nucleation is dependent on the supersaturation of the system and surface energy of the available surfaces. This indicates that, other than supersaturation, it is dependent only on the presence of particles/seeds but not on the number of particles. However, secondary nucleation and growth rates are more controlled mechanisms

of crystallization, and occur in a seeded environment. These crystallization mechanisms are necessary in a continuous process where crystals are constantly being lost to the outflows. They are both dependent on the available crystal surface area of the crystallizing salt (see Equations 2.11 and 2.13). Therefore, the secondary nucleation and growth rates are enhanced while primary nucleation is reduced, as the overall crystal surface area increases and supersaturation of the crystallizing species decreases. This means that the crystals become larger and the overall crystallization rate of the salt, given sufficient supersaturation, increases as the surface area of seeds increases. The overall crystallization rate reaches a maximum or equilibrium when the crystal growth rate is high enough to consume all available supersaturation provided in the specified residence time.

In systems with slow growth and secondary nucleation rates, especially as observed in preferential crystallization of chiral compounds, continuous seeding or in situ formation of seeds is required (Chaaban et al., 2013, Vetter et al., 2015). For example, a ball mill may be included in a recycle stream to break up the crystals. A very high stirring rate can also provide shear, inter-particle collisions and mechanical collisions which can cause crystal breakage and ensure a high crystallization rate by increasing the crystal surface area.

Seeding can be undertaken at the initiation of the process in continuous systems, therefore during the transient stages of crystallization, or it can be undertaken continuously, by adding a recycle or by in situ crystal breakage. In either case, seeding may determine which species crystallize, and by affecting the primary and secondary nucleation and growth rates of each species differently, it also determines the yield and particle size of each species that forms. The supersaturation of the species that is crystallizing at a slower rate is constantly higher, producing smaller crystals through a larger primary nucleation rate. The species with a significant presence of crystals forms mainly by secondary nucleation and growth, producing large crystals and ensuring that its substantial presence is maintained.

Seeding may further influence the length of time taken to reach steady state as it affects the rate at which the supersaturation is consumed. Between temperature, concentration and particle size distribution, it is known that particle size distribution takes the longest to stabilise (Mullin, 2001), as it tends to oscillate as nucleation and growth rate increase alternately. In some cases it may not stabilize at all. With the presence of an additional potentially crystallizing species, this may further lengthen the time required to reach stability. However, the stability of a

crystallizing system increases with an increase in growth rate and magma density, and a decrease in product withdrawal rate. It also increases with continuous seeding (Mullin, 2001).

In a typical continuous process where one supersaturated species is crystallized out, only sufficient seeds to initiate nucleation are required, as the crystals continuously nucleate and grow until the crystallization rate matches the rate of supersaturation formation. Over time, the species form an unchanging crystal size distribution at steady state which is independent of the initial seed mass and surface area. However, this is not so straightforward in a multi-supersaturated system. In this type of system, the introduction of seeds has an impact on the crystallization of multiple species.

In a non-eutectic system, a maximum yield is obtained as the system approaches equilibrium. The supersaturation decreases while surface area increases for a given coolant temperature, causing the growth rate to decrease as equilibrium is reached (Qamar et al., 2013; Zhang et al., 2017). However, in eutectic freeze crystallization, the crystallization of one species increases the supersaturation of the other species, such that supersaturation does not change significantly with residence time as two species continuously crystallize. As residence time increases, the surface area of the crystallizing species increases as they continue to crystallize with time. Therefore, crystal growth likely remains constant or potentially increases as residence time increases as the growth rate is also dependent on the available surface area or magma density. The limitation of the system is therefore defined by the desired solids density or required yield (Randall et al., 2011). Seeding surface area is therefore likely to increase the crystallization rates of the crystallizing species and therefore the yield of products obtained.

Few studies have considered seeding in continuous crystallization for inorganic salt systems. In pharmaceuticals, seeding is used within a kinetic window where a single enantiomer can be separated from its antipode (Rougeot and Hein, 2015), and is usually required in the form of continuous seeding to encourage an increased crystal growth rate. A study by Chaaban et al. (2013) investigated two different initiation seeding cases in the formation of a conglomerate forming chiral system. The study made use of a continuous coupled preferential crystallizer and found that the original experiments produced a pure product of the one enantiomer and a mixed product (92 – 100% purity) of the other enantiomer. Using the same mass of seeds but milling them to increase the surface area, resulted in an increased purity (100%) and yield (1.64 – 2.08% vs 0.88 – 1.62%) of both enantiomers. The increased surface area was therefore able to improve the selectivity of each product while also increasing the crystallization rates of the

respective enantiomers. It is therefore observed that the seed surface area, as with supersaturation, impacts nucleation and growth rates, and determines the rate of supersaturation consumption directly after seeding and the ratio of products formed over time.

The available knowledge and fundamental understanding of seeding in a multi-supersaturated continuous system suggests that an increase in seed mass, and therefore seed surface area, will increase both the crystallization and growth rate of the seeded species, thus increasing the relative crystallization rate of this salt over other species. This also increases its average particle size, with associated improved settling rate. The increased crystallization rate and average particle size will ensure that more of this species reports to the underflow. It is expected that in all cases, if the metastable limit of the unseeded salt is reached, it will spontaneously nucleate, causing the overall salt crystals within the crystallizer to be of a low purity. However, as long as these crystals are small, ice formation rate is large, and the mixing rate is also high, a significant amount of these crystals may get entrained with the ice and report to the overflow. This could result in an underflow salt product that has low levels of contamination of the unseeded species. A combination of these factors would result in an increased purity and yield of the seeded species in the underflow product. Separation and melting of fines from the final salt product may also ensure the production of a pure product.

3.3 Structure and hydration of magnesium sulphate crystals

The hydration of a salt species determines many of its properties. For example, $MgSO_4 \cdot 7H_2O$ is vastly different from $MgSO_4 \cdot 11H_2O$ in terms of both metastability and solubility-temperature dependence. It is therefore critical to ensure that the information used for the salt in question is for the correct hydrated form.

There are two schools of thought regarding the form of magnesium sulphate hydrate which crystallizes around -5°C, or at the ternary eutectic temperature of the Na_2SO_4-$MgSO_4$-H_2O system. In geology, where multiple studies have been conducted on ice core samples, it is assumed and has been shown that the meridianite ($11H_2O$) form is present. This form is well known and understood. However, in crystallization chemistry, it has long been assumed that the correct form is $12H_2O$ (see list of sources in Genceli, 2008), until recently some studies showed otherwise, which has resulted in some debate on the topic.

Himawan et al. (2006) and Genceli (2008) both undertook studies which provide information on the crystal structure of this salt. Himawan undertook research which up to that point assumed that magnesium sulphate formed as $MgSO_4 \cdot 12H_2O$ at EFC operating conditions,

which was unlike what Genceli found, who determined that it formed as $MgSO_4 \cdot 11H_2O$. Himawan used a majority magnesium sulphate solution with small percentages of impurities, while Genceli used both a pure magnesium sulphate aqueous solution and a solution containing impurities. The studies therefore overlapped in terms of the type of system investigated. The images for these two forms of salts (Figure 3.3) show some slight differences, therefore it cannot be determined by the images alone whether they are the same or if they are different salts. Both studies agreed that either of the above magnesium sulphate crystals morphed into the $MgSO_4 \cdot 7H_2O$ hydrate form once the temperature increased to close to zero. $MgSO_4 \cdot 11H_2O$ had a triclinic crystal form (Genceli, 2008), while $MgSO_4 \cdot 12H_2O$ had a relatively square form, and both disintegrated into needle-like particles once they had changed form into $MgSO_4 \cdot 7H_2O$ (Himawan et al., 2006). As the crystals formed in a structure with minimal impurities, the disintegration into needle-like particles during and after filtration did not have a major effect on the purity of the salt. The crystals are shown below.

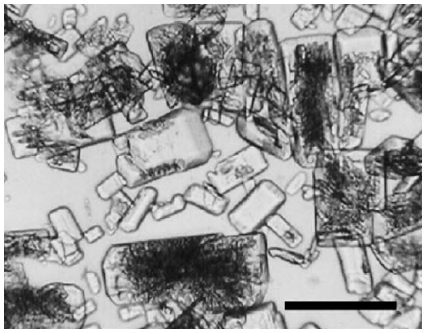

a)

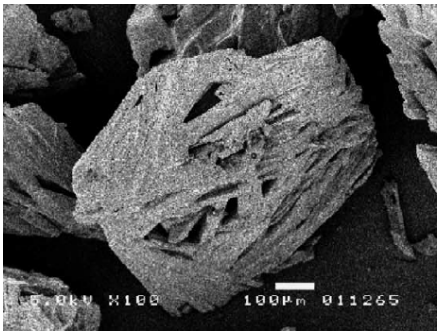

b)

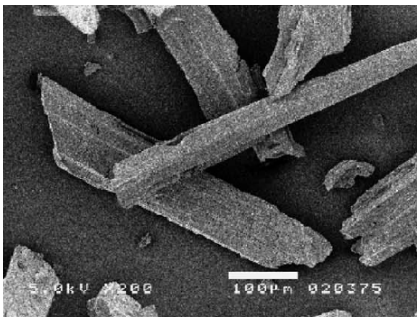

c)

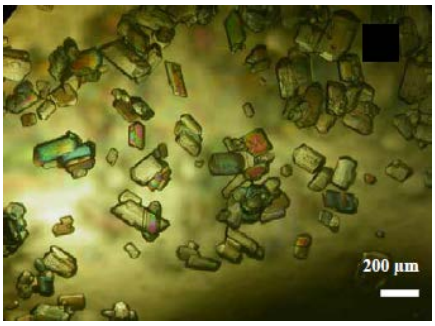

Figure 3.3: (a) $MgSO_4 \cdot 12H_2O$ (bar = 500microm); (b) pseudomorph particles after drying (bar = 500microm); (c) $MgSO_4 \cdot 7H_2O$ crystals after drying (bar = 100 microm) [taken from Himawan et al., 2006]; (d) $MgSO_4 \cdot 11H_2O$(bar = 200micron) [taken from Genceli, 2008]

In the above studies, only Genceli (2008) conducted measurements on the salt structure and tried to prove that it was indeed the $11H_2O$ form, while Himawan's study was conducted with the assumption that it was the $12H_2O$ form as it had always been understood. Furthermore, it

is noted that both studies used a very similar solution (flue gas desulfurisation solution) which suggests that the more recent study (Genceli) may be correct. It is also noted that modelling tools assume the $12H_2O$ form and do not include meridianite in any of its simulations, and therefore its results cannot be taken as conclusive as they may be outdated.

The purpose of the current study is not to determine the form of the salt that is crystallized. However, as seen in Section 4.6, analysis of the salt constituents suggest that the salt may be the $11H_2O$ form. Therefore the assumption was made that the $MgSO_4 \cdot 11H_2O$ form is crystallized as according to the study done by Genceli (2008). The actual identity of the salt, based on calculations made on the seed and salt product, will be further commented on in the results section.

3.4 Research Motivation

The majority of brines produced in South Africa are multi-component in nature. Therefore, it is expected that once sufficient solvent and major salt are removed from the system, the concentration of the solution will change such that two or more salts could eventually crystallize simultaneously at the same conditions. Due to the significant metastability of $Na_2SO_4 \cdot 10H_2O$ and $MgSO_4 \cdot 11H_2O$, which are two of the most common salts typically found in saline wastewater in South Africa, the possibility exists for selective recovery of a pure salt in a system that is supersaturated in multiple species.

Selective recovery of a pure salt in a multiple-supersaturated system can be achieved by making use of seeding (Rousseau & O'Dell, 1980; Randall et al., 2009; Rodriquez Pascual, 2009; Randall, 2010). Alternatively, insofar as a finite residence time is used, differences in crystal growth rates and crystal size can potentially be used to produce a salt with a different ionic composition to the feed stream, or allow separation of the final product through a crystal size based separation step. In this study, selective recovery by salt and ice seeding was investigated.

Numerous studies have investigated binary salt-water systems, and multi-component systems with one major salt in eutectic freeze conditions. These studies have shown that pure ice and salt crystals can be formed, as the crystallization rate in a eutectic freeze crystallization process is slow enough to allow rejection of impurities, except in the case where the impurity ion is very similar to the host ion and is thus substituted into the salt product (Apsey, 2011).

Studies have additionally been conducted on ternary salt-salt-water systems, where supersaturation is provided by cooling, but the solvent is not removed in the form of ice. These studies have shown that the potential for selective recovery of one salt is dependent on the nature of the salt pair in question. Some salts have very low metastability, and thus crystallize out regardless of the type of salt that is seeded. In other cases, a salt may have a very low solubility-temperature dependence. Therefore, with a significant reduction in suspension temperature below saturation, the supersaturation for this salt remains insignificant, such that it may not crystallize even in the presence of seeding material (Rousseau & O'Dell, 1980; Randal et al., 2011).

In this study, $MgSO_4 \cdot 11H_2O$ and $Na_2SO_4 \cdot 10H_2O$ were used as the salts of choice for investigating selective recovery of salts by seeding. As the temperature metastable zone width of $Na_2SO_4 \cdot 10H_2O$ is likely smaller than that of $MgSO_4 \cdot 11H_2O$, it is expected that $Na_2SO_4 \cdot 10H_2O$ will crystallize out at a lower supersaturation with no salt or ice seeding. The

concentration metastable zone of $MgSO_4 \cdot 11H_2O$ may be smaller than that of $Na_2SO_4 \cdot 10H_2O$, although the literature is not clear on this. The solubility-temperature dependence of $MgSO_4 \cdot 11H_2O$ is, however, higher than that of $Na_2SO_4 \cdot 10H_2O$. These two factors suggest that a change in concentration due to solvent removal through ice crystallization is more likely to cause $MgSO_4 \cdot 11H_2O$ concentration to exceed its metastable limit. Therefore, where the temperature is close to the eutectic temperature combined with a significant concentration supersaturation, thus where ice is seeded before any spontaneous salt nucleation has occurred, it is expected that $MgSO_4 \cdot 11H_2O$ would crystallize out first. This is due to a greater solubility-temperature dependence combined with a possible lower metastability in terms of concentration.

Seeding is vital for selective recovery as it allows selective crystallization of a species in a system that would otherwise be metastable. It also allows some control over the crystallization rate of the various species by providing a surface for crystal nucleation and growth. The presence of salt seeds provides a surface for heterogeneous nucleation of the dissolved salt species (Rodriquez Pascual, 2009). This is due to the reduction in wetting angle, and therefore reduction in interfacial energy required for nucleation. The wetting angle of a species with a more similar structure to the seed surface will be smaller, and therefore result in a lower supersaturation requirement for secondary nucleation. Therefore, where supersaturation is sufficient, seeding will result in the crystallization of the seeded species. However, the reduction in interfacial energy may also be significant for the non-seeded species. With the crystallization of the seeded species and ice, the concentration of the unseeded species increases due to solvent removal. This may increase the supersaturation of the unseeded species above its supersaturation requirement for nucleation, such that spontaneous nucleation occurs. The nucleation of the unseeded species may result in a reduction of the purity of the salt product. Therefore, the presence of seeds at sufficient supersaturation will result in the crystallization of the seeded species. However, if the supersaturation is too high, spontaneous nucleation of the unseeded species will also occur, resulting in a reduction of product purity.

The surface area of salt seeds also affects the crystallization rate of the seeded species (Chaaban et al., 2013). As the surface area of seeds is increased, the available growth surface is increased. This allows the seeds to grow at a faster rate by overall mass, as the supersaturation can be distributed over this large growth surface. The result of this faster rate of growth of the seeded salt species is an increase in the rate at which the crystallizing species' supersaturation is consumed, thereby increasing the supersaturation of the non-seeded species. This

supersaturation is created through solvent removal both by ice crystallization and by removal of waters of hydration as the seeded salt crystallizes. This could then potentially result in spontaneous heterogeneous nucleation of the unseeded species. However, as the seeded salt forms on the initial seed surfaces, a greater mass of seeds will increase the proportion of seeded salt in the salt product during the transient phase. This larger surface area promotes an increased secondary nucleation and growth rate, while the other species is formed mainly by primary nucleation due to a high supersaturation, and may continue to show these characteristics over time. With a finite residence time, equilibrium is not reached due to continuous heat removal that provides supersaturation, and kinetics of crystallization that are different for the different crystallizing species. At steady state, although seeds and newly formed crystals leave the crystallizer with time, the effects of an increased nucleation and growth rate are still present.

In EFC supersaturation can be increased by changing initial temperature. Therefore, an additional variable can be changed to affect the initial growth rate of the seeded salt, and that is by changing the seeding temperature. The resultant increased growth rate of the seeded salt increases the concentration of the unseeded salt. This may increase the likelihood of the second salt's supersaturation increasing above its required energy barrier for nucleation and therefore cause it to spontaneously crystallize out. In addition to this, decreasing the seeding temperature increases the temperature-related supersaturation, which would encourage $Na_2SO_4 \cdot 10H_2O$ nucleation above nucleation of $MgSO_4 \cdot 11H_2O$ based on their MSZWs (Mersmann, 2001; Himawan et al., 2006). With the combined effect of seeding temperature on initial temperature-related supersaturation, and subsequent increased supersaturation of the unseeded species, it is expected that an increase in the initial supercooling will decrease the purity of the salt product, with an increased likelihood of $Na_2SO_4 \cdot 10H_2O$ crystallizing out.

3.4.1 Hypothesis

Effect of nature of crystallizing species on purity and yield of salt product

Due to its smaller temperature-related metastable zone width, $Na_2SO_4 \cdot 10H_2O$ is more likely to spontaneously nucleate in the absence of any seeds compared to $MgSO_4 \cdot 11H_2O$. However, in the presence of ice crystals, the system experiences a low supercooling combined with a change in concentration due to solvent removal. In this case it is expected that $MgSO_4 \cdot 11H_2O$ will crystallize out first due to both its possibly lower concentration-related metastable zone width as well as its higher solubility-temperature dependence. These factors mean that $MgSO_4 \cdot 11H_2O$ is more likely to exceed its metastable limit due to a small change in temperature or concentration. It is therefore hypothesized that, given a eutectic solution, seeding with $MgSO_4 \cdot 11H_2O$ and ice will produce a higher purity salt product compared to the purity of the product produced when seeding with $Na_2SO_4 \cdot 10H_2O$ and ice. As $MgSO_4 \cdot 11H_2O$ is more likely to crystallize at the given conditions and aided by its dominance in the system due to a larger concentration, $MgSO_4 \cdot 11H_2O$ seeding is expected to produce a higher yield of product than a similar mass of $Na_2SO_4 \cdot 10H_2O$ seeds.

Effect of seeding material on purity and yield of salt product

The presence of seed material results in a reduction in wetting angle and therefore interfacial energy required for crystallization of the salt species. This required energy will be lower for the seeded species. Therefore, given a sufficient solubility-temperature dependence, and therefore sufficient supersaturation of the seeded species, the presence of seeds is expected to result in crystallization of the seeded salt. However, with a high enough solubility-temperature dependence and therefore high enough supersaturation or the unseeded species, this species could also potentially crystallize out due to spontaneous heterogeneous nucleation on the seed material. This occurrence is more likely with $MgSO_4 \cdot 11H_2O$ due to its greater solubility-temperature dependence. Therefore, it is hypothesized that the presence of seeds will result in the crystallization of the seeded material but may also result in a reduction of product purity due to crystallization of the unseeded salt, with an increased likelihood of impurity formation when seeding with $Na_2SO_4 \cdot 10H_2O$.

Effect of seed surface area on product purity and yield

An increase in the seed surface area will increase the crystallization rate of the seeded salt. This will increase both the yield and proportion of seeded salt in the salt product, while also increasing the concentration of the unseeded salt in the solution. This may result in the spontaneous nucleation of the unseeded salt due to the presence of lower energy surfaces for nucleation and an increased supersaturation with time. Therefore, it is hypothesized that an increase in the seed surface area will increase the yield of the seeded salt product and the potential for crystallization of the unseeded salt. However, as the surface area of the seeded salt increases, it also increases the secondary nucleation and growth of this species, which may also increase the proportion of seeded salt in the system at steady state. Therefore, it may be possible to produce both a high yield and high purity product with a large seed surface area.

Effect of seeding temperature on product purity and yield

A decrease in the seeding temperature increases the initial supersaturation for all species. As $Na_2SO_4 \cdot 10H_2O$ has a smaller temperature-related MSZW of the two salt species, a lower seeding temperature could encourage spontaneous nucleation of $Na_2SO_4 \cdot 10H_2O$. However, in the absence of any spontaneous nucleation, the increase in initial supersaturation, as with seed surface area, will cause the yield of seeded salt in the product to increase. As the yield, or surface area, of the seeded salt increases, the growth and nucleation rate of this salt will increase in turn, allowing this trend to continue to steady state. However, this increased yield will cause an increase in supersaturation of the unseeded salt, which will also increase the likelihood of spontaneous nucleation of the unseeded salt.

3.4.2 Key Questions

Effect of nature of crystallizing species on yield and purity

I. Which salt forms first via spontaneous nucleation when only ice is seeded?
II. How does the yield and purity compare for the salts in the absence of salt seeding?

Effect of seeding material on yield and purity

I. How does the yield and purity compare for different salt seeds?

Effect of seed surface area on product purity and yield

I. At what seed masses does the crystallization of the undesired salt negatively impact the purity?
II. What is the effect of seed mass on the yield and purity of salt product obtained?

Effect of seeding temperature on product purity and yield

I. How does seeding temperature affect product yield?
II. How does seeding temperature affect product purity?

4 Materials and Methods

This study aimed to determine the effect of seeding on purity and yield of salt product from the ternary $MgSO_4$-Na_2SO_4-H_2O system. The investigation is split into two sections, ie. thermodynamic modelling and laboratory experiments. The modelling aimed to determine the eutectic composition and temperature of the system on which the experiments could be based.

4.1 Thermodynamic modelling

Thermodynamic modelling was done on OLI Stream Analyser 9.5 thermodynamic modelling tool. The model made use of the Helgeson-Kirkham-Flowers (HKF) equation of state to determine the saturation temperatures of the various species. The modelling work determined that the eutectic composition of the system was 16.55 wt.% magnesium sulphate and 2.74 wt.% sodium sulphate at a temperature of -5.13°C.

4.2 Experimental setup and reagents

Synthetic aqueous solutions of 2.74 wt.% sodium sulphate and 16.55 wt.% magnesium sulphate were prepared using analytical grade sodium sulphate decahydrate ($Na_2SO_4 \cdot 10H_2O$), pharmaceutical grade magnesium sulphate heptahydrate ($MgSO_4 \cdot 7H_2O$) and ultrapure water.

The experiments were conducted in a scraped and stirred jacketed and insulated 2 ℓ glass crystallizer. The experimental setup is shown in Figure 4.1 below.

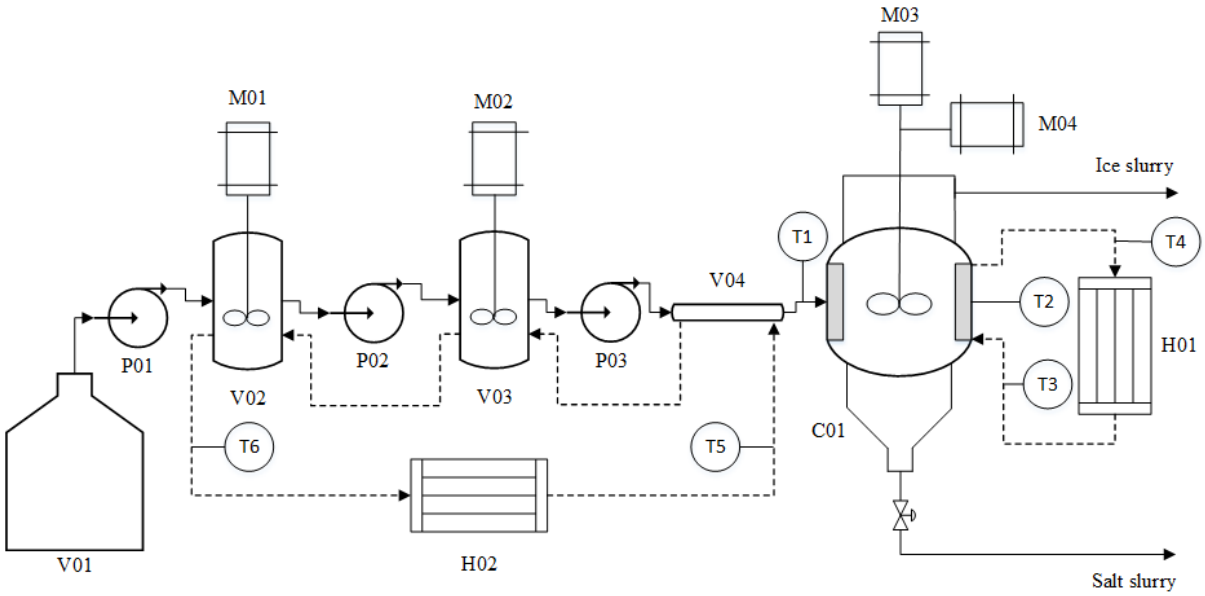

Figure 4.1: Experimental setup, showing vessels (V01-V04), crystallizer (C01), stirrers (M01-M04), peristaltic pumps (P01-P03) and chillers (H01 and H02)

A stirred 50 ℓ drum (V01) was used as combined feed storage and warming vessel, ensuring that the reconstituted brine from the crystallizer outflows were melted, and further ensured a constant feed temperature and concentration to the first pre-cooler. Watson Marlow peristaltic pumps were used to transfer process liquid between each vessel. The pre-cooling system consisted of 3 pre-cooler vessels and a Lauda Proline chiller model RP855. The cooling liquid used was Kryo 51. The first two vessels were 2 ℓ jacketed glass vessels stirred using overhead variable speed stirrers, followed by a glass double pipe. This combination allowed the feed temperature to be reduced to a minimum temperature of approximately -3.6°C, using a coolant temperature set-point of -6.45°C, without scaling. All pre-cooling vessels and piping were insulated with a layer of heavy-duty foil and neoprene rubber. The active volume of the crystallizer was 2ℓ while the overflow and underflow stilling sections added up to 1 ℓ total volume. The underflow rate was controlled using a ball valve to limit blockages. The crystallizer was cooled by a separate chiller, namely a Thermo Scientific A40 model, using Kryo 40 as the cooling liquid. The inner crystallizer walls were scraped using high density polyethylene (HDPE) scrapers, held in place by cadmium coated steel springs. The variable speed stirrer was located in the centre of the active volume of the crystallizer and rotated in the opposite direction to the scrapers to improve mixing. The scraper speed was set to 62.5 rpm and stirrer speed was set to 800 rpm. The temperature measurements at all points were taken by PT100 temperature probes, connected to an F252 precision thermometer setup with a 16 channel SB 500 multi-port. This system had an accuracy of ±0.01°C. Online recording was accomplished through ASL ULog software.

All of the experiments were conducted at 30 minutes' residence time with a supercooling of approximately 6°C (coolant temperature of -11°C) with a resultant operating temperature between -5.0°C and -5.1°C depending on the feed solution. Four batches of feed solution were used, and it was found that a slight change in feed composition resulted in a significant difference in operating temperature, hence coolant temperature was chosen as the control to maintain a similar operational supersaturation.

A syringe fitted with a 0.2 μm membrane filter was employed for drawing samples of the residual mother liquor from the crystallizer for the first steady state experiments. For all other experiments, underflow and overflow samples were used to determine purity and yield of the salt and ice products, as well as the mother liquor composition. Due to the high number of dilutions required, and therefore error introduced, in using typical Atomic Absorption Spectroscopy (AAS) or Inductively Coupled Plasma – Optical Emission Spectroscopy (ICP-

OES), a complexometric titration method with EDTA was used to measure magnesium ions and $BaSO_4$ volumetric titration was used to measure sulphate, from which sodium was calculated by subtraction. It is noted that samples from the initial steady state experiments were measured using AAS, for magnesium and sodium ions, prior to the development of the titration techniques.

4.3 Seed preparation

This study aimed to investigate the effect of seed surface area on the purity and yield of the salt product. There are two methods of changing the seed surface area. The first is by grinding the seeds in order to change the particle side and thereby changing the surface area. The second is by changing the mass of seeds but keeping the average particle size constant. If the crystals are too small, they would get entrained out of the system with the overflow, and may also cause difficulties with sample collection and filtration. Therefore, it was decided to use a difference in seed mass to change the seed surface area. The variation in the seed size was deemed to be relatively constant across various experimental runs as the same method of seed generation or procurement was used for all seeds.

$Na_2SO_4 \cdot 10H_2O$ seeds were taken directly from the reagents which were also used to prepare the feed solution. The was no special preparation of ice seeds. $MgSO_4 \cdot 11H_2O$ seeds were produced in a batch crystallizer using a hyper-eutectic binary solution of magnesium sulphate and water with a composition of approximately 23 wt.% $MgSO_4$, which was prepared using pharmaceutical grade magnesium sulphate heptahydrate ($MgSO_4 \cdot 7H_2O$) and ultrapure water. The jacketed batch crystallizer was operated in a temperature-controlled room at temperatures between -1 and -3°C to ensure that the crystals obtained would not change into heptahydrate crystals, which is the most stable form above approximately 4-5°C. The solution was seeded at -1°C and a residence time of 30 min was provided for crystal growth, while the solution temperature continued to drop to approximately -2.5°C. The hydrated magnesium sulphate salt was filtered out using filter paper with 22µm pore size to ensure that the average particle size of the filtered salt would be large enough to reduce melting between storage in the freezer and seeding the crystallizer in the room temperature laboratory, and also to ensure that the particle size would be relatively similar to that of the $Na_2SO_4 \cdot 10H_2O$ seeds. The batch process had to be conducted three times to produce sufficient seed material for all of the experiments. The batch time and coolant temperature were kept constant for each of these experiments to ensure a similar particle size distribution of the seed material could be obtained.

Multiple photographs of seed crystals from each salt were acquired on a microscope before the seeds could melt or change form (in the case of $MgSO_4 \cdot 11H_2O$). 200 individual crystals were counted for each salt, and the areas of the crystals were used to calculate their equivalent sizes. The resulting particle size distributions are shown in Figure 4.2 below.

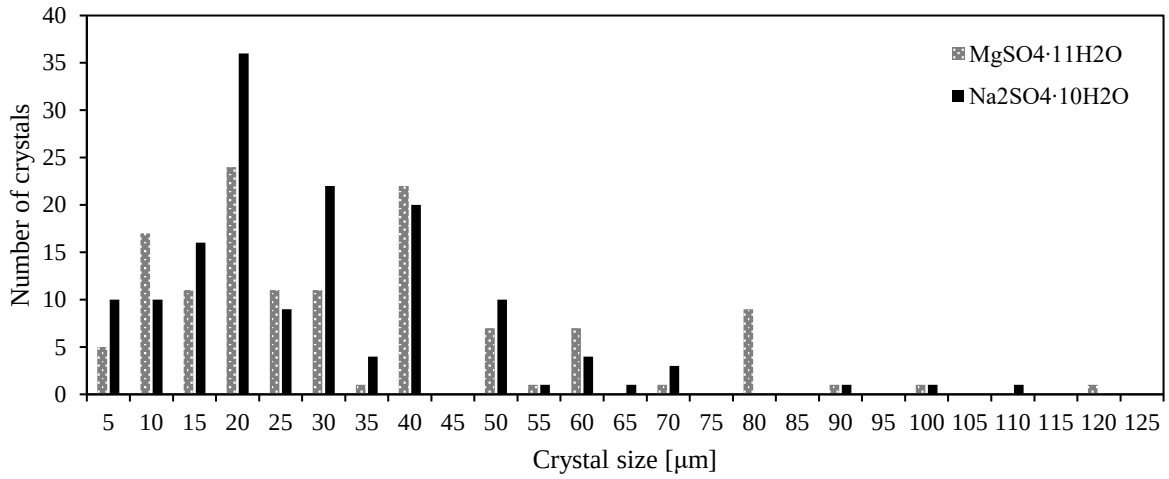

Figure 4.2: Particle size distribution of seed material

The particle size distribution of the two seeding materials were comparable. The median and mean particle sizes of the $MgSO_4 \cdot 11H_2O$ seeds were 30 µm and 37 µm, respectively. The median and mean particle sizes of the $Na_2SO_4 \cdot 10H_2O$ seeds were 25 µm and 29 µm, respectively.

4.4 Experimental design

The experiments were conducted according to Table 4.1. According to the design, all experiments were to be done in triplicate. Two seed materials were used, namely $Na_2SO_4 \cdot 10H_2O$ and $MgSO_4 \cdot 11H_2O$. For each seed material, experiments were conducted at three different seed masses for one seed temperature (-5.3°C), and three different seed temperatures for one seed mass (10x the critical seed mass). The highest temperature was chosen for the seed mass experiments as this provided the best control and reduced the potential for spontaneous nucleation prior to seeding. The largest seed mass was chosen for the seed temperature experiments as this mass maximised the potential for the crystallization of the seeded material. In all experiments, salt was seeded first, and ice was seeded 2 min after salt seeding at a solution temperature of -5.3°C, 4 min after salt seeding at -5.6°C and directly after seeding at -5.9°C. The timing of ice seeding for the -5.3°C and -5.6°C experiments was chosen based on the change in temperature that was observed after salt seeding, as the temperature drop was steeper at higher temperatures. This was done to ensure that the temperature drop

after salt seeding was similar for these cases. However, for the -5.9°C case, ice seeding had to be done immediately as ice nucleation occurred spontaneously immediately after or during salt seeding at this temperature. In all cases, 0.3 g of ice was used as ice seeds.

Table 4.1:Seeding conditions for all experiments

Aim	**$Na_2SO_4 \cdot 10H_2O$ seed mass [g]**	**$MgSO_4 \cdot 11H_2O$ seed mass [g]**	**Solution temperature at seeding [°C]**
Investigate the effect of nature of crystallizing species on purity and yield	0	0	-5.3
Investigate the effect of seed material on purity and yield	0.04	0	-5.3
	0	0.08	
Investigate the effect of seed surface area on purity and yield	0	0.08	-5.3
		3	
		30	
	0.04	0	
	0.25		
	2.5		
Investigate the effect of seeding temperature on purity and yield	2.5	0	-5.3
			-5.6
			-5.9
	0	30	-5.3
			-5.6
			-5.9

The critical seed mass was determined using the method provided in Lewis et al. (2015), where the critical seed loading ratio was estimated from a graph once the seed particle sizes were known. This ratio could then be used to calculate the critical mass of seeds which fulfil this ratio, as follows:

$$C_s^* = m_{seed}^*/\Delta m \qquad 4.1$$

In this equation, C^*_s is the critical seed loading ratio, m^*_{seed} is the critical seed mass and Δm is the mass of solids formed in the process. This Δm was assumed as the maximum theoretical

yield of each of the salts, respectively. The critical seed masses were determined to be 3 g for $MgSO_4 \cdot 11H_2O$ and 0.25 g for $Na_2SO_4 \cdot 10H_2O$. This method is designed for a batch process as no continuous process seed design could be obtained. Using an instantaneous moment in time with negligible inflow and outflow rates, and with excellent mixing characteristics, the initial seeding process can be estimated to be similar to a batch process.

From these numbers, the seed masses for each run were chosen as shown in Table 4.2.

Table 4.2: Determination of seed masses for seed variation experiments

Seeding case	**Description**
Case 1	No salt seeds
Case 2	Just enough seeding material to initiate crystallization
Case 3	Critical seed mass
Case 4	10x the critical seed mass

4.5 Experimental procedure

4.5.1 Start up

The full setup was located in a laboratory at room temperature. The first step in the start up of the process was the mixing of the solution for a few minutes to ensure that there was no stratification in the storage drum. The pre-coolers and crystallizer were filled with solution using peristaltic pumps, whereafter the chillers were switched on to initiate cooling. Since the double pipe cooled the solution very quickly, the startup was done in continuous mode to prevent scale formation in the double pipe. The pre-cooler chiller was set to -6.45°C, at which it remained for the duration of the run. The crystallizer chiller was set to -8.5°C for initial cooling to ensure that the crystallizer temperature did not drop too quickly, as it would make exact control of seeding difficult. At these chiller set points, the pre-cooling section cooled down far more efficiently than the crystallizer, ensuring that the feed temperature was already at the desired set point for some time before the crystallizer was cooled to the selected seeding temperature. The overflow rate from the crystallizer was measured, with the underflow valve in closed position, once the crystallizer temperature was near the steady state operating temperature, to ensure that the feed solution pumping rate was correct.

The seed material was weighed, covered and placed in the freezer in preparation for seeding while the experimental setup was still cooling down. This seed material was introduced into the crystallizer immediately as the required seeding temperature was reached. The salt seeds

were introduced first, and the required waiting time provided, as explained in the Experimental Design section, before ice seeding. Immediate and abundant ice nucleation was observed as ice was seeded. Due to this, and a limitation on the amount of seeds that could be added at one time in the seeding port, a change in mass of ice seeds was not included in the experimental plan as it would not be possible to investigate this with the experimental setup used, and it was expected to have a limited effect on ice and salt crystallization. In contrast, salt seeding did not result in an immediate change in temperature, thus allowing multiple additions of salt seeds to be introduced prior to any major response in the system. As soon as the temperature jump associated with heat of formation of ice was observed, the crystallizer chiller temperature was reduced to -11°C, which was kept constant for the remainder of the experiment. This temperature was chosen as it provided a steady state operating temperature which was low enough to be within the metastable zone of all species according to predictions from Version 9.5 of OLI Stream Analyser, while also producing a significant yield of solids.

The scrapers and selected operating conditions ensured that scaling did not occur in the crystallizer, as an ice scale layer would have an-effect on the operating temperature and often cause damage to the scrapers. However, there was some accumulation of ice agglomerates between the scrapers, which left the crystallizer in clumps. Therefore, there was some accumulation during the transient phase, but the average mass of ice and salt entrapped in the ice became constant with time. Although this was a limitation of the experimental setup, it was not expected to have significant effects on the results. It was not possible to determine the mass of accumulated material as it was not physically attached to the crystallizer internals, and therefore left the crystallizer when it was emptied.

4.5.2 Steady state operation

All of the operating conditions, such as pumping rate and coolant set points, were kept constant throughout the experiment once the seeding process was successfully completed. The feed temperature into the crystallizer was approximately -3.48 – 3.59°C. The salt product slurry was harvested from the bottom of the crystallizer using a valve for flow control, and the ice product overflowed from the top of the crystallizer. These streams were combined and directed into the 50 ℓ vessel which fed the process, to close the cycle. The process was allowed to operate for 12 τ for initial steady state experiments and for 10 τ for the remaining experiments once it had been determined that this was long enough for mother liquor concentration-related steady state to be reached. In the steady state experiments, it has been calculated that sampling was conducted before and after all seeds were washed out of the system. During the remaining

experiments, sampling was only undertaken after 99.995% of the seeds were washed out of the system. See the Appendix B1 for the calculations.

Although 10 τ was found to be approximately double of the operating time required to reach steady state in terms of concentration, it is noted that solids flow and particle size distribution were not measured. Therefore, the possibility exists that steady state in terms of particle size distribution may not have been reached. However, the recovery of filtered salt in the underflow and overflow was relatively constant towards the end of each run, which suggests that changes in particle size distribution were no longer likely to be significant.

It is further noted that the steady state operating temperatures of all the experiments were above the modelled eutectic temperature, which was -5.14°C according to OLI Stream Analyser Version 9.5 and -6°C according to Version 9.6. All laboratory experiments indicate that all species were able to crystallize simultaneously at the operating conditions, suggesting that all species were supersaturated. By this reasoning, it can be surmised that the modelled eutectic temperatures of both versions are inaccurate. This inaccuracy causes temperature-based supersaturation calculations to be impossible, as they would find that the system is under saturated, as at temperatures between -5.01 and -5.10°C all species crystallized.

Experiments were randomised to ensure that different feed batches were used for each seed type, mass and temperature. Effects by varying feed composition are reflected in the error bars.

4.5.3 Sampling

For the steady state experiments, a syringe filter, fitted to a syringe and tube was used to extract mother liquor directly from the crystallizer into sampling containers. Three samples were taken every 2 residence times starting from 4 τ until 12 τ. Although the only available opening was from the top, which could result in a slightly dilute sample as some ice is expected to melt in this region, the differences in concentrations between the samples was sufficient to determine if concentration-based steady state had been reached.

In all further experiments, samples were only taken after 10 τ. The temperature of the temperature-controlled room was set to -6°C a few hours before sampling time, to allow the room to cool down. Samples were not taken until or unless the refrigerated laboratory temperature was at least -3.5°C or lower, to prevent salt and ice from melting during the sampling and analysis process. This may have added up to 2 τ to the total experimental time. It is noted that the temperature-controlled room undergoes de-frost cycles in which the room is automatically heated up to prevent ice build-up in the cooling system. In some experiments,

the de-frost cycle started halfway through sampling, in which case, sampling was completed as quickly as possible before the room temperature became very high. Simultaneous sampling of the underflow and overflow was conducted, using a vacuum flask and doubly-insulated cylinder, respectively, for three 2-minutes intervals. These samples were transferred immediately to the temperature-controlled room to be filtered. Unwashed ice, salt and their respective filtrates were individually weighed and stored in sampling containers. Hereafter, a further sample of the underflow was collected by opening the underflow valve to obtain a significant volume with minimal melting time, which was filtered and washed, and collected for the purpose of measuring the salt purity. It is noted that a limitation of the process was that no similar significant instantaneous sample volume could be obtained from the overflow, therefore the overflow salt purity is affected by some melting. All sampling related equipment was kept in the temperature-controlled room at all times, to ensure that it was cold at the time of sampling.

In the washing of the salts, acetone was used. This was chosen because it is a liquid at the sampling temperatures (between 0 and -6°C), salt does not dissolve in it, and it is not soluble in water. The assumption was that the acetone would wash off any mother liquor on the salt particles, and the moisture associated with the filtered salt would be replaced by acetone. The analysis results showed that there was some addition of mass to the solid product, which was not magnesium, sodium or sulphate. However, the variation in purity was seen to be reduced by the washing process, as it is caused by variations in filtering efficiency across the sample, and would therefore be improved as mother liquor was washed off. Furthermore, the addition of mass to the salt as a result of phase change of water or acetone, or variation in moisture associated with these liquids, was unlikely to affect the structure and composition of the salt product itself. Therefore, it was determined that the analysis of the washed salt product was a more accurate measure of salt purity than that taken from the unwashed salt product. However, the waters of hydration calculation and the total mass of salt measurement required the use of the unwashed salt.

4.6 Analysis of magnesium sulphate hydration

The magnesium ion concentration was determined by complexometric titration with EDTA with an accuracy of ±0.1%. Sulphate was measured by barium sulphate volumetric titration with an accuracy of ±0.5%. The sodium ion and water amounts were calculated by subtraction. The accuracy of the sodium concentration was determined by propagation of errors method to be ±2.6%.

As the total mass of salt product and concentration of magnesium and sulphate were measured, it was possible to calculate the sodium concentration by the method of difference using the molar ratio of magnesium to sulphate in the salt. Thereafter, knowing the waters of hydration of sodium sulphate decahydrate, the remaining waters were assumed to be bonded to the magnesium sulphate salt. Due to analytical error and variations in filtration efficiency, it was not expected for the hydration calculation results to be exact, and the range was large. However, out of 32 experiments, the 10^{th} and 90^{th} percentile values for all of the unwashed salt products was 10.83 and 11.96, with an average of 11.31 and a median value of 11.14. The average waters of hydration for 3 samples of the generated seed material was 11.2. These calculations suggest that the magnesium sulphate product formed at these temperatures, in a binary $MgSO_4$-H_2O system and a ternary $MgSO_4$-Na_2SO_4-H_2O system, could in fact be $MgSO_4 \cdot 11H_2O$.

5 Results and Discussion

This section presents the results of both the thermodynamic modelling and the experimental work done to determine the effect of seeds on salt product purity and yield.

5.1 Modelling

In order to determine the ternary eutectic temperature and concentrations, the Na_2SO_4-$MgSO_4$-H_2O system was modelled theoretically using version 9.5 of OLI Stream Analyser, which is a thermodynamic modelling tool. The results shown in Figure 5.1 were obtained for an aqueous feed solution containing 2.74 wt.% Na_2SO_4 and 16.55 wt.% $MgSO_4$ with a basis of 1000 g of solution.

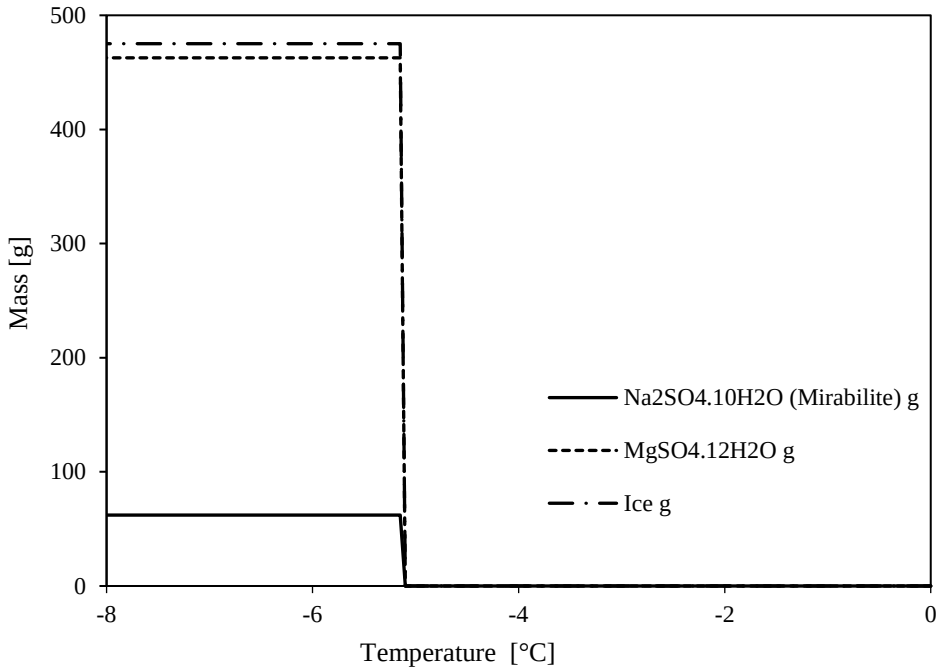

Figure 5.1:OLI modelling results showing eutectic temperature of the ternary system

It is noted that the modelling tool assumed that the $MgSO_4$ form is $12H_2O$ as shown in the figure, but this salt has been shown to most likely be the $11H_2O$ form. As shown in Figure 5.1, simultaneous crystallization of $MgSO_4 \cdot 11H_2O$, $Na_2SO_4 \cdot 10H_2O$ and ice occurs at a temperature of -5.14^oC if this solution is cooled. This is the ternary eutectic temperature of the system. The solution used in this study was at the eutectic concentration and thermodynamically all the three species were expected to crystallize at -5.14^oC. Figure 5.1 shows that eutectic crystallization of such a feed solution results in a theoretical mass of $MgSO_4 \cdot 11H_2O$ similar to the mass of ice produced while that of $Na_2SO_4 \cdot 10H_2O$ is far less. The waters of crystallization become part of the hydrated salt structure and are therefore subtracted from the potential mass

of ice that could be formed. Therefore, the ice produced would be far less than the amount of water (80 wt.%) in the initial solution.

The total mass of each species shown in Figure 5.1 is the maximum yield of each species, which may not be possible in a single stage, single-pass continuous crystallizer. Furthermore, the crystallization rates of the components and other factors such as residence time and operating temperature determine the actual yields achievable during the crystallization process. Figure A1.1 in Appendix A1 shows an example of a system with a salt feed concentration higher than eutectic, in this case specifically higher in $MgSO_4 \cdot 11H_2O$. In this theoretical system, salt(s) and/or ice form to bring the system towards the eutectic concentration, at which point all three species crystallize out until all species are in solid form or all supersaturation has been consumed and the system is at equilibrium.

The thermodynamic model suggests that all species crystallize out simultaneously. However, the kinetics of each species is unique. Each of the species crystallizes at different supersaturations, growth and nucleation rates, and are further affected by the masses of other species in solution, which is further linked to whether a common ion is shared with the other species. All of these factors can be used to encourage the crystallization of one species over another, or to affect the particle sizes such that the species report differently to the underflow and overflow.

In the following sections it is stated that magnesium sulphate **hendecahydrate** is crystallized out as one of the potential salts in the product, as has been shown in Section 4.6 through analyses of the salt product obtained in the experiments and also of the seeding material. It was not the purpose of this study to investigate the crystal structure of the salt. However, this assumption has a negligible effect on the yield and purity of the magnesium sulphate hydrate salt product, and no effect on the trends obtained.

Of importance in this study, is the model version used to determine the eutectic composition, as well as the accuracy of the modelling information. During this study, a new version of OLI Stream Analyser was released (version 9.6) which showed slightly different concentrations and temperatures for the phase lines of the ternary system compared to the previous version. A ternary diagram was drawn from these models, showing a comparison of the two OLI versions at the relevant concentrations, and is shown below in Figure 5.2.

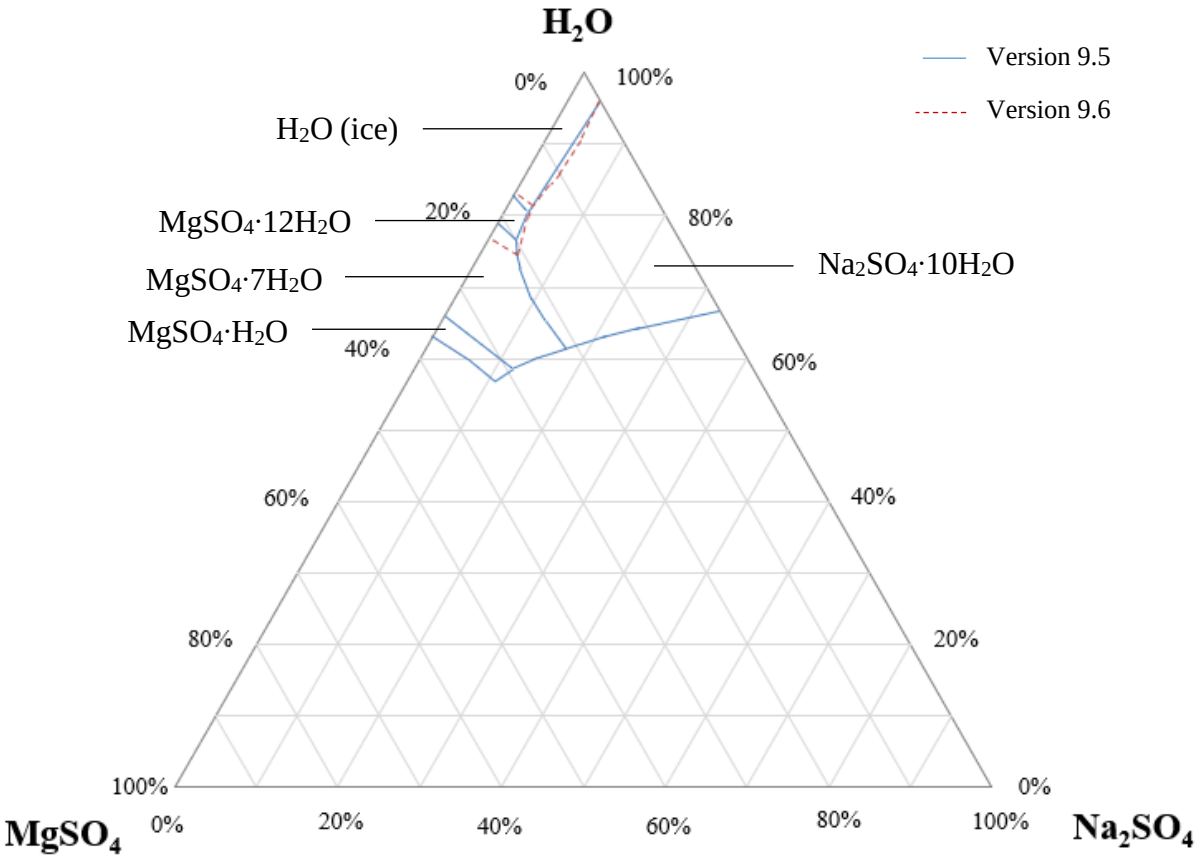

Figure 5.2: Ternary diagram comparing OLI Stream Analyser model versions

The ternary diagram was drawn for the low temperature region only, and is limited to the temperatures and concentrations that follow a proportional solubility-temperature relationship. In this diagram, the two models appear very similar, where the major difference is a change in the eutectic point composition towards the water side of the diagram. In other words, if the feed solutions were exactly on the eutectic point according to version 9.5, they would now be more concentrated than the eutectic in terms of both salt species, according to version 9.6. The eutectic temperature according to version 9.6 is also significantly lower (-6°C). It is further noted that the model was designed for use in high temperature applications and the data would thus be inaccurate at low temperatures. Both versions are therefore just estimates and could be relatively different from experimental or practical reality. These inaccuracies make supersaturation calculations impractical, as the experimental system shows signs of supersaturation when the model predicts undersaturation.

5.2 Experimental results

5.2.1 Typical experimental run

In all the conducted experiments, it was assumed that a residence time of 10 τ was sufficient to attain steady state conditions. This was based on findings of preliminary experiments which

measured the mother liquor concentrations in the crystallizer over time using a solution at the ternary eutectic composition.

Figure 5.3 below shows an example of a typical temperature-time plot of an experiment. A -5.9°C seeding temperature run was chosen as an example as the initial temperature jump after seeding was significant in this run and was not as clearly observed on temperature profile graphs of other experiments. Besides the magnitude of the initial temperature jump, all other aspects of the temperature profile was almost identical in all other experiments.

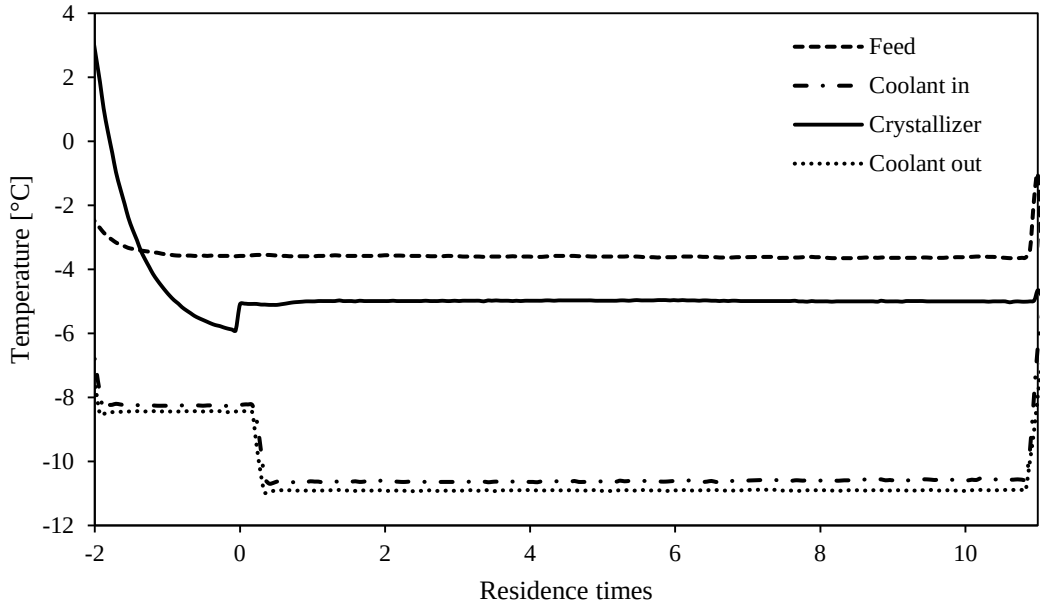

Figure 5.3: Temperature profile of typical experimental run at 30min residence time and -5.9°C seeding temperature, with 30g $MgSO_4 \cdot 11H_2O$

The time at which seeding was conducted is shown as zero on the residence times axis. This is associated with an initial sharp increase in suspension temperature caused by the release of heat of crystallization. It is noted that the coolant temperature was -8.5°C at the point of seeding. This was to ensure that the cooling rate of the crystallizer contents was not too rapid, allowing finer control of seeding temperature. After the initial temperature jump had been observed, the coolant temperature was dropped to -11°C and was maintained at this value for the remainder of the experiment. This ensured a higher temperature difference for heat transfer to produce a potentially high yield of ice and salt.

The initial temperature increase which occurred directly after seeding was very sharp, and was therefore associated with ice formation as it is the solvent and has fast crystallization kinetics (Lewis et al., 2010). However, because salt had also been seeded, salt may also have been crystallizing but its rate may have been slow enough to be hidden by the more obvious effects

of ice crystallization on temperature. When enough initial supersaturation had been consumed and sufficient ice crystal surface area had been formed to increase the crystal growth rate to balance the heat removal rate, the suspension temperature stopped climbing. Once this had happened, the temperature started to drop over time. The drop in temperature and change in concentration due to solvent crystallization increased the supersaturation of other species, until a more gradual temperature jump was observed at approximately 0.5 τ. This temperature jump was associated with salt crystallization. Since salt was seeded upfront, this was unlikely to be the first presence of salt in the system. Therefore, it is expected that the temperature increase was caused by the occurrence of a second nucleation event. Although it is not clear what caused this event, it is possible that spontaneous nucleation of the unseeded salt occurred, which then increased the supersaturation of both the seeded salt and ice, resulting in a greater crystallization rate of all species than before. This greater crystallization rate would then result in an increased release of heat of crystallization, hence the increased suspension temperature. These crystallization rates eventually eased off to new, constant crystallization rates as concentration-related steady state was reached by approximately 5 τ.

Figure 5.4 below shows a magnified view of the ternary diagram close to the ternary eutectic point. This diagram shows the feed and mother liquor concentrations of the various experiments. Similar concentrations were combined into single points, to make the spread more visible. The mother liquor concentrations were determined by filtration of the underflow and overflow products, respectively. The ternary diagram shows the OLI Stream Analyser version 9.5 equilibrium lines as a solid blue line and version 9.6 equilibrium lines as a red dotted line.

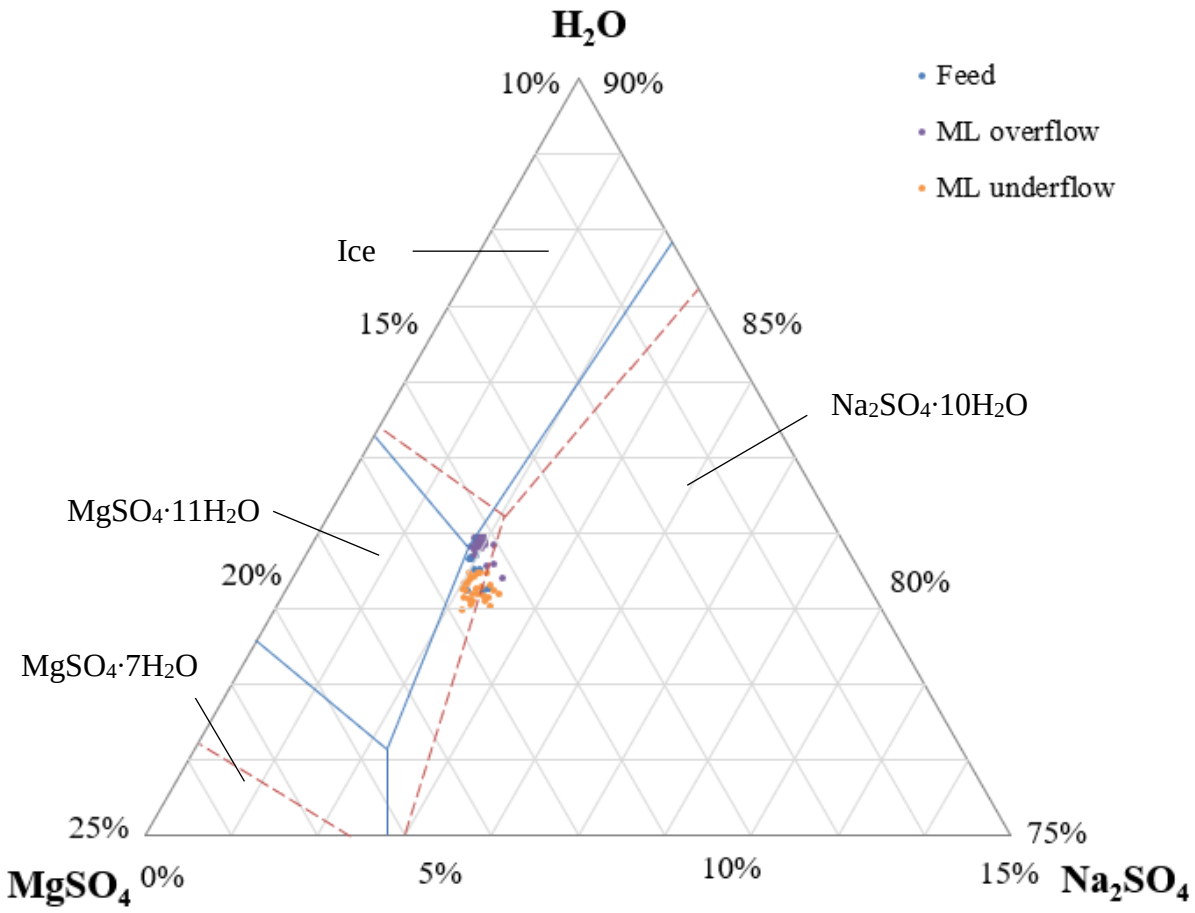

Figure 5.4: Ternary diagram showing concentrations of feed and mother liquor obtained from overflow and underflow filtrate.

On the ternary diagram it can be seen that the feed concentrations were very similar, and were all slightly off but close to both the original eutectic and the updated model's eutectic point. The mother liquor concentration from the underflow was slightly more concentrated in terms of both salts, while the mother liquor concentration from the overflow was dilute.

It has been seen from literature (Rousseau & O'Dell, 1980; Rodriguez Pascal, 2009, Randall, 2010; among others) that if the feed solution is close to a eutectic, the metastability of the species plays an important role, as the less metastable species always crystallizes out first regardless of the concentration. In this ternary diagram, according to OLI Stream Analyser version 9.5, sodium sulphate decahydrate would be more likely to crystallize out as the solution was more concentrated in this salt. On the other hand, according to version 9.6, ice would not form until some of the salts crystallized out allowing the solution to become more diluted. However, the experiments found that ice always crystallized immediately upon seeding, which was comparable to the findings of Himawan et al. (2006). Magnesium sulphate hendecahydrate (meridianite) was always the majority salt in the salt product above the thermodynamic expectation, and sodium sulphate decahydrate almost always crystallized as well. This

indicates that the feed solution was very close to the real eutectic and within the metastable zone of all three species.

The residual mother liquor results can be used to determine the amount of salt and/or ice melting that took place during the sampling and filtration process in the refrigerated laboratory space. This means that the actual mother liquor concentration would be in between these two concentrations, therefore very similar to the feed concentration. This indicates that either not much ice or salt was crystallizing out, or that all of the three species were crystallizing out resulting in a small change in mother liquor concentration. It is also noted that ice melting is more significant than salt dissolution in a practical laboratory setting, which could indicate that the mother liquor was in fact slightly more concentrated than the feed solution. This is further substantiated by a larger yield of ice obtained as a percentage of the feed than that of the salts combined in all cases.

5.2.2 Seeding with sodium sulphate decahydrate

Experiments were conducted to determine the effect of seeding on salt yield and purity. This section provides results of the experiments in which sodium sulphate decahydrate and ice were seeded.

In Figure 5.5 below, the change in yield of the salt product is shown for various seed masses of sodium sulphate decahydrate. The seeds were added to the 2 ℓ crystallizer initially in a single dose.

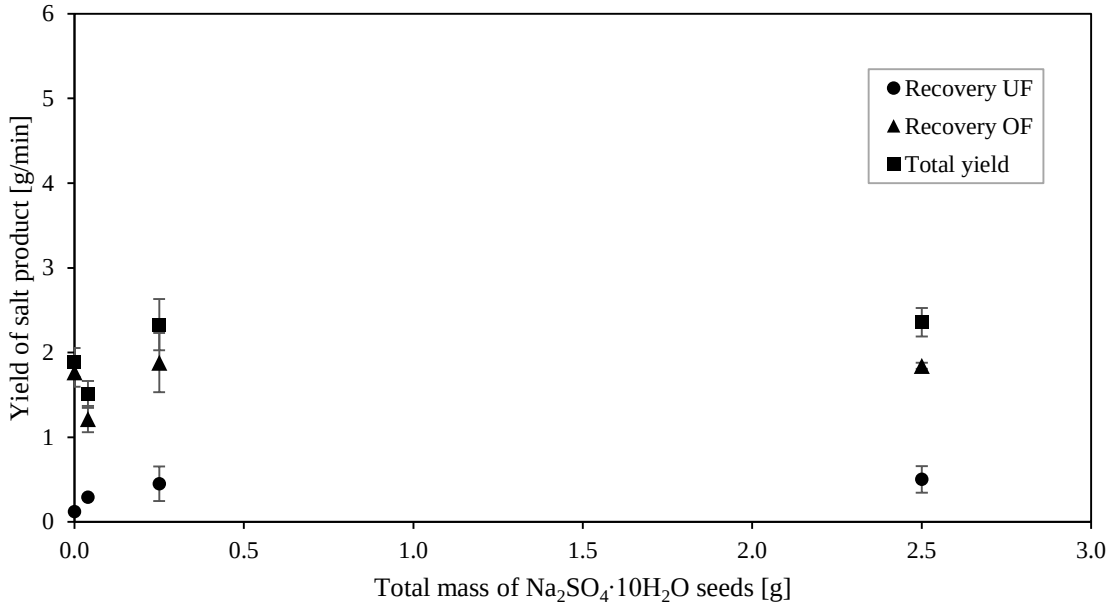

Figure 5.5: Recovery of salt in overflow (OF), underflow (UF) and yield with $Na_2SO_4 \cdot 10H_2O$ seeding at constant temperature.

This graph shows that the recovery of the salt product, both in the underflow and in the overflow, increased with an increase in the mass of salt seeds, and plateaued below 0.25 g of seeds. Furthermore, the overflow had a higher recovery than the underflow.

The difference in the underflow and overflow recovery indicates that most of the salt reported to the overflow due to small particle sizes, hence entrainment occurred with the ice. This could be attributed to a relatively large supersaturation in the system caused by solvent removal which may have encouraged a high nucleation rate, as expected according to the primary nucleation equation (Equation 2.10). Additionally, large scraper and stirrer speeds were used in the crystallizer to prevent scale formation, thus resulting in large mixing rates. These mixing rates provided little opportunity for salt settling and produced high shear and impact forces which resulted in particle breakage, thus producing small particle sizes. The increase in underflow salt recovery with an increase in seed mass indicates that the seeds encouraged crystal growth, which resulted in a greater mass of larger crystals which were able to settle to the underflow. This is as expected according to the growth rate equation (Equation 2.13).

A drop in yield of salt product was observed between the no salt seeding case, and the crystallization initiation case (0.04 g of seeds) which was observed in all experiments and was also observed when seeding with $MgSO_4 \cdot 11H_2O$. This trend was, furthermore, also visible in the total yield (see Figure A1.7 and Figure A1.8 in Appendix A1). This suggests that this trend is reproducible for different seeding materials. It is not clear why this occurred, as the heat

removed in each case was similar, and therefore the supersaturation affecting the kinetics could only be due to a difference in the seeding mass and seeding material. A potential explanation may be the high level of supersaturation achieved in the no salt seeding case, such that when spontaneous nucleation occurred, a large number of crystals were formed. This large presence of crystals may have had a similar effect as seeding with a larger mass of crystals, therefore resulting in a significant surface area for crystal growth. However, when a very small mass of seeds (0.04 g) was introduced at low supersaturations, the available surface area for crystal growth was very low.

The purity and yield of salt in an experimental run are interlinked as they are both dependent on the crystallization mechanisms occurring in the crystallizer. For instance, a higher crystallization rate of one salt increases the supersaturation of the other salt, which may encourage spontaneous nucleation of this salt, but may also hinder its growth rate. Therefore, knowledge of the yield of salt product is insufficient information to understand the interactions between the salts and their individual crystallization mechanisms. It is therefore necessary to consider the purity of the salt product, shown in Figure 5.6 below, for a better understanding of these mechanisms.

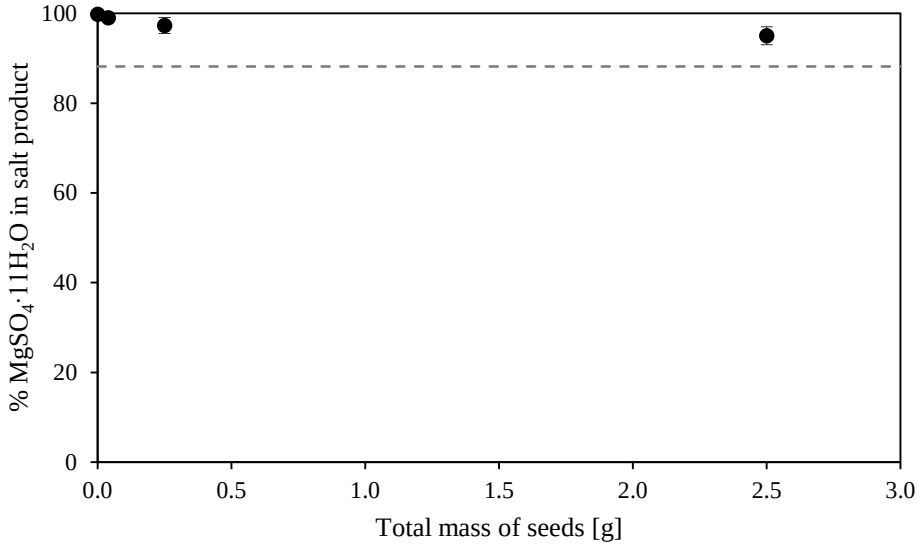

Figure 5.6: Purity of underflow salt product with $Na_2SO_4 \cdot 10H_2O$ seeding at constant seeding temperature

The dotted line in Figure 5.6 shows the purity of the salts if they formed according to their thermodynamic ratios. This graph shows that the purity of the salt was higher than the thermodynamic ratio for all experiments. Therefore, the content of $MgSO_4 \cdot 11H_2O$ in the salt product was very high, in contrast to the salt that had been seeded ($Na_2SO_4 \cdot 10H_2O$). The content of $MgSO_4 \cdot 11H_2O$ in the overflow product was also above the thermodynamic ratio (see

Figure A1.3 in Appendix A1) and total salt purity ranged between 92.9 and 99.3% for these runs. A further observation from Figure A1.3, is that the percentage of $Na_2SO_4 \cdot 10H_2O$ in the underflow was lower than that in the overflow for lower seed masses, but there was a cross over as the seed mass increased from 0.25 g to 2.5 g, where the percentage of $Na_2SO_4 \cdot 10H_2O$ was highest in the underflow.

These findings suggest that the $Na_2SO_4 \cdot 10H_2O$ crystal sizes increased with an increase in seed mass, allowing more of this salt to settle to the underflow. Furthermore, a slight decrease in purity was observed as the mass of seeds was increased. This could also be seen as an increase of the proportion of $Na_2SO_4 \cdot 10H_2O$ as the mass of this salt's seeds was increased. These results can be compared to findings by Chaaban et al. (2013), who observed that an increase in seed surface area increased both the yield and proportion of seeded species in the product.

In order to determine if the increase in the recovery in the underflow salt split ratio was caused just by an increase in sodium sulphate decahydrate (as seen by a decrease in the purity of the salt) or if magnesium sulphate hendecahydrate also increased, a stacked graph was plotted (see Figure 5.7), which shows the masses of each salt species that were formed in the process.

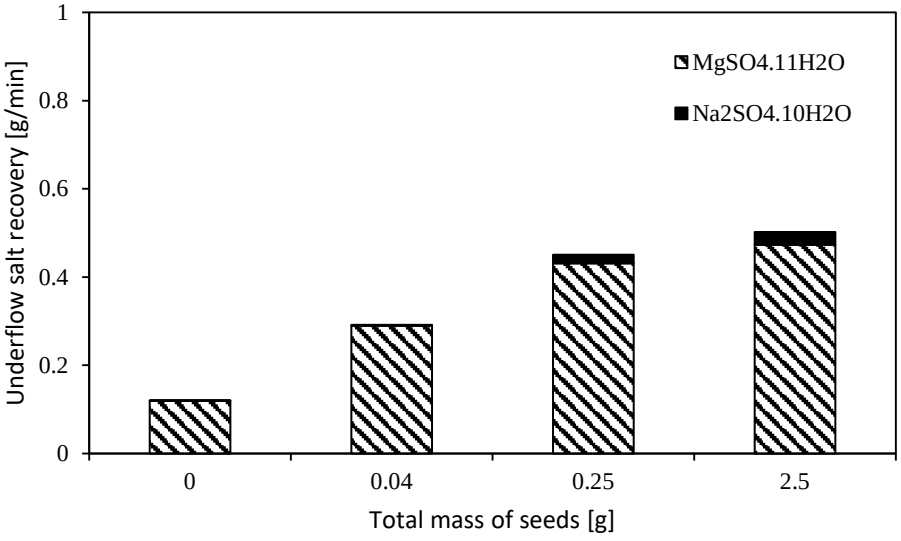

Figure 5.7: Underflow salt recovery as a function of $Na_2SO_4 \cdot 10H_2O$ seed mass

This graph shows that the recovery of $MgSO_4 \cdot 11H_2O$ increased significantly with the introduction of a small mass of seeds compared to seeding with ice only. This occurred without a change in the mass of $Na_2SO_4 \cdot 10H_2O$ formed. However, a further increase in seed mass increased the recovery of both $Na_2SO_4 \cdot 10H_2O$ and $MgSO_4 \cdot 11H_2O$.

The change in underflow salt recovery and purity was different for each seeding case. This suggests that, insofar as concentration and salt recovery are concerned, multiple steady states were possible in a $MgSO_4$-Na_2SO_4-$10H_2O$ ternary eutectic system, where the final state was determined by the method of seeding, as all other conditions were kept constant. This compares to the study by Chaaban et al. (2013), where different seed surface areas resulted in a difference in salt product purity and yield, therefore multiple steady states were observed due to seed engineering. An alternative reasoning for the difference in purity and yield for each seeding case could be that steady state had not been reached. However, the total salt yield for each case was observed to remain relatively constant, which suggests that the maximum yield had been obtained for the given heat transfer driving force, and the system had therefore reached steady state in terms of concentration, yield and solids flow.

In Figure 5.7 it can be observed that in all cases, $MgSO_4 \cdot 11H_2O$ formed and became the dominant salt product, above the thermodynamic ratio. This means that it was the salt that required the smallest supersaturation to form as well as having faster overall crystallization kinetics.

There are several potential explanations why $MgSO_4 \cdot 11H_2O$ would form first with no salt seeding. The first is that the feed solution used in the experiments could have been slightly concentrated in $MgSO_4 \cdot 11H_2O$ compared to the eutectic point, which would explain why it crystallized out first. However, the ternary diagram (Figure 5.4) shows that for either model version, the feed solution was not concentrated with $MgSO_4 \cdot 11H_2O$ any more than $Na_2SO_4 \cdot 10H_2O$. Furthermore, both salts formed in this study, therefore the system was metastable for both salts, at least by the time steady state was reached, therefore the feed solution was close to the ternary eutectic composition.

A second explanation is that $MgSO_4 \cdot 11H_2O$ was the majority salt in the solution, therefore, once it had crossed the energy barrier for initial nucleation, it would form far more crystals than $Na_2SO_4 \cdot 10H_2O$. This would result in greater overall secondary nucleation and growth rates, assuming kinetic nucleation and growth constants which would otherwise be within the same order of magnitude. Even if $Na_2SO_4 \cdot 10H_2O$ had slightly faster initial nucleation and growth kinetics, it would quickly reach a point where all its supersaturation would be consumed, from which point $MgSO_4 \cdot 11H_2O$ would continue to form and eventually overtake the $Na_2SO_4 \cdot 10H_2O$ in total crystal mass and surface area. Therefore, it could be possible that regardless of the initial kinetics, a larger crystal mass and surface area of one salt could ensure

a larger secondary nucleation and growth rate (in mass per time), both of which are related to crystal surface area. This would cause the minority salt to gradually get washed out of the system as its secondary nucleation and growth rate become insufficient to keep up with the rate of salt removal from the system. Over time, the supersaturation for this salt would increase, and it would start to form by primary heterogeneous nucleation rather than secondary nucleation and growth, as the surface area of the crystals would be insufficient to consume its supersaturation. However, this second explanation does not support the findings that an increase in seed mass of the minority salt increases the yield of this salt and its overall particle size. This is because this explanation assumes that the minority salt will always end up crystallizing mainly by primary heterogeneous nucleation and that there is no possibility for multiple steady states. This reasoning therefore indicates that final yields of products are not necessarily related to the relative concentrations of each crystallizing resource within a eutectic system.

The only remaining possibility is the relation of the solubility of the salt to temperature. In the current study, $MgSO_4 \cdot 11H_2O$ has a higher solubility-temperature dependence than $Na_2SO_4 \cdot 10H_2O$ near eutectic conditions, and by this reasoning it would seem to fit with findings from other studies. In Randall et al.'s (2009) study using a ternary Na_2SO_4-$MgSO_4$-H_2O system on the binary eutectic of $Na_2SO_4 \cdot 10H_2O$ and $MgSO_4 \cdot 7H_2O$ at 14.1°C, he found that $Na_2SO_4 \cdot 10H_2O$ consistently crystallized out as the majority salt regardless of the seeding material. In this system, the solubility-temperature dependence of $Na_2SO_4 \cdot 10H_2O$ was higher than that of $MgSO_4 \cdot 7H_2O$ (see Figure A1.2 in Appendix A1). Similarly, in his later study investigating the consecutive crystallization of ice, $CaSO_4 \cdot 2H_2O$ and $Na_2SO_4 \cdot 10H_2O$, it was found that $CaSO_4 \cdot 2H_2O$ would not crystallize in EFC conditions but only crystallized at room temperature after ice removal in an EFC crystallizer (Randall et al., 2011). In this case, $CaSO_4 \cdot 2H_2O$ has a very weak solubility-temperature relationship thus causing its supersaturation to be very low even with a large change in temperature below its saturation point. Its kinetics of crystallization are also very low at low temperatures. Rousseau and O'Dell (1980) observed a similar phenomenon using a solution of K_2CrO_7-K_2SO_4-H_2O saturated at 25°C, where K_2CrO_7 always crystallized out regardless of seeding material due to K_2SO_4's very low solubility-temperature dependence. However, solubility-temperature dependence is purely thermodynamic and does not necessarily explain kinetic effects, especially at a ternary eutectic at which all species experience a similar supercooling, and initial concentration supersaturation prior to crystallization of any species is negligible. The response of the system

therefore combines metastability and solubility-temperature characteristics of the crystallizing salts. This is in agreement with the hypothesis that states that $MgSO_4 \cdot 11H_2O$ is more likely to crystallize out as well as forming a larger yield of salt than $Na_2SO_4 \cdot H_2O$.

The increase in the yield from no salt seeds to 0.04g salt seeds indicates that the presence of $Na_2SO_4 \cdot 10H_2O$ provided a lower energy surface which allowed heterogeneous nucleation of $MgSO_4 \cdot 11H_2O$ to occur, as according to the equation for heterogeneous nucleation (Equation 2.10) and as observed by Rodriguez Pascal (2009). This likely occurred early in the experiment, before all the supersaturation had been consumed by the ice, which was seeded in all experiments. This then allowed the $MgSO_4 \cdot 11H_2O$ to crystallize into a significant mass of crystals over time until steady state was reached.

When no salt seeds were added, $MgSO_4 \cdot 11H_2O$ still crystallized out but only once the supersaturation of the system due to solvent removal through ice crystallization had increased enough to allow primary nucleation of this salt. The required supersaturation for nucleation of $MgSO_4 \cdot 11H_2O$ was higher in the presence of ice crystals than $Na_2SO_4 \cdot 10H_2O$ crystals as it was more dissimilar to ice in structure. This means a longer time period was required for this supersaturation to grow, in which time ice was continuously crystallizing. By this point, a significant mass of ice was present with larger rates of secondary nucleation and growth encouraged by its large crystal surface area. By the time $MgSO_4 \cdot 11H_2O$ spontaneously nucleated, it crystallized predominantly by primary nucleation, with limited opportunity for secondary nucleation and growth. Although the large surface area produced by this primary nucleation resulted in a large total yield of salt, the underflow recovery was very low due to a small average particle size. This means that a larger recovery of $MgSO_4 \cdot 11H_2O$ underflow salt product can be obtained in the presence of a small mass of $Na_2SO_4 \cdot 10H_2O$ seeds compared to when no salt seeds are added.

The underflow salt recovery of $MgSO_4 \cdot 11H_2O$ continued to increase with an increase in $Na_2SO_4 \cdot 10H_2O$ seed mass above 0.04g of seeds. The equation for primary heterogeneous nucleation only includes the effect of surface properties of the seed material on Gibbs free energy required for nucleation. This means that an increase in surface area is unlikely to affect this energy requirement. However, an increase in the available nucleation sites may have increased the probability and extent of nucleation which may have led to the increase in the overall crystallization rate.

The absence of $Na_2SO_4 \cdot 10H_2O$ in the underflow salt product in the 0.04 g seeding case could be explained by an initial difference in supersaturation for each of the salt species. The supersaturation for $Na_2SO_4 \cdot 10H_2O$ may not have been high enough to cause significant $Na_2SO_4 \cdot 10H_2O$ crystallization at the time of seeding. As spontaneous heterogeneous nucleation of $MgSO_4 \cdot 11H_2O$ occurred, the higher initial supersaturation for $MgSO_4 \cdot 11H_2O$ crystallization caused by its larger solubility-temperature dependence, resulted in a far greater degree of $MgSO_4 \cdot 11H_2O$ crystallization. This salt crystallization, along with ice crystallization, resulted in a large presence and surface area of these crystals, which allowed them to consume all of the available cooling. This resulted in an initial rise in temperature such that there was very little opportunity for initial $Na_2SO_4 \cdot 10H_2O$ secondary nucleation and growth. With continued $MgSO_4 \cdot 11H_2O$ and ice crystallization, the $Na_2SO_4 \cdot 10H_2O$ supersaturation increased thus resulting in crystallization predominantly through primary nucleation with limited potential for growth. This would cause $Na_2SO_4 \cdot 10H_2O$ crystals to remain in miniscule amounts, and also ensured that very little of this salt was able to settle to the underflow product.

Figure A1.3 in Appendix A1 shows that the mass of $Na_2SO_4 \cdot 10H_2O$ was significant in the overflow whenever $Na_2SO_4 \cdot 10H_2O$ was seeded. This indicates that it was crystallizing within the crystallizer. This leads to the question of the particle size distribution of the salts. If the purity of the underflow and overflow were significantly different, it indicates that the salt species were crystallizing with different particle size distributions. Therefore, one salt formed by secondary nucleation and growth, producing larger crystals, while the other salt formed mainly by primary heterogeneous nucleation, producing small salt crystals. This suggests that $Na_2SO_4 \cdot 10H_2O$ formed mainly by primary nucleation when insufficient seeding material was provided, while $MgSO_4 \cdot 11H_2O$, as long as some salt seed material was provided, consistently formed some large crystals which reported to the underflow. This also means that the supersaturation for $MgSO_4 \cdot 11H_2O$ formation was not as high as for $Na_2SO_4 \cdot 10H_2O$ once crystallization had been initiated, allowing the crystals to grow and not just form small nuclei.

A mass of 2.5 g of $Na_2SO_4 \cdot 10H_2O$ was used to seed at various seeding temperatures. This mass was chosen as it produced the highest supersaturation for the unseeded salt, and a decrease in seeding temperature would further increase this supersaturation. These results would therefore show the greatest effect of initial supersaturation on yield and purity of the salt product. The results of these experiments are shown in Figure 5.7 and Figure 5.9 below.

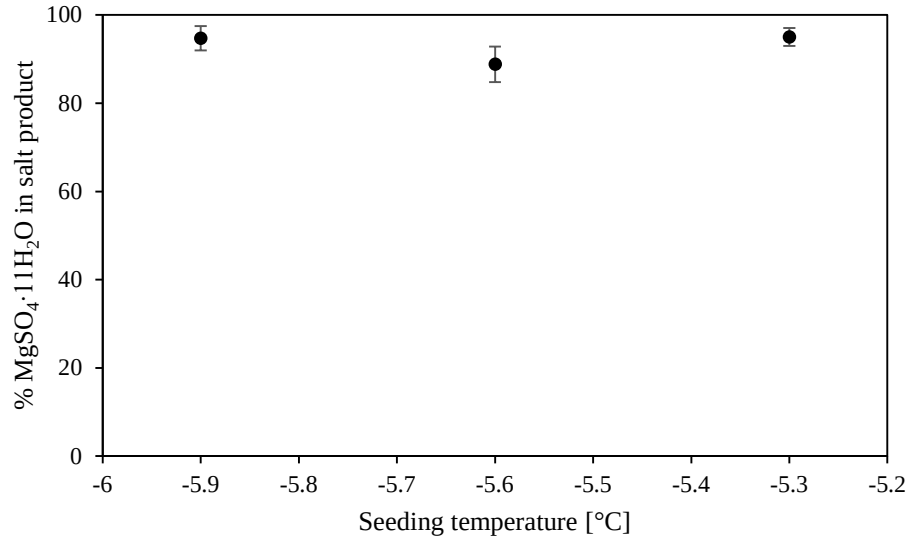

Figure 5.8: Purity of underflow salt split fraction with $Na_2SO_4 \cdot 10H_2O$ seeding at constant mass of seeds

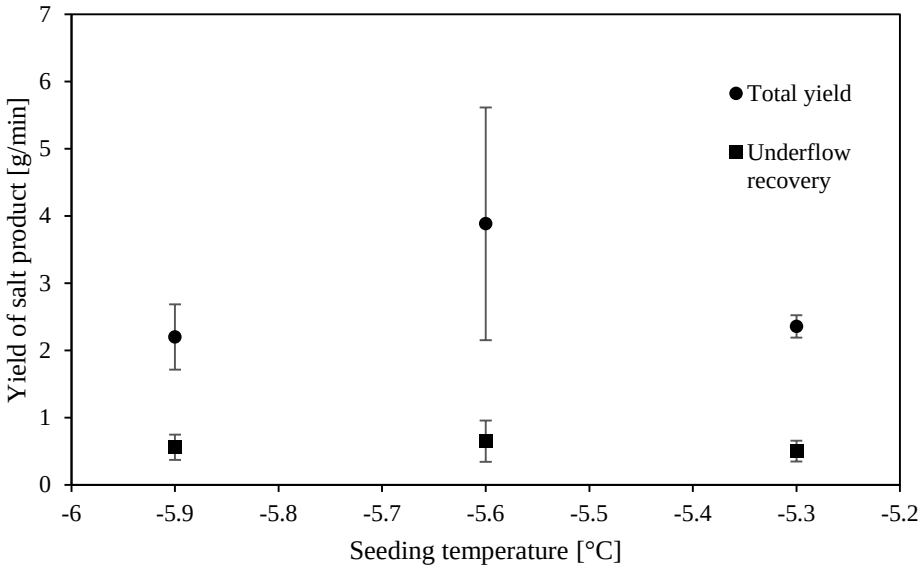

Figure 5.9: Underflow salt split fraction and yield with $Na_2SO_4 \cdot 10H_2O$ seeding at constant mass of seeds

There was no obvious change in either the yield or purity with seeding temperature, but large variations were evident. The lack of a change indicates that the seeding temperature did not have a significant effect on the crystallization of the salts in the crystallizer. The cause of the high variability in yield and purity is not certain. However, heterogeneous nucleation is stochastic in nature, which may also impact crystallization in multicomponent systems, which could have resulted in this variability in purity and yield.

According to typical design heuristics, mixed suspension tanks are operated at up to 40 wt.% solids, and in some cases 50 wt.% where unmixed pockets are desired to increase energy

efficiency. For a continuous crystallization process, it is necessary to reduce the total solids to allow some space for movement of solids, thus allowing ice to rise and salt to sink. This was observed by Randall et al. (2011), who operated his batch crystallizer in series to avoid increasing the solids content above 30% of ice. Therefore, the total yield of ice and salt cannot be far above this to ensure efficient mixing and production of individual crystals with reduced entrainment and agglomeration, assuming there is no melting of the product crystals back into the filtrate. In the highest $Na_2SO_4 \cdot 10H_2O$ seeding mass cases, the total yields of ice and salt in both the underflow and overflow were 3.9 g and 2.4 g, respectively, which works out to a total feed conversion of 7.7% to solid crystals. Taking melting into account, as seen by the mother liquor concentrations (see Figure 5.4), this yield could have been up to 10% of the crystallizer contents. Furthermore, the total mass of solid crystals in the crystallizer was physically measured and found to be less than the calculated conversion (between 4.3 and 6.3%), likely due to physical constraints in the laboratory resulting in increased melting. Nevertheless, the conversion obtained was significantly less than the practical maximum obtainable in such a process. However, as the yield as a response to seed surface area plateaued between 0.25 and 2.5 g and was unlikely to increase further with an increase in seed mass, this indicates that the design of the process in terms of heat transfer surface area and heat capacity of coolant requires improvement to increase this yield.

5.2.3 Seeding with magnesium sulphate hendecahydrate

Similar experiments were done to the above, in which $MgSO_4 \cdot 11H_2O$ was seeded instead of $Na_2SO_4 \cdot 10H_2O$. Figure 5.10 shows the change in the yield of salt with an increase in $MgSO_4 \cdot 11H_2O$ seeding mass. Seeds were added once initially into the 2 ℓ crystallizer. It is noted that no error bars are shown for the 3g seeding case as only one successful experiment could be conducted at these conditions.

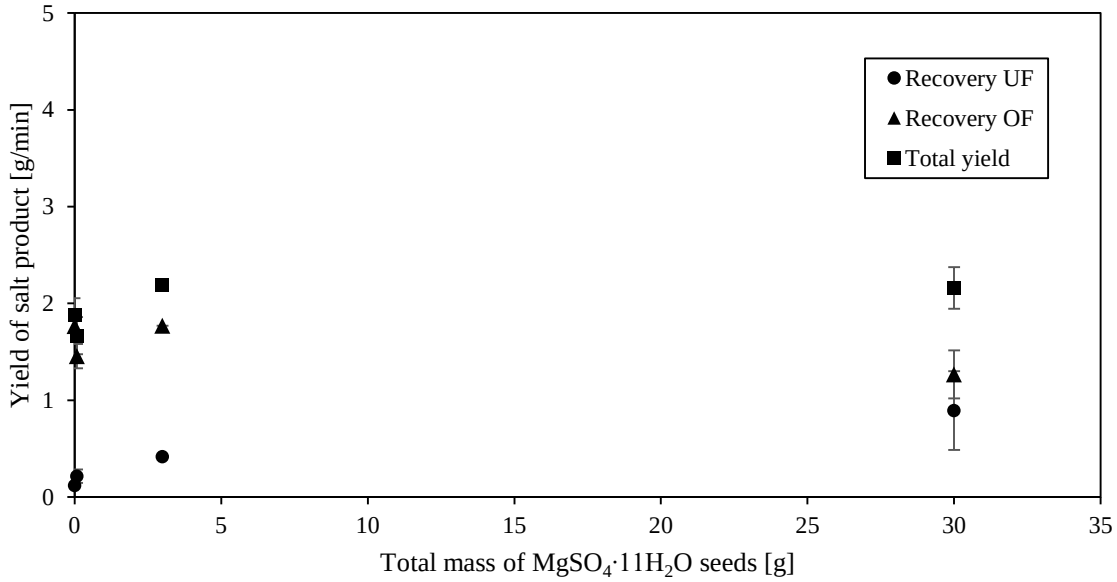

Figure 5.10: Recovery of salt in overflow (OF), underflow (UF) and yield with $MgSO_4 \cdot 11H_2O$ seeding at constant seeding temperature

This graph shows a clear relationship between the mass of seeds and the yield of salt, especially that of the underflow salt fraction. Furthermore, the error bars are small enough to indicate that variation is not just due to feed composition and flow rate. However, there are some differences between the overflow, underflow and total salt yield. Although all of the yield measurements increased from no seeds to 3 g of salt seeds, the total salt yield reached a plateau at 3 g of seeds, while the overflow product decreased between 3 g and 30 g of $MgSO_4 \cdot 11H_2O$ seeds. This graph further shows that the overflow contained a higher recovery of salt than the underflow.

The differences in the recoveries of the overflow and underflow yields between 3 g and 30 g of seeds (1.77 g and 1.27 g overflow yield in each respective case), and the similarity of the total yield in these two cases (2.19 and 2.16 g, respectively), indicates that the total yield of salt remained unvarying, but the average particle size possibly increased since more salt reported to the underflow. Due to this, less salt was entrained with the ice in the overflow. These findings suggest that the yield limit was reached, in that the supersaturation available for $MgSO_4 \cdot 11H_2O$ crystallization was fully used in both the 3 g and 30 g seeding cases. However, the increased seed surface encouraged more crystal growth than nucleation, therefore producing larger crystals, in agreement with the findings made by Chaaban et al. (2013).

The purity of the salt product is shown in Figure 5.11 below.

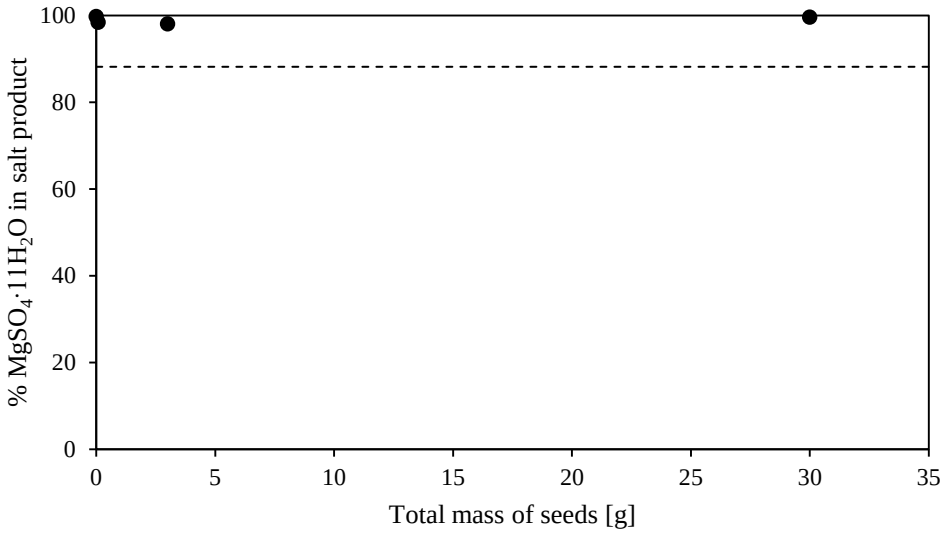

Figure 5.11: Purity of underflow salt product with $MgSO_4 \cdot 11H_2O$ seeding at constant seeding temperature

Figure 5.11 demonstrates that the purity was very high regardless of the seed mass. A closer inspection reveals that the purity was highest when no salt was seeded (ice seeding only) and when 10x the critical seeding mass (30 g) of $MgSO_4 \cdot 11H_2O$ was seeded.

These results indicates that a relatively high purity product was obtained regardless of the seed loading (above 98%). This shows that the system had a high selectivity towards $MgSO_4 \cdot 11H_2O$. Furthermore, a very high purity (above 99.4%) was obtained when only ice seeds were added, and when 30 g of $MgSO_4 \cdot 11H_2O$ was seeded. These results agree with the hypothesis that selectivity would be higher for $MgSO_4 \cdot 11H_2O$ due to its larger solubility-temperature dependence.

When only ice was seeded, the ice proliferated, forming many crystals, which caused its crystallization rate to increase. The concentrating up effect that ice crystallization had on the dissolved salts with time eventually caused spontaneous nucleation of $MgSO_4 \cdot 11H_2O$ as its supersaturation increased. However, due to a combination of high supersaturation and the vast presence of ice, the $MgSO_4 \cdot 11H_2O$ formed mainly through primary nucleation with limited opportunity for growth, and therefore the yield of this salt was low. The purity of the overflow product (see Figure A1.4 in Appendix A1) shows that $Na_2SO_4 \cdot 10H_2O$ also formed by primary heterogeneous nucleation and was therefore also present in the crystallizer. However, the $Na_2SO_4 \cdot 10H_2O$ crystals formed predominantly by primary nucleation, to a greater extent than $MgSO_4 \cdot 11H_2O$. This small particle size, together with a small overall mass of crystals, resulted in an absence of this species in the underflow product.

In the latter case, where 30 g of seeds were added, the seeds ensured that the salt formed at a significant secondary nucleation and growth rate. This likely resulted in the formation of large crystals, which reported to the underflow, resulting in the largest underflow yield while reducing the yield of salt in the overflow. It is of interest to note that the overflow product (see Figure A1.4 in appendix) also contained a high purity of $MgSO_4 \cdot 11H_2O$. This suggests that the combined crystallization of $MgSO_4 \cdot 11H_2O$ and ice resulted in a very high supersaturation of $Na_2SO_4 \cdot 10H_2O$. This resulted in $Na_2SO_4 \cdot 10H_2O$ crystallization through primary nucleation with associated suppression of its growth rate to the extent that very little of this salt could be detected even in the overflow product.

30 g $MgSO_4 \cdot 11H_2O$ seeds produced the optimal results of all the seeding cases, as both a high yield and high purity product could be achieved. Furthermore, the overflow and underflow salt products could be combined, and the overflow product would not need to be melted and recrystallized, as its purity was high.

A stacked graph is included below which shows the underflow salt fraction recovery and quality for $MgSO_4 \cdot 11H_2O$ seeding.

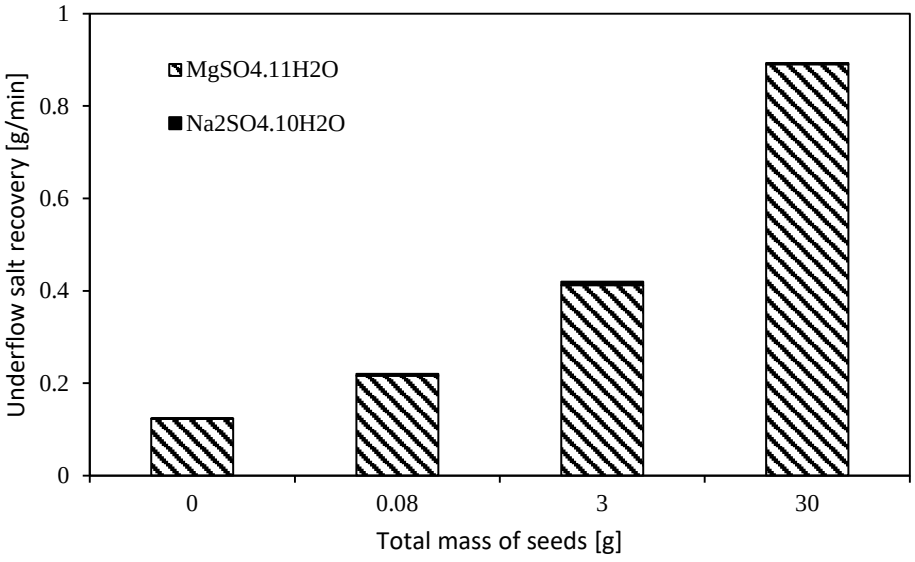

Figure 5.12: Underflow salt recovery as a function of $MgSO_4 \cdot 11H_2O$ seed mass

The stacked graph shows that the underflow salt product consisted of predominantly $MgSO_4 \cdot 11H_2O$, and that $Na_2SO_4 \cdot 10H_2O$ did not form in any significant quantity when $MgSO_4 \cdot 11H_2O$ was seeded. The increase in underflow recovery with seed mass further indicates that multiple steady states did exist even when the product purity remained relatively constant. The presence of multiple steady states is substantiated by other studies (Chaaban et

al., 2013). As the total salt yield displayed an insignificant change with seed mass, and produced the same trend for $Na_2SO_4 \cdot 10H_2O$ seeding (see Figure A1.7 and Figure A1.8), it is observed that steady state had been reached in terms of yield and solids flow. Therefore, the difference in split fraction recovery and purity was not due to a requirement for longer operating times to reach steady state. Furthermore, the yield of salt obtained in the 6-minute sampling time was substantial and could therefore not be due simply to residual seed material that had been added initially, but was due to significant salt crystallization over time.

The high purity for all seeding cases shows that, as with $Na_2SO_4 \cdot 10H_2O$ seeding, an increase in seed mass encouraged the crystallization of the seeded species and not that of the unseeded species. This can be confirmed by similar findings in literature (Chaaban et al., 2013).

As with the $Na_2SO_4 \cdot 10H_2O$ seeding cases, it can be seen from Figure 5.13 and Figure 5.14 below, that there was no clear trend in the product yield and purity with a change in seeding temperature.

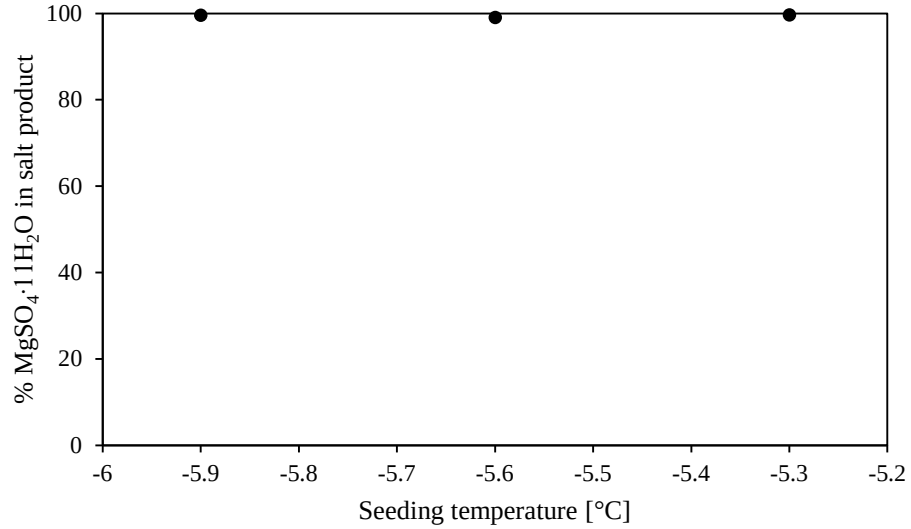

Figure 5.13: Purity of underflow salt product when seeded with 30 g $MgSO_4 \cdot 11H_2O$ with changing seeding temperature

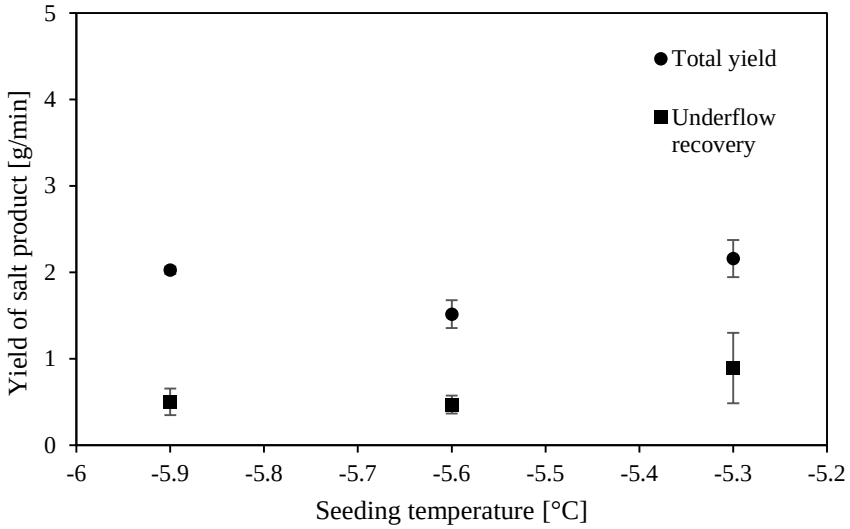

Figure 5.14: Recovery of underflow salt fraction and yield when seeded with 30 g $MgSO_4 \cdot 11H_2O$ with changing seeding temperature

The above graphs show that the purity of the salt product formed in all the experiments was high, with very little variation. Therefore, this was a reproducible finding, independent of seeding temperature. However, there was a large variation in the yield of the salt without showing any definite trend.

The large variation in the yields, as with $Na_2SO_4 \cdot 10H_2O$ seeding, indicates that the spontaneous nucleation of the unseeded salt may have been stochastic in nature, and that the difference in the yield at -5.3°C compared to the lower two temperatures was likely just due to differences in the initial nucleation time and rate for ice and $MgSO_4 \cdot 11H_2O$ and does not provide clear information in terms of a trend. However, the variation in yields for the $MgSO_4 \cdot 11H_2O$ could also be explained by some practical laboratory aspects. The large mass of seeds caused some difficulties during the seeding process, in that a large portion of the seeds melted as they were fed through a small and warm feed port, and started to clog up the port with time, which was problematic for the 30 g seeding case. This could also have resulted in the variations in the yield, as a different mass may have melted to $MgSO_4 \cdot 7H_2O$ in different experiments. This also indicates that the actual mass of $MgSO_4 \cdot 11H_2O$ seeds needed to produce a pure product may be significantly lower than 30 g since all the experiments at this seed mass consistently produced a high purity salt product.

The high mass of seeds chosen (10x critical seeding mass) for the different seeding temperature runs ensured a seeded salt crystallization rate high enough to consume available supersaturation. This hindered the growth of the unseeded salt to the extent that very little of this salt could be detected in the product. Therefore, even if the temperature was decreased,

and the supersaturation was increased, no change is expected to be seen in the purity. It is recommended that future experiments be conducted at lower seeding masses to determine whether a change in seeding temperature has any notable effect when this high level of supersaturation has not been reached.

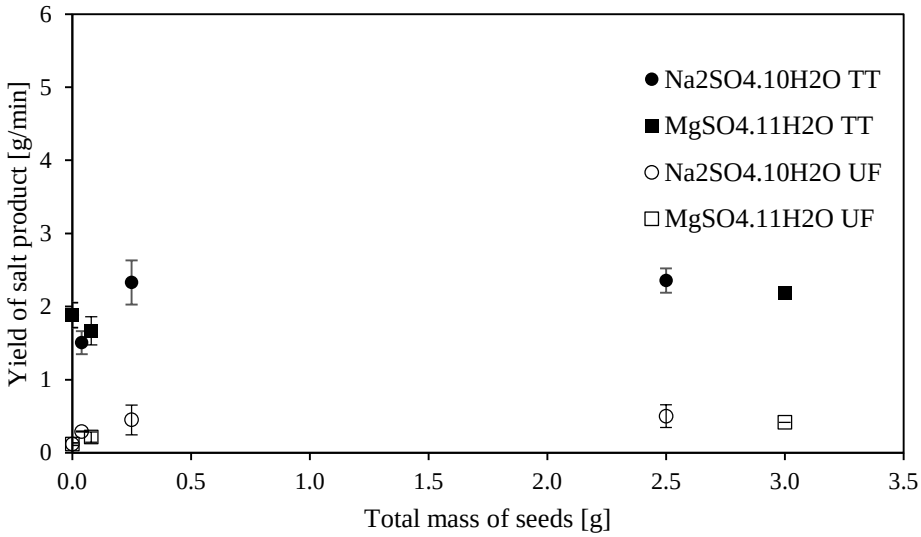

Figure 5.15: Figure comparing underflow recovery and yield for $MgSO_4 \cdot 11H_2O$ and $Na_2SO_4 \cdot 10H_2O$ seeding

Comparing the yield of the salt product for similar seed masses of $Na_2SO_4 \cdot 10H_2O$ and $MgSO_4 \cdot 11H_2O$, it is clear that $MgSO_4 \cdot 11H_2O$ always crystallized out as the majority salt and formed at a far higher purity when it was seeded. However the above graph shows that there was not much difference in yield in the underflow and total recoveries when a similar mass of $MgSO_4 \cdot 11H_2O$ was seeded as $Na_2SO_4 \cdot 10H_2O$. As the seed particle size distributions for the different salts were very similar, with $Na_2SO_4 \cdot 10H_2O$ being only slightly smaller, this can be approximated to a similar seed surface area. This shows that an increase in seed surface area increased the total salt yield regardless of what seed material was used, up to a point, where it reached a plateau. It also shows that seed surface area had a similar effect on total salt secondary nucleation and growth rate regardless of the seeding material used. This similarity could be due to the salt product consisting mostly of $MgSO_4 \cdot 11H_2O$ in all cases, therefore its growth and nucleation kinetics were dominant and $Na_2SO_4 \cdot 10H_2O$ crystallization rates did not produce a significant change in total yield.

The results further indicate that the critical seed mass was sufficient to produce the highest potential yield of salt. This is due to the total salt yield remaining relatively constant between the critical seed mass and 10x the critical seed mass cases (see Figure A1.7 and Figure A1.8 in Appendix A1). However, a further increase in seed mass resulted in an increase in the average

particle size, such that the yield in the overflow split fraction decreased (see Figure A1.5 and Figure A1.6 in Appendix A1) as the yield in the underflow split fraction increased.

In overall, the experiments show that ice had the largest crystallization rate, by producing a mass larger than expected according to thermodynamic ratios with the salts. $MgSO_4 \cdot 11H_2O$ had the second largest crystallization rate as it produced more crystals than its thermodynamic ratio with $Na_2SO_4 \cdot 10H_2O$ predicted.

In the highest $MgSO_4 \cdot 11H_2O$ seeding mass cases, the total yields of ice and salt in both the underflow and overflow were 2.5 g and 2.2 g, respectively, which works out to a total feed conversion of 5.8% to solid crystals. Taking melting into account, this yield could have been up to 7% of the crystallizer contents. This is much less than the practical maximum obtainable in such a process, indicating that the design of the process needs to be improved in terms of heat transfer surface area and heat capacity of the coolant. Furthermore, although the salt yield for a similar mass of seed material was comparable to that when $Na_2SO_4 \cdot 10H_2O$ was seeded, the ice yield was significantly lower when $MgSO_4 \cdot 11H_2O$ was seeded, reducing the overall conversion in the crystallizer. However, for producing a high yield and purity salt product, rather than ice, seeding with $MgSO_4 \cdot 11H_2O$ was required.

These experiments show that the supersaturation in the system was high enough to ensure that all species crystallized out at these conditions, whether seeded or not. Therefore, selective recovery could not rely on remaining within the metastable zone of the unseeded salt in this system, but had to be accomplished through of seed engineering, and thus taking into account the surface area of seeds. In these experiments, it was found that selective recovery was possible for two specific cases, namely with the seeding of only ice and of 30g of $MgSO_4 \cdot 11H_2O$, respectively. Seeding with 30 g of $MgSO_4 \cdot 11H_2O$ produced the highest recovery of underflow salt product as well as a consistently high purity of salt reporting both to the underflow and the overflow regardless of seeding temperature.

5.3 Implications of study

This is the first study of its kind, where selective recovery is attempted in a continuous crystallizer, using inorganic salts. This study showed that although solvent is removed in the form of ice in this process, increasing the supersaturation substantially, the salts responded very similarly to what is found in the selective crystallization of organic compounds. The similarity between these systems included the presence of multiple steady states, and an increase in

selectivity and yield towards the seeded species with an increase in seed surface area. Therefore, findings from one system can, with caution, be applied to the other.

It was found that multiple steady states exist for the $MgSO_4$-Na_2SO_4-H_2O system, at the same operating conditions. These multiple steady states are made possible by the presence of multiple crystallizing species, which impact on the other species' supersaturations. These supersaturations result in variations in the species nucleation and growth rates. One of the outcomes of these interactions is a difference in particle sizes of the various salt species, as seen by a difference in the purities of the overflow and underflow salt split fractions. The study therefore showed that, although yield reached a plateau with an increase in seed mass, the average particle sizes of the salts could be engineered using seed surface area to increase the purity of the underflow salt split fraction.

Furthermore, it was found that simultaneous salt crystallization occurred in this system. It was not possible to operate such that the unseeded salt did not spontaneously nucleate. However, seed engineering was found to have the potential for maximising the formation of one salt while suppressing that of the other salt. Hereby, the possibility exists to selectively recover one salt from a multi-supersaturated system.

Of further interest is the form of magnesium hydrate that was crystallized in this process. Analysis of the seed material and the salt product showed that the possibility exists that the salt product may consist predominantly of $MgSO_4 \cdot 11H_2O$, rather than $MgSO_4 \cdot 11H_2O$, as initially expected.

6 Conclusions

The aim of this study was to determine the effect of seeding on the yield and purity of the salt product in a Na_2SO_4-$MgSO_4$-H_2O system supersaturated with all three species. Experiments were conducted at a coolant temperature of -11°C and residence time of 30 minutes in a 2 ℓ scraped and stirred glass crystallizer.

Comparing the results of the two seeding materials, it was observed that a similar seed mass of each salt produced a similar total salt yield. Furthermore, regardless of the seeding material used, $MgSO_4 \cdot 11H_2O$ always formed at a higher ratio to $Na_2SO_4 \cdot 10H_2O$ than the thermodynamic expectation, showing that the system had a higher selectivity to this salt. This indicates that $MgSO_4 \cdot 11H_2O$ had faster crystallization kinetics. As $MgSO_4 \cdot 11H_2O$ formed the majority of the salt product, the similarity in yield with seeding of different materials was attributed to this salt's kinetics being predominant in all cases.

An increase in seed mass, which relates to an increase in seed surface area, was shown to increase the recovery of the seeded salt in the underflow. This means that, in the $Na_2SO_4 \cdot 10H_2O$ seeding case, although a greater yield of $MgSO_4 \cdot 11H_2O$ was always obtained, the proportion of $Na_2SO_4 \cdot 10H_2O$ in the underflow increased with an increase in seed mass. In the case of $MgSO_4 \cdot 11H_2O$ seeding, 30 g of this material increased the abundance of this salt to such an extent that growth of the unseeded salt ($Na_2SO_4 \cdot 10H_2O$) was suppressed, resulting in a high purity salt product in both the underflow and overflow salt split fractions. It was further found that an increase in seed mass increased the total yield of salt up to the critical seed mass, after which the yield plateaued. This indicated that the critical seed mass was sufficient to produce the highest potential yield of salt. However, a further increase in seed mass resulted in an increase in the average particle size, such that the yield in the overflow split fraction decreased as the yield in the underflow split fraction increased. Therefore, an increase in seed mass increased both the recovery and purity of the seeded salt in the underflow split fraction.

In these experiments, it was found that seeding temperature did not have a significant effect on the yield and purity of the salt product. This was likely because these experiments were undertaken with large masses of each seeding material, therefore the initial supersaturation upon initiation of crystallization was already high in all cases, such that increasing the initial supercooling did not have a noticeable impact on the steady state outcome.

This study shows that multiple steady states exist for the $MgSO_4$-Na_2SO_4-H_2O system at the same operating conditions, with a change in seeding conditions, as far as could be observed without analysing the PSD. Although there was no significant impact on the overall salt yield, an increase in seed mass increased the average particle size of the seeded salt. This resulted in an increase in the underflow recovery and proportion of the seeded salt. In the case where the salt with a higher selectivity was seeded, this resulted in a highly pure product at a high yield. Through this mechanism, it was found that selective recovery of a pure salt product was made possible in a multi-supersaturated system.

8 Recommendations

This study was conducted on a single salt-salt-water system which revealed that there was a higher selectivity towards one of the salts, which resulted in the production of a high purity and high yield salt when seeded with a large mass (30 g/2 ℓ solution) of this salt. It is recommended that studies be conducted on other salt-salt-water systems, to determine whether this characteristic is system-specific or if it can be applied in other systems. Although there was variation in the feed composition, the range of concentrations was narrow. It would therefore also be beneficial to determine the range of concentrations at which the high selectivity for $MgSO_4 \cdot 11H_2O$ continues to exist.

Furthermore, it is recommended that the seeding temperature runs be undertaken at lower seeding masses, so that the initial supersaturation experienced by the salt species would be provided predominantly by the low temperatures. In this way, the seeding temperature may have a larger impact on initial nucleation and growth rates, rather than allowing these rates to be determined more significantly by a very large seed base. This will allow the researcher to determine whether seed temperature holds any significance in determining the final steady state.

9 References

Aamir, E., Nagy, Z.K., Rielly, C.C. 2010. Optimal seed recipe design for crystal size distribution control for batch cooling crystallization processes. *Chemical Engineering Science* 65: 3602 - 3614

Apsey, G. 2011. Impurities in crystals formed by eutectic freeze crystallization. M.Eng. Dissertation. University of Cape Town, South Africa

Balomenos, E., Panias, D., Paspaliaris, I. 2006. A semi-empirical hydrogen model (SEHM) for describing aqueous electrolyte solutions. *Fluid Phase Equilibria* 243: 29 - 37

Beckmann, W. 2013. *Crystallization: Basic Concepts and Industrial Applications*. Wiley-VCH, p. 42 - 44

Bergfors, T. 2003. Seeds to Crystals. Journal of Structural Biology 142: 66 - 76

Bock, C.W., Markham, G.D., Katz, A.K., Glusker, J.P.. 2006. The arrangement of first- and second-shell water molecules around metal ions: effects of charger and size. *Theoretical Chemistry Accounts* 115: 100 - 112

Chaaban, J.H., Dam-Johansen, K., Skovby, T., Kiil, S. 2013. Separation of enantiomers by continuous preferential crystallization: Experimental realization using a coupled crystallizer configuration. *Organic Process Research and Development* 17: 1010 - 1020

Deng, T. 2012. Stable and Metastable Phase Equilibria in the Salt-Water Systems, Advances in Crystallization Processes, Dr. Yitzhak Mastai (Ed.), ISBN: 978-953-51-0581-7, InTech, Available: http://www.intechopen.com/books/advances-in-crystallization-processes/stable-and-metastable-phaseequilibria-of-the-salt-water-system

Denton, W.H., Smith, M.J., Klaschka, J.T., Forgan, R., Diffey, H.R., Rumary, C.H., Dawson, R.W. 1974. Experimental Studies on Washing and Melting Ice Crystals in the Immiscible Refrigerant Freezing Process. *Desalination* 14: 263-290

Gartner, R.S., Genceli, F.E., Trambitas, D.O., Witkamp, G.J. 2005. Impurity gradients in solution-grown ice and MgSO4.12H2O crystals measured by cryo-laser ablation and high-resolution-induced-coupled plasma mass spectrograph. *Journal of Crystal Growth* 275, e1773 – e1778

Genceli, F.E., Himawan, C., Witkamp, G.J. 2005. Inline determination of supersaturation and metastable zone width of MgSO4.12H2O with conductivity and refractive index measurement techniques. *Journal of Crystal Growth* 275: e1757-e1762

Genceli, F.E. 2008. Scaling-up Eutectic Freeze Crystallization. Ph.D. Thesis. Technical University of Delft, The Netherlands

Goldschmidt, V.M. 1937. The principles of distribution of chemical elements in minerals and rocks. *Journal of the Chemical Society.* Issue 0,1937

Haggard, E.L., Sheridan, C.M., Harding, K.G. 2015. Quantification of water usage at a South African platinum processing plant. *Water SA.* 41: No. 2

Himawan, C. 2005. Characterization and population balance modelling of Eutectic Freeze Crystallization. Ph.D. Thesis. Technical University of Delft, The Netherlands

Himawan, C., Kramer, H.J., Witkamp, G.J. 2006. Study on the recovery of purified MgSO4.7H2O crystals from industrial solution by eutectic freezing. *Separation and Purification Technology* 50: 240 - 248

Hofmann, S., Raisch, J. 2013. Solutions to inversion problems in preferential crystallization of enantiomers – Part II: Batch crystallization in two coupled vessels. *Chemical Engineering Science* 88: 48-68

Jin, M., Frohberg, P., Sun, Y., Li, P., Yu, J., Ulrich, J. 2015. Study on metastable zone width and crystal growth of a ternary system: case study $MgCl_2 \cdot 6H_2O \cdot$1,4-dioxane. *Chemical Engineering Science* 133: 181-189

Jones, A.G. 2002. *Crystallization Process Systems.* London, UK: Butterworth Heinemann

Kadam, S.S., Kulkarni, S.A., Ribera, R.C., Stankiewicz, A.I., ter Horst, J.H., Kramer, H. J. 2012. A new view on the metastable zone width during cooling crystallization. *Chemical Engineering Science* 72: 10-19

Kane, S.G., Evans, T.W., Brian, P.L., Sarofim, A.F. 1975. The kinetics of the secondary nucleation of ice: implications to the operation of continuous crystallizers. *Desalination* 17: 3 - 16

Lewis, A, Nathoo, J., Reddy, T., Randall, D., Zibi, L., Jivanji, R. 2010. Novel technology for recovery of water and solid salts from hypersaline brines: eutectic freeze crystallization. University of Cape Town, South Africa

Lewis, A., Seckler, M., Kramer, H., van Rosmalen, G. 2015. *Industrial Crystallization.* Cambridge University Press

Mantri, R.V., Sanghvi, R., Zhu, H. 2017. Developing solid oral dosage forms (second edition). *Pharmaceutical Theory and Practice*. 3 - 22

Margolis, G., Sherwood, T.K., Thibaut Brian, P.L. Sarofim, A.F. 1971. The Performance of a Continuous Well Stirred Ice Crystallizer, *Industrial and Engineering Chemistry Fundamentals* 10: 439-452

Markov, I.V. 1995. *Crystal growth for beginners: Fundamentals of Nucleation, Crystal Growth and Epitaxy*. Bulgaria. World Scientific Publishing Co. Pte. Ltd

Mersmann, A. 2001. *Crystallization technology handbook.* 2nd ed. USA. Marcel Dekker, Inc

Mitchel, N.A. & Frawley, P.J. 2010. Nucleation kinetics of paracetamol-ethanol solutions from metastable zone widths. *Journal of Crystal Growth* 312: 2740-2746

Mullin, J.W. 2001. *Crystallization*. Ed 4. Reed Educational and Professional Publishing Ltd

Myerson, A.S. 2002. *Handbook of Industrial Crystallization, 3rd ed.* A.S. Myerson, Ed. London: Butterworth Heinemann.

Nathoo, J., Jivanji, R., Lewis, A.E. 2009. Freezing Your Brines Off: Eutectic Freeze Crystallization for Brine Treatment, *International Mine Water Conference*, Pretoria, South Africa, p. 431 – 437

Peters, E.M. 2015. Effect of antiscalants during eutectic freeze crystallization of a reverse osmosis retentate. M.Eng. Dissertation. University of Cape Town, South Africa

Qamar, S., Galan, K., Elsner, M.P., Hussain, I., Seidel-Morgenstern, A. 2013. Theoretical investigation of simultaneous continuous preferential crystallization in a coupled mode. *Chemical Engineering Science* 98: 25-39

Randall, D.G. 2010. Development of a brine treatment protocol using Eutectic Freeze Crystallization. Ph.D. Thesis. University of Cape Town, South Africa

Randall, D.G., Nathoo, J., Lewis, A.E. 2009. Seeding for selective salt recovery during eutectic freeze crystallization. International Mine Water Conference, 639 - 646

Randall, D.G., Nathoo, J., Lewis, A.E. 2011. A case study for treating a reverse osmosis brine using eutectic freeze crystallization – approaching a zero waste process. *Desalination* 266: 256-262

Randall, D.G., Nathoo, J., Genceli-Guner, F.E., Kramer, H.J., Witkamp, G.J., Lewis, A.E. 2012. Determination of the metastable ice zone for a sodium sulphate system. *Chemical Engineering Science* 77: 184-188

Reddy, S., Lewis, A. 2009. Waste minimisation through recovery of salt and water from a hypersaline brine. Mine Water and Innovative Thinking. Wolkersorfer, 179-183

Reddy, S., Lewis, A., Witkamp, G., Kramer, H., van Spronsen, J. 2010. Recovery of Na2SO4.10H2O from a reverse osmosis retentate by eutectic freeze crystallization technology. *Chemical Engineering Research and Design* 88, No. 9: 1153-1157

Remko, M. 1997. Structure and gas phase stability of complexes L… M, where M = Li+, Na+, Mg2+ and L is formaldehyde, formic acid, formate anion, formamide and their sila derivatives. *Molecular Physics: An International Journal at the Interface between Chemistry and Physics* 91: 5

Rodriguez Pascual, M. 2009. Physical aspects of scraped heat exchanger crystallizers. Ph.D. Thesis. Technical University of Delft, The Netherlands

Rougeot, C., Hein, J.E. 2015. Application of continuous preferential crystallization to efficiently access enantiopure chemicals. *Organic Process Research and Development* 19: 1809-1819

Rousseau, R.W., O'Dell, F.P. 1980. Separation of multiple solutes by selective nucleation. *Industrial and Engineering Chemistry Product Research and Development.* 603-608

Sadek, S. 1966. Nucleation and Growth of Ice in Saline Solutions. Sc.D. Thesis. M.I.T., Cambridge, Massachusetts

Saito, N., Yokota, M., Fujiwara, T., Kubota, N. 2001. A note of the purity of crystals produced in batch crystallization. *Chemical Engineering Journal* 84: 573 – 575

Tavare, H.S. 1995. *Industrial Crystallization.* Manchester, UK: Springer Science + Business Media, LLC

Thomsen, K. 1997. Aqueous electrolytes: model parameters and process simulation. Ph.D. Thesis. Technical University of Denmark, Denmark

Ulrich, J. and Jones, M.J. 2006. Heat and mass transfer operations – Crystallization. In *Chemical Engineering and Chemical Process Technology.* J Bridgwater, M Molzahn, R Pohorecki, Eds. Oxford, UK: Eolss Publishers

Vaessen, R. 2003. Development of scraped eutectic crystallizers. Ph.D. Thesis. Technical University of Delft, The Netherlands

Van der Ham, F. 1999. Eutectic Freeze Crystallization. Ph.D. Thesis. Technical University of Delft, The Netherlands

Van der Ham, F., Seckler, M.M., Witkamp, G.J. 2004. Eutectic freeze crystallization in a new apparatus: the cooled disk column crystallizer. *Chemical Engineering and Processing* 43: 161-167

Van Spronsen, J., Rodriguez Pascual, M., Genceli, F.E., Trambitas, D.O., Evers, H., Witkamp, G.J.. 2010. Eutectic freeze crystallization from the ternary Na_2CO_3-$NaHCO_3$-H2O system: A novel scraped wall crystallizer for the recovery of soda from an industrial aqueous stream. *Chemical Engineering Research and Design* 88: 1259-1263

Vetter, T., Burcham, C.L., Doherty, M.F. 2015. Separation of conglomerate forming enantiomers using a novel continuous preferential crystallization process. *American Institute of Chemical Engineers AIChE J* 61: 2810-2823

Villamil Ramirez, O.K. 2016. Preferential crystallization of a racemic compound via its conglomerate co-crystals. M.Eng. Dissertation. Delft University of Technology, The Netherlands

Witkamp, G. 2008. Treatment of molybdate containing waste streams. WO 2008/115063 A1

Zhang, D., Xu, S., Du, S., Wang, J., Gong, J. 2017. Progress of pharmaceutical continuous crystallization. *Engineering* 3, Issue 3: 354-364

Zhang, G. and Grant, D. 1999. Incorporation mechanism of guest molecules in crystals: solid solution or inclusion. *International journal of pharmaceutics* 181, p. 61 – 70

Appendix A1

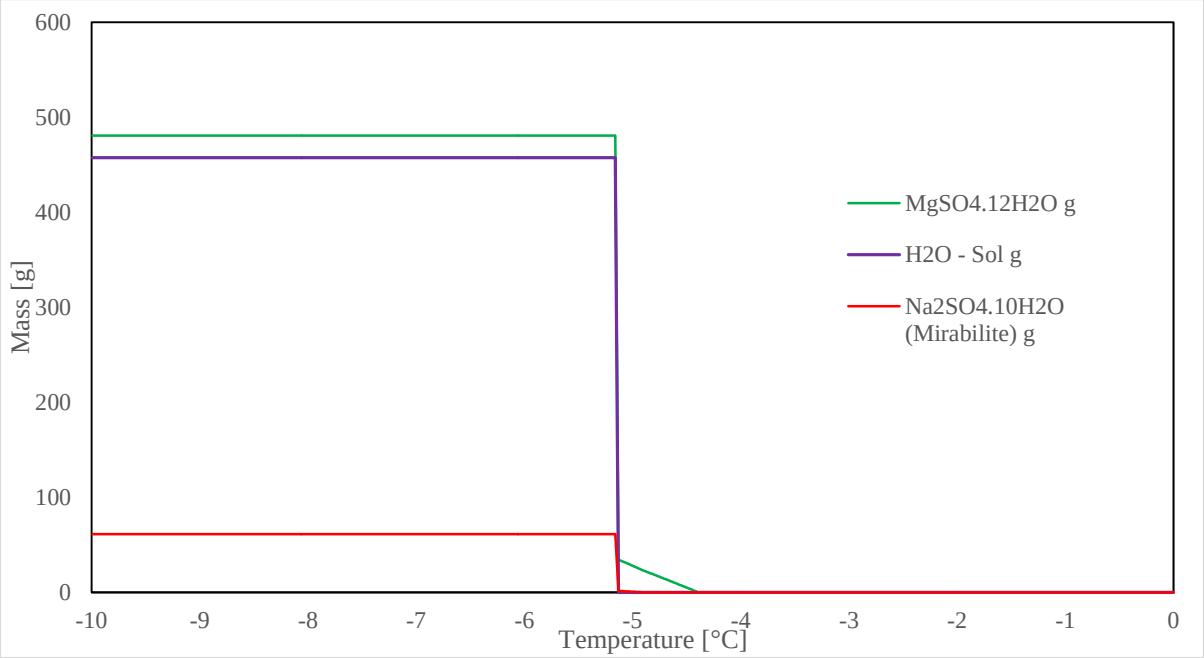

Figure A1.1: Example of OLI thermodynamic modelling of a ternary system not at eutectic

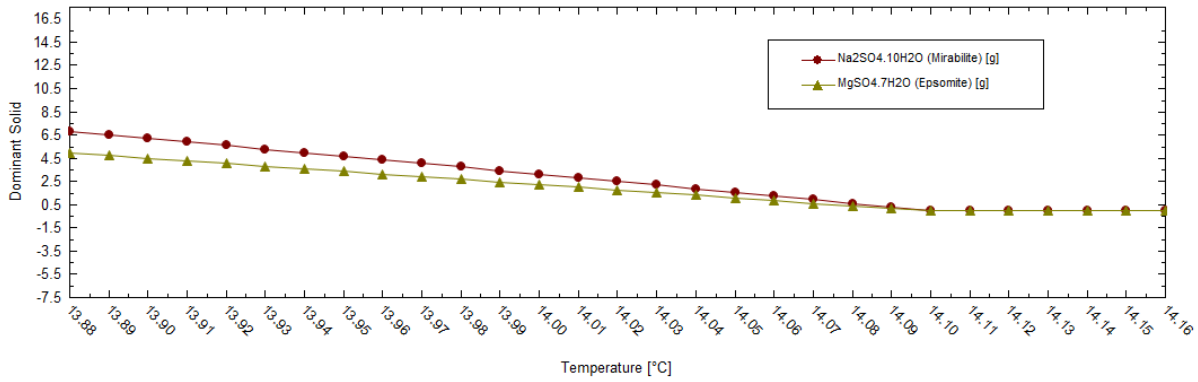

Figure A1.2: Change in mass of solid crystallized as a function of temperature, based on a saturated Na_2SO_4-$MgSO_4$-H_2O composition on the salt binary line at 14.1°C

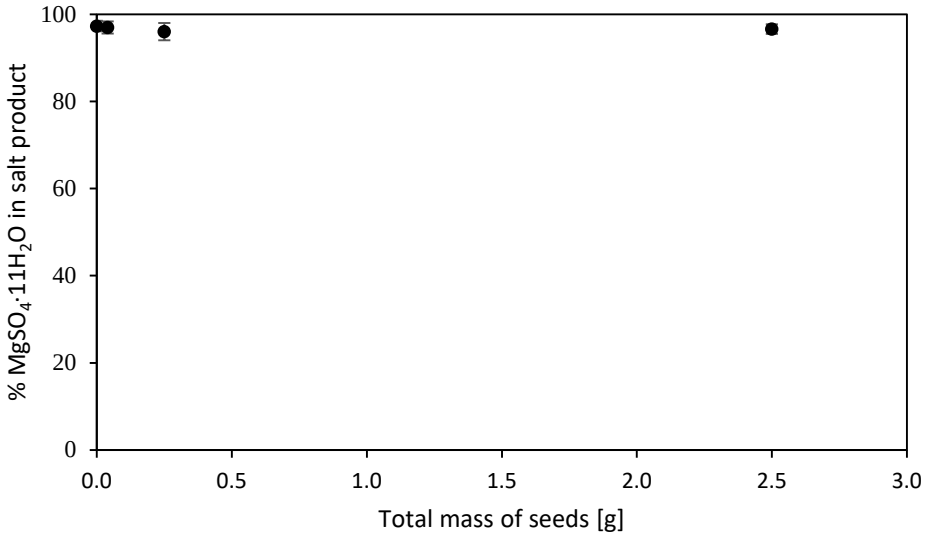

Figure A1.3: Purity of overflow salt split fraction with $Na_2SO_4 \cdot 10H_2O$ seeding at constant mass of seeds

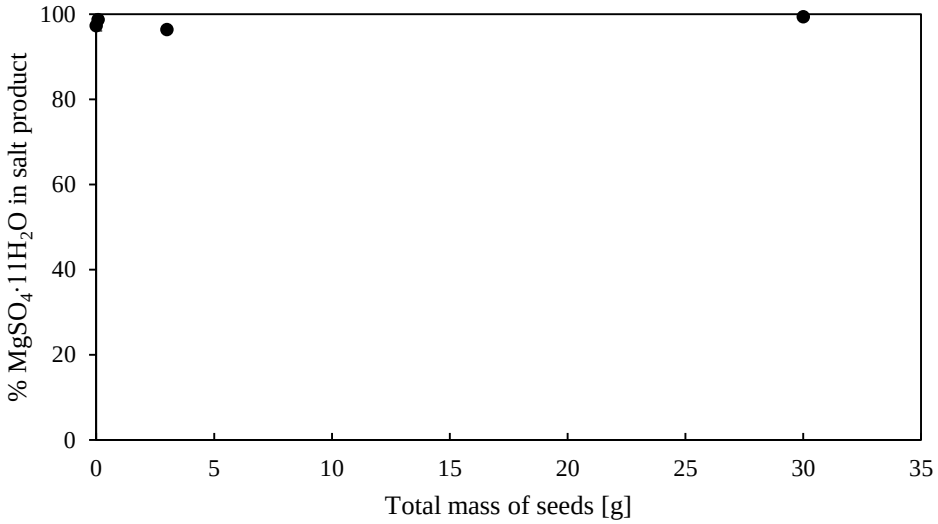

Figure A1.4: Purity of overflow salt split fraction with $MgSO_4 \cdot 11H_2O$ seeding at constant mass of seeds

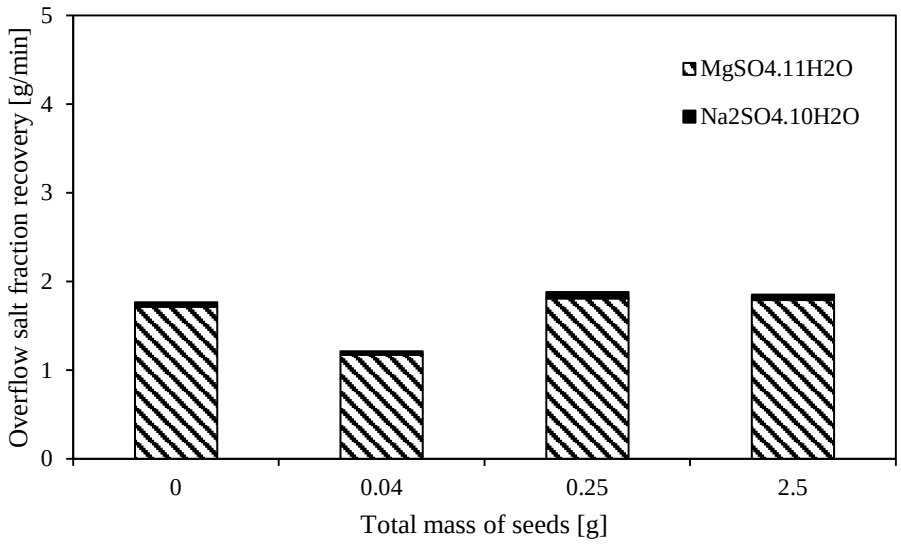

Figure A1.5: Recovery of overflow salt product species with a change in $Na_2SO_4 \cdot 10H_2O$ seed mass

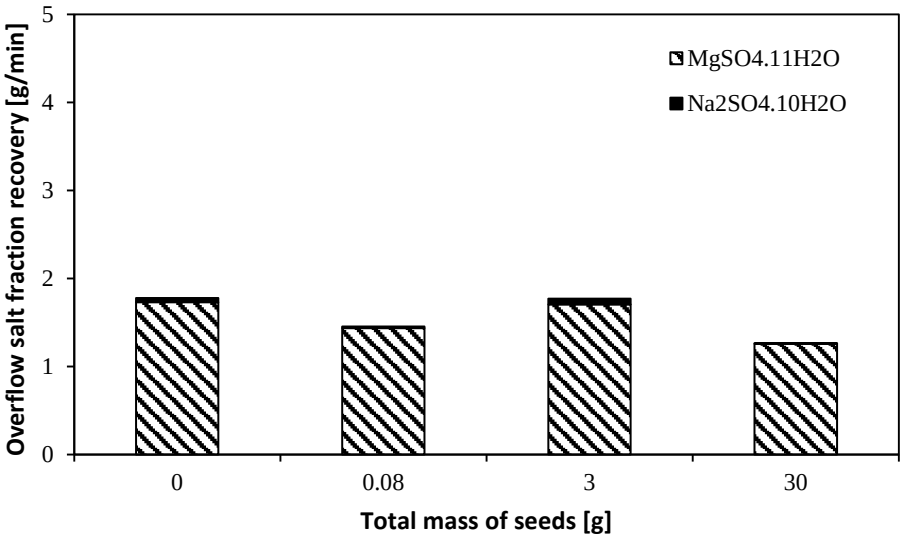

Figure A1.6: Recovery of overflow salt product species with a change in $MgSO_4 \cdot 11H_2O$ seed mass

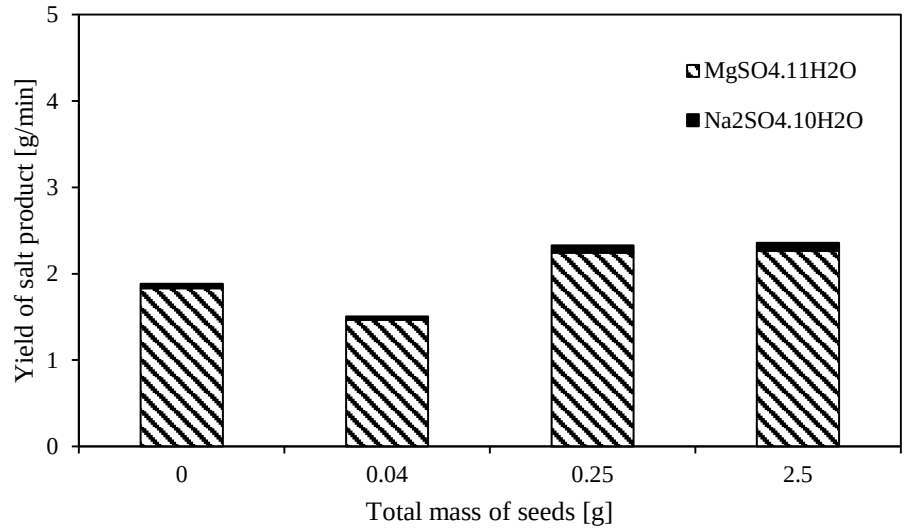

Figure A1.7: Total yield of salt product species with a change in $Na_2SO_4 \cdot 10H_2O$ seed mass

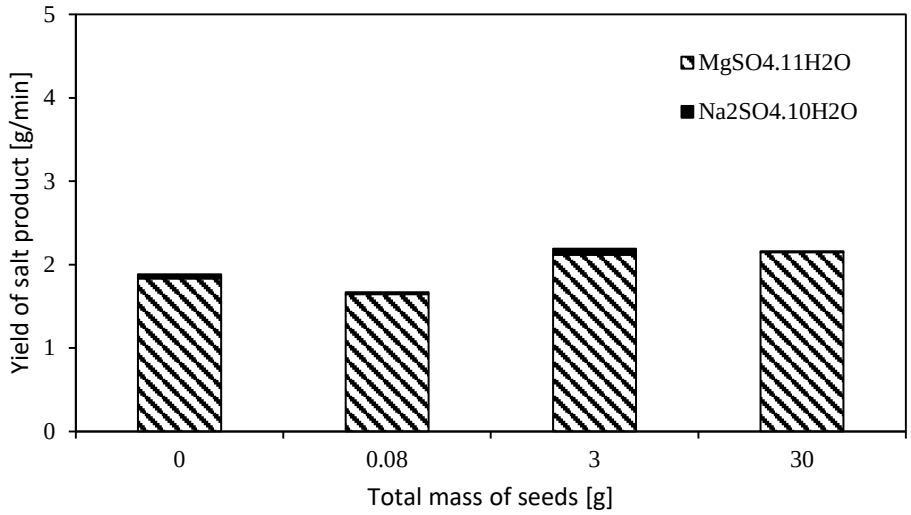

Figure A1.8: Total yield of salt product species with a change in $MgSO_4 \cdot 11H_2O$ seed mass

Appendix B1

In order to estimate the fraction of seeds remaining in the crystallizer over time, an estimated calculation was used based on a tracer study equation, assuming CSTR or MSMPR continuous crystallizer operation.

The equation used is as follows:

$$\frac{C(t)}{C_0} = e^{-t/\tau} \quad \text{B1.1}$$

The percentage of seeds that have washed out of the crystallizer is therefore:

$$\left(1 - \frac{C(t)}{C_0}\right) \times 100\% \quad \text{B1.2}$$